THERMAL AND ENERGY PERFORMANCE OF NANOFLUID OPERATED HEAT RECOVERY EXCHANGER

LEONG KIN YUEN

**THESIS SUBMITTED IN FULFILMENT
OF THE REQUIREMENTS
FOR THE DEGREE OF DOCTOR OF PHILOSOPHY**

**FACULTY OF ENGINEERING
UNIVERSITY OF MALAYA
KUALA LUMPUR**

2013

UNIVERSITY OF MALAYA

ORIGINAL LITERARY WORK DECLARATION

Name of Candidate: Leong Kin Yuen

Registration/Matric No: KHA100008

Name of Degree: Doctor of Philosophy

Title of Project Paper/Research Report/Dissertation/Thesis ("this Work"):

Thermal and Energy Performance of Nanofluid Operated Heat Recovery Exchanger

Field of Study: Heat Transfer and Energy

I do solemnly and sincerely declare that:

(1) I am the sole author/writer of this Work;
(2) This Work is original;
(3) Any use of any work in which copyright exists was done by way of fair dealing and for permitted purposes and any excerpt or extract from, or reference to or reproduction of any copyright work had been disclose expressly and sufficiently and the title of the Work and its authorship had been acknowledge in this Work;
(4) I do not have any actual knowledge nor ought I reasonably to know that the making of this work constitutes an infringement of any copyright work;
(5) I hereby assign all and every right in the copyright to this Work to the University of Malaya ("UM"), who henceforth shall be owner of the copyright in this Work and that any reproduction or use in any form or by any means whatsoever is prohibited without the written consent of UM having been first had and obtained;
(6) I am fully aware that if in the course of making this Work I have infringed any copyright whether intentionally or otherwise, I may be subject to legal action or any other action as may be determined by UM.

Candidate's Signature Date:

Subscribed and solemnly declared before,

Witness's Signature Date:

Name:

Designation:

Abstract

In recent years, there has been a substantial increase in energy demand due to industrialization. This raises concern on issues such as depletion of fossil based energy and emission of green house gasses. It is reported that a high portion of industrial energy is wasted as flue gas/hot gas from heating plants, boilers, etc. Hence, optimization of energy use through heat recovery device is one of the possible approaches to address this problem. However, conventional heat transfer fluids feature low thermal conductivity.

The development in nanotechnology has enabled the introduction of nanofluids as a new generation of heat transfer fluid. Nanofluids are suspensions of nanoparticles in a base fluid. The inclusion of nanoparticles into a base fluid significantly increases the thermal conductivity of the base fluid. This study attempts to investigate the thermal and energy performance of a shell and tube heat exchanger and thermosyphon air-preheater operated with nanofluids. It focuses on recovering waste heat from hot gases/ flue gas produced by a heating plant. The analysis was conducted based on the thermo-physical properties of nanofluids obtained from literatures, mathematical correlations and present experimental data.

The thermo-physical properties measured in this study include thermal conductivity, viscosity and density. The study reveales that, the thermal conductivity of ethylene glycol/water based Al_2O_3 (0.5vol.%, partice size: 13nm) increases about 8.9% compared to base fluid. About 12.9% augmentation is also observed for water based Al_2O_3 (0.5vol.%, particle size :13nm). Thermal conductivity of nanofluids increases with the increase of particle volume percentage or decrease of particle size. Viscosity and density also show increasing trend with the addition of nanoparticles.

The thermal performance of shell and tube heat recovery exchanger improved with the addition of nanoparticles. About 7.8% heat transfer augmentation was observed

for the ethylene glycol-based nanofluids containing 1 vol.% of copper nanoparticles at 26.3 kg/s flue gasses' mass flow rate and 111.6 kg/s coolant's mass flow rate. For water containing 2 vol.% of copper, 4.5% heat transfer enhancement was recorded. At constant coolant mass flow rate, lower pumping power is needed when nanofluids are applied. About 10.99% less power was observed at 1vol. % of copper nanoparticle compared to ethylene glycol base fluid.The study on the size reduction of heat exchanger, implied that nanofluids provide opportunity to reduce the size of heat exchanger without decreasing its thermal performance.

Analysing the total dimensionless entropy generation revealed that, 10.8% reduction is observed with an addition of 7 vol.% of Al_2O_3 into water. About 9.7% reduction is observed for water-based TiO_2 (4 vol.%) nanofluid. Other factors that influence total dimensionless entropy generation are dimensionless temperature difference, fluid mass flow rate, tube diameter and length.

Moreover, the study revealed that the change of nanofluid thermo-physical properties only plays a minor role in improving the thermal performance of the thermosyphon heat exchanger. Slight increase of overall heat transfer coefficient and cold air outlet temperatures are observed with increasing nanoparticle volume fraction. However, the thermal performance of thermosyphon heat exchanger increases when the hot air velocity elevates from 2.5 to 4.75m/s.

Abstrak

Kebelakangan ini, terdapat peningkatan dalam permintaan tenaga akibat dari pembangunan industri. Ini telah meningkatkan perhatian terhadap isu-isu seperti kekurangan sumber tenaga berasaskan fosil dan pembebasan gas rumah hijau. Laporan telah menunjukkan sebahagian besar tenaga industri dibazirkan dalam bentuk gas serombong/gas panas dari loji pemanasan, dandang dan sebagainya. Oleh itu, pengoptimunan tenaga melalui alat penukar haba merupakan salah satu cara untuk menyelesaikan masalah ini. Walaubagaimanapun, bendalir haba konvensional mempunyai ciri terma konduksi yang lemah.

Pembangunan dalam bidang nanoteknologi memungkinkan kewujudan bendalir nano sebagai bendalir haba generasi baru. Bendalir nano terdiri dari campuran nanopartikel dan bendalir asas. Penambahan nanopartikel ini ke dalam bendalir asas dapat meningkatkan ciri-ciri konduksi terma. Oleh yang demikian, projek ini bertujuan untuk mengkaji prestasi terma dan tenaga bagi penukar haba jenis *shell* dan *tube* serta thermosifon udara pra-pamanas yang beroperasi mengunakan bendalir nano. Alat-alat penukar haba ini berfungsi untuk mengembalikan baki haba dari gas serombong/gas panas yang dihasilkan dari loji pemanasan. Analisa yang dijalankan adalah berpandu kepada ciri-ciri terma dan fisikal bendalir nano yang didapati dalam literatur, korelasi matematik dan juga eksperimen data dari projek ini.

Eksperimen terma fizikal yang dijalankan meliputi konduksi haba, kelikatan dan ketumpatan. Projek ini mendapati bahawa konduksi haba bagi campuran *ethylene gycol*/air yang mengandungi Al_2O_3 (0.5% konsentrasi isipadu, partike saiz: 13nm) meningkat sebanyak 8.9% berbanding dengan bendalir asas. Peningkatan sebanyak 12.9% juga direkodkan pada bendalir nano berasakan air yang mengandungi Al_2O_3 (0.5% konsentrasi isipadu, partikel saiz: 13nm). Ia juga dilaporkan bahawa konduksi haba bagi bendalir nano meningkat seiring dengan peningkatan konsentrasi isipadu

nanopartikel. Ciri-ciri lain seperti kelikatan dan ketumpatan bendalir nano juga meningkat apabila konsentrasi isipadu nanopartikel meningkat.

Kajian juga mendapati prestasi terma penukar haba *shell* and *tube* meningkat dengan pertambahan nanopartikel ke dalam bendalir asas. Sebanyak 7.8% peningkatan haba dicatatkan bagi *ethylene glycol* yang mengandungi 1% konsentrasi isipadu nanopartikel jenis tembaga pada kadar alir jisim 26.3 kg/s (gas serombong) dan 111.6 kg/s (bendalir nano). Bagi air berasaskan 2% konsentrasi isipadu tembaga pula, peningkatan haba sebanyak 4.5% dicatatkan pada pengaliran jenis laminar. Pada kadar alir jisim bendalir yang tetap, kuasa pam yang lebih rendah diperlukan apabila bendalir nano digunakan. 10.99% pengurangan kuasa pam didapati apabila ethyelene glycol bendalir asas ditambahkan dengan 1% konsentrasi isipadu tembaga. Kajian juga mendapati penggunaan bendalir nano menyediakan peluang bagi pengecilan saiz alat penukar haba tanpa menjejaskan prestasinya.

Kajian juga mendapati jumlah entropi tanpa dimensi menurun sebanyak 10.8% dicatatkan apabila 7% konsentrasi isipadu Al_2O_3 ditambahkan ke dalam bendalir asas berasaskan air. Sebanyak 9.7% penurunan dicatatkan pula bagi bendalir nano berasaskan 4% konsentrasi isipadu TiO_2. Faktor-faktor lain seperti perbezaan suhu tanpa dimensi, kadar alir jisim bendalir, paip diameter and panjang juga mempengaruhi jumlah entropi tanpa dimensi.

Kajian juga mendapati bahawa perubahan dalam ciri-ciri termo-fizikal bendalir nano hanya memainkan peranan kecil dalam peningkatan prestasi terma termosifon penukar haba. Hanya sedikit peningkatan dari segi perolakan haba keseluruhan dan suhu keluar gas sejuk dicatatkan. Walaubagaimanapun, prestasi terma termosifon penukar haba meningkat apabila kadar alir udara panas meningkat dari 2.5 m/s ke 4.75 m/s.

Acknowledgements

First and foremost, I would like to express heartiest thanks to my supervisors, Professor Dr Saidur Rahman, Associate Professor Dr Yau Yat Huang and Professor T.M.Indra Mahlia for their consistent encouragement, advice and invaluable guidance throughout the course of this project.

I would also like to express my deepest appreciation and gratitude to my family members and Miss Ng Lee Yin for their love, sacrifice, motivation and support during the course of this project. I am thankful to and acknowledge the HIRG-MoHE for their financial support under UM.C/HIR/MHE/ENG/40.

And last but not least, I would like to thank those who have contributed directly or indirectly towards the success of this project.

Table of Contents

List of Figures

List of Tables

List of Abbreviations and Symbols

Abbreviations

A	Area, m^2
A_s	Total tube outside heat transfer area, m^2
$A_{c,f}$	Cross flow area, m^2
$A_{o,t}$	Tube side flow area per pass, m^2
Al_2O_3	Aluminium oxide, alumina
Au	Gold
B	Baffle length, m
C	Capacity rate, W/K
CO_2	Carbon dioxide
c_p	Specific heat, J/kgK
Cu	Copper
CuO	Copper oxide
Cu_2O	Copper(I)oxide
CL	Tube layout constant
CTAB	Cetyltrimethylammonium bromide
CTP	Constant
D,d	Diameter,m
DNP	Diamond
dP	pressure drop, Pa
dx	length of the tube,m
EG	Ethylene glycol
E	Energy consumption (MWh)
$\dot{e}$	Energy consumption needed for 1 kg material processing
Ec	Eckert number
f_s	fin spacing, mm
F,f	Friction factor
Fe	Ferum
Fe_2O_3	Iron(III)oxide
g	Gravity acceleration, m/s^2
h	Convective heat transfer coefficient,W/m^2K

H	Height (m)
H_2O	Water
IEP	Isoelectric point
j	Colburn factor
k	Thermal conductivity, kW/mK
L	Length of tube, m
l	fin length for heat conduction from primary to midpoint between plates, m
LMTD	Log mean temperature different
m	Mass, kg
MWCNT	Multiwall carbon nanotube
$\dot{m}$	Mass flow rate, kg/s
N_2	Nitrogen
Nu	Nusselt number
NTU	Number of heat transfer units
$N_{t,p}$	Number of tubes per pass
N_t	Total number of tubes
N_{TC}	$\frac{D_s}{P_t}$
O_2	Oxygen
P	Pump power, kW
PEO	Poly(ethylene oxide)
Pr	Prandtl number
PR	Pitch ratio
PVP	Polyvinylpyrrolidone
P_t	Square tube pitch, mm
Q, q	Heat transfer rate, kW
R	thermal resistance, m^2K/W
Re	Reynolds number
SWCNH	Single wall carbon nanohorn
$\dot{S}_{gen}$	entropy generation (W/K)
St	Stanton number
s_t	transverse pitch, mm
s_l	longitudinal pitch, mm

SiO_2	Silicon dioxide
SDBS	Sodium Dodecyl Benzene Sulfonate
SDS	Sodium Dodecyl Sulfate
T	Temperature, ^oC
TEM	Transmission electron microscopy
TiO_2	Titanium dioxide
U, U_o	Overall heat transfer coefficient, W/m^2K
u	Velocity,m/s
V	Volumetric flow rate, m^3/s
v	Volume
WO_3	Tungsten trioxide
W	Weight (m)
ZnO	Zinc oxide

Greek symbol

ρ	Density, kg/m^3
∅	Volume fraction
μ	Dynamic viscosity, Ns/m^2
ε	Heat exchanger effectiveness
Δp	Pressure drop,Pa
η_o	Total surface temperature effectiveness
α	heat transfer area/ volume
ψ	total dimensionless entropy generation $\dot{S}_{gen}/[Q/(T_w - T_i)]$
λ	dimensionless length
τ	dimensionless wall and fluid temperature different $[(T_w-T_i)/T_w]$

Subscripts

bf	base fluid
c	cross section
cond	condenser
cf	Cross flow
e	Equivalent

eff	Effective
eva	evaporator
f	Fluid/ basefluid/fin
fg	Flue gas
g	Gas
h	Hydraulic
i	Inner or inlet
l	longitudinal, liquid
m	Mean
max	Maximum
min	Minimun
n	Number of row
nf	Nanofluids
o	Outer, outlet, overall
p	Particle
red	Reduction
s	Shell, spacing
sav	Saving
t	Tube, transverse, total
w	Wall

List of Appendices

CHAPTER 1 INTRODUCTION

1.1 Introduction

Challenges such as climate change, increase of fuel price and fuel security have garnered significant attention from the international communities. There are growing concerns on these issues as industrial revolution increases the demand for energy substantially. Having said this, much attention has been focused towards introducing highly efficient devices and heat recovery systems for better utilization of energy. It is also reported that, 80% of the total energy consumption in the industry is originated from fossil fuel based energy (Abdelaziz et al., 2011). United States Energy Information Administration (2012) reported that 2.47×10^{15} Joule energy was consumed by the industrial sector in 2009 while Teke et al., (2010) revealed that about 26% of the industrial energy is wasted in the form of hot gas or fluid. Consequently, any small improvement in the efficiency of heat recovery systems can result in significant energy savings.

Heat recovery systems utilize heat exchangers to recover the waste heat. This provides benefits in terms of energy and cost saving as well as reducing green house gas emissions. Adding fins and increasing the heat transfer area are the common methods used to enhance the efficiency of the heat recovery systems. However, these approaches lead to a larger and bulkier heat exchanger. Furthermore, Kulkarni et al., (2008) have concluded that the usage of fins and micro channels have reached the optimum limit of its efficiency.

The efficiency of a thermal system correlates with the thermal conductivity of heat transfer fluids (Murshed et al. 2008a). Conventional heat transfer fluids such as water, ethylene glycol and engine oil are widely used in heat recovery systems. They are cheap but possess low thermal conductivity. For instance, the thermal conductivity of water and ethylene glycol are 0.613W/mK and 0.252W/mK, respectively (Incropera

et al., 2007). Choi (2009) revealed that the efforts to improve the performance and design of compact engineering equipment are hindered by the low thermal conductivity of conventional heat transfer fluids.

Therefore, there is an urgent need to develop a new generation of heat transfer fluid with higher thermal conductivity. The development in nanotechnology has enabled the suspension of nano-sized particles into a base fluid which results in a product known as nanofluid. The pioneering works of nanofluids were started by Argonne laboratory in the early 90's. Nanofluid is a suspension of nanoparticles (Al_2O_3 , TiO_2 , Cu, CuO, etc) in conventional base fluids (water, ethylene glycol, engine oil, etc). Keblinski (2009) stated that the typical size of nanoparticles used in nanofluids ranges from 1 – 100nm. The base fluid thermal conductivity are substantially improved through the addition of nano-sized particles (Eastman et al., 2001; Beck et al., 2008; Evans et al., 2008; Han, 2008; Murshed et al., 2008b; Nasiri et al., 2012; Paul et al., 2012). It is also known that the thermal conductivity of the fluid is proportional to convective heat transfer. Extensive studies found that convective heat transfer augmentation does correlate with nanoparticles volume fractions (Daungthongsuk and Wongwises, 2007; He et al., 2007; Kim et al., 2009). With these characteristics, nanofluids have the potential to replace conventional heat transfer fluids in various heat exchanger applications.

Besides thermal conductivity, viscosity of nanofluids also plays an important role in determining its performance. It is known that fluid's viscosity determines the pumping power of the system. Mahbubul et al., (2012) conducted a comprehensive review on the nanofluids viscosity characteristics. The effects of particle loading, size and shape, temperature on the nanofluids viscosity are discussed thoroughly in this review. Most of the researchers indicate that nanofluids viscosity increases with particle concentration (Duan et al., 2011; Yang et al., 2012; Fedele et al., 2012; Bobbo et al., 2012).

However, other thermo-physical properties such as density and specific heat have received limited attention. Vajjha et al., (2009) investigated three types of ethylene glycol/water-based nanofluids: aluminium dioxide, antimony-tin oxide and zinc oxide nanofluids. As expected, density of these nanofluids is higher than base fluid. It is also found that the density slightly decreases with the increase of temperature. There are also few experimental studies which focused on the specific heat of nanofluids. For instance, Zhou and Ni (2008) studied water based aluminium oxide nanofluids. Findings implied that the specific heat of water decreases when the aluminium oxides nanoparticles volume fraction increases from 0 to 21.7%. Similar conclusion is derived by Zhou et al., (2010) who investigated the specific heat of copper oxide/ethylene glycol nanofluids. Another researcher, Jung et al., (2010) investigated three types of water-based nanofluids: silicon dioxide, titanium dioxide and aluminium oxide nanofluids. They concluded that the specific heat of nanofluids decreases as the nanoparticles mass loading increases from 0.5% to 20%. In addition, it is observed that nanoparticle size has limited or minor effect on the nanofluids' specific heat.

Because of its improved thermo-physical properties and its myriad of applications, nanofluid has received substantial attention among researchers. The applications include engine cooling system (Leong et al., 2010; Peyghambarzadeh et al., 2011a; Peyghambarzadeh, 2011b, Charyulu et al.,1999), electronic cooling (Roberts and Walker, 2010; Ijam and Saidur, 2012; Tsai and Chein, 2007), air conditioning (Park and Jung, 2007), water heater (Kulkarni et al.,2009), solar collector (Yousefi et al., 2012; Otanicar et al., 2010) and etc. Most of the studies indicated that the thermal systems operated with nanofluids showed enhanced efficiency. This again shows that nanofluids have the potential to emerge as a new generation of heat transfer fluid.

1.2 Background of problem

Hot gases are common by-products in the industrial sector especially through operation of boilers or heating plants. During this operation fuel combustion releases its chemical energy to produce combustion products with high temperature. Saidur et al., (2010) reported that the main source of heat loss (10–30%) in a boiler is through the flue gasses. Figure 1.1 describes the typical energy balance of a boiler. It can be seen that 10 to 30% of the energy content releases through flue gasses in operation of the boiler.

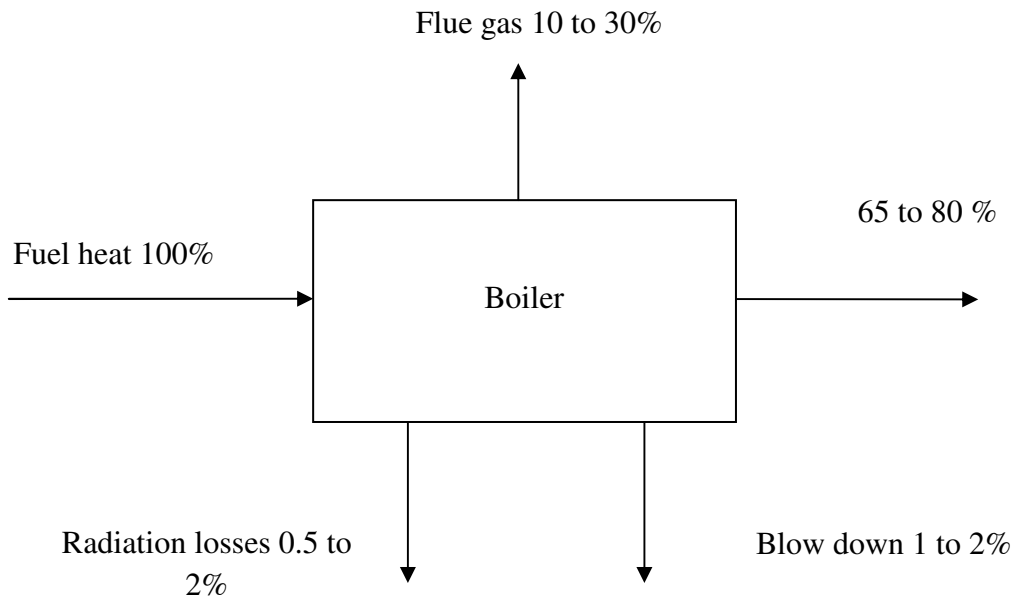

Figure 1.1 Typical energy balance of a boiler (Jayamaha, 2008)

The remaining waste heat in the flue gasses can be recovered by using heat recovery exchanger. Shell and tube heat exchanger and heat pipe or thermosyphon air-preheater are commonly used for this purpose. For instance, Pandiyarajan et al., (2011) utilized shell and tube exchanger to recover waste heat from the engine diesel exhaust. Saneipoor et al., (2011) studied the same type of heat exchanger used in a cement plant. Shi et al., (2011) used fin and tube heat exchanger to recover sensible and latent heat from the heat recovery steam generator. Thermosyphon or heat pipe heat exchanger has

also been used in various heat recovery applications (Yang et al., 2003; Noie and Majideian, 2000; Srimuang and Amatachaya, 2012).

The optimization of energy use in industry through heat recovery exchanger can reduce the emission of green house gasses such as CO_2 and lead to social and economy benefits (Stijepovic and Linke, 2013; Xu et al., 2013). Therefore, this study investigates the thermal and energy performance of heat recovery exchanger operated with nanofluids. Nanofluids are selected due to its enhanced thermal conductivity compared to that of base fluid. Application of this novel fluid will lead to thermal performance improvement of the heat recovery exchanger.

The experimental study on thermal conductivity, viscosity and density of nanofluids are included in the present study. It tried to evaluate nanofluid's thermo-physical characteristics as a heat transfer fluid. The selected heat recovery devices are shell and tube heat exchanger and thermosyphon air preheater. It focuses on recovering waste heat from hot flue gas produced by a heating plant. The recovered waste heat can be used to pre-heat air for combustion process, building heating, and etc. Estimation on size reduction of the shell and tube heat exchanger without altering its thermal performance is also included. Furthermore, the energy required to heat the air for combustion process have been estimated.

The advantages of using nanofluids compared to base fluid cannot be merely judged by their thermal performance as viscosity should also be taken into consideration. It is known that viscosity of the base fluid increases with the increase of particle volume fractions; consequently, it will affect the friction loss characteristic. There must be an optimum trade-off between both parameters to justify performance of nanofluid as a new generation of heat transfer fluid. Entropy generation analysis included in the present study is a powerful approach to study on this aspect. From here, both heat transfer enhancement and friction loss are evaluated.

Overall, this study aims to answer the following questions

(a) What is the effect of adding nanoparticle on the thermo-physical properties of base fluid?

(b) What is the thermal and energy performance of shell and tube heat recovery exchanger and thermosyphon air-preheater operated with nanofluid used to recover waste heat from flue gas/hot gas?

(c) What is the performance of nanofluids flowing in a circular tube under constant wall temperature in terms of entropy generation?

To the best of author's knowledge, there has not been any study which focuses on using nanofluids for heat recovery application. Most studies focused on the fundamental properties of the nanofluids such as thermal conductivity, viscosity and convective heat transfer performance. On the entropy analysis aspect, author found that up to now, none of the study focuses on the nanofluids flow through a circular tube under constant wall temperature. Literatures revealed that most of the studies emphasize on the constant heat flux condition. It is hope that the present study not only fills the gap in this area but also provide alternative approach to optimize the energy consumption in the industry.

1.3 Overview of the study

Schematic diagram as shown in Figure 1.2 depicts the overvall study on thermal and energy performance of heat recovery exchanger operated with nanofluids. The first section covers the investigation of thermo-physical properties of nanofluids which includes thermal conductivity, viscosity and density. Thermo-physcical properties are obtained from literatures, mathematical correlations and present experimental data. This is because of the pure metallic (such as copper) based nanofluids are not suitable to be produced via two-step method due to particles' oxidation process. Particles' oxidation

will affect its thermal conductivity characteristics. Therefore, data from literatures and mathematical correlations are required. In the latter section, nanofluids were used as heat transfer fluids in the heat exchanger. Kern and effective-NTU methods are combined to conduct the analysis of shell and tube heat exchanger. These approaches are rarely used in analysis of nanofluids operated heat exchanger. For the thermosyphon heat exchanger, effective-NTU approach is used to investigate its thermal and energy performance. The function of heat exchangers is to recover heat from flue gas/ hot gas released. Entropy generation analysis to investigate the efficiency of nanofluids as heat transfer fluid was also conducted in the present study.

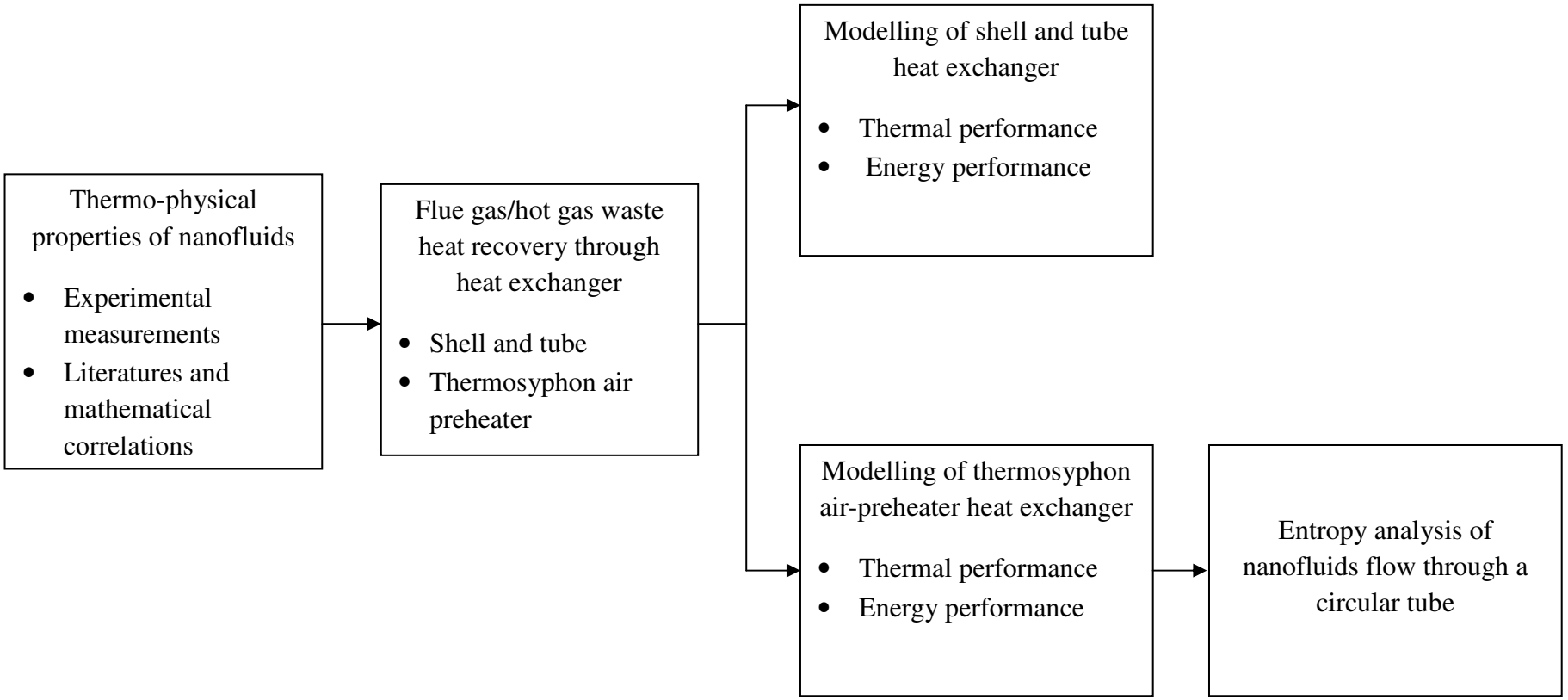

Figure 1.2 Overview of the study

1.4 Objectives of the study

There are considerable nanofluid related researches found in the existing literatures. It is noted that most of the works focused on the thermal conductivity, viscosity and convective heat transfer characteristic of nanofluids. These studies found that nanofluids have the potential to replace conventional heat transfer fluids in the thermal systems. However, there is limited study focusing on recovering waste heat from the flue gas or hot gas using nanofluids. The recovered heat can be used for many other applications which eventually leads to energy saving and reduction of green house gas emission. Keeping this in mind, the objectives of present study are as follows:-

(a) To investigate the effect of aluminium oxide and titanium dioxide based nanoparticles on thermo-physical properties (thermal conductivity, viscosity and density) of water and ethylene glycol/water mixtures-based fluids

(b) To extend a mathematical model for the heat transfer and energy performance of shell and tube heat recovery exchanger operated with ethylene glycol and water-based copper nanofluid and ethylene glycol/water mixtures based aluminium oxide and titanium dioxide nanofluids

(c) To analyse the entropy generation of water-based aluminium oxide and titanium dioxide nanofluids flow using circular tube with constant wall temperature

(d) To evaluate the performance of air-preheater operated with water-based aluminium oxide and titanium dioxide nanofluids as a working fluid.

1.5 Scope of the study

The scope of the present study is as follows:

(a) Water and ethylene glycol/water mixture were used as base fluid in the experimental works.

(b) Thermal conductivity, viscosity and density were the thermo-physical properties measured in the present study. Aluminium oxide, Al_2O_3 (particle size: 13nm and less than 50nm) and titanium dioxide, TiO_2 (particle size: 21nm) were the nanoparticle used in the experiment.

(c) Two types of heat recovery exchanger were used to recover the waste heat from flue gas/hot gas. They are shell and tube and thermosyphon air-preheater heat exchanger.

(d) Analysis of the nanofluids application in shell and tube and thermosyphon air-preheater heat exchangers was done using mathematical modelling. Experiments are not conducted since there is no experimental facility in University of Malaya. Moreover, it is very expensive to establish a flue gas heat recovery system. Ethylene glycol and water-based copper nanofluid and ethylene glycol/water mixtures-based aluminium oxide and titanium dioxide were used in the shell and tube heat exchanger modelling while, water-based titanium dioxide and aluminium oxide nanofluids were considered in the thermosyphon air-preheater and entropy generation modelling.

(e) In the mathematical modelling, nanofluids properties are assumed to remain constant or invariant when applied to the heat recovery exchangers. It is presumed that the nanoparticles in the base fluid are well dispersed and the nanofluids exhibit optimum thermal properties.

1.6 Outline of the thesis

This thesis is divided into 5 chapters. Each of the chapters is briefly explained as follows:

Chapter 1: Background of problem, overview, problem statement, purpose (objective) and scope of the study are presented and discussed thoroughly in this chapter.

Chapter 2: This chapter covers in-depth literature on the nanofluids as heat transfer fluid, its thermo-physical characteristics, convective heat transfer, entropy generation and application of nanofluids in heat pipe and shell and tube heat exchanger. Potential of energy saving using nanofluids is also discussed in this chapter.

Chapter 3: This chapter explains in detail the method used in the present study. It includes the synthesis of nanofluids, nanofluids thermo-physical properties measurement, modelling of thermal and energy performance of shell and tube heat exchanger, size prediction of heat exchanger, entropy generation of nanofluids flow and thermal performance of thermosyphon air pre-heater heat exchanger.

Chapter 4: The result and discussion of the project are included in this chapter. They are presented in graphical form (graphs) which includes thermo-physical properties of nanofluids, thermal and energy performance of heat recovery exchangers, and entropy analysis of nanofluids flow. The results are critically analysed and discussed which covers the theory and physical mechanism contributing to the results.

Chapter 5: This is the last chapter of the thesis where the conclusion deduced from this project is presented. Apart from that, author also suggests few recommendations for future research work.

CHAPTER 2 LITERATURE REVIEW

2.1 Introduction

This section reviews the preparation method of nanofluids, its thermo-physical properties such as thermal conductivity, viscosity, density and specific heat. The nanofluids convective heat transfer performances, entropy generation as well as the application of nanofluids in heat pipe and shell and tube heat exchanger are discussed in the later sections. In the last section, the potential of energy saving through nanofluids researches are presented.

2.2 Heat transfer with nanofluids

The addition of small particles into base fluid to improve base fluid's thermal conductivity has been in use since the establishment of Maxwell treatise. However, this effort is focused on the mili-micrometer sized particles. Murshed et al., (2008a) and Sarit et al., (2008) revealed that the limitations of this method include the rapid settling of particles, wear out of the heat transfer device's surface and increase of pressure drop and pumping power.

The concept of suspending nanoparticles in the base fluid (known as nanofluids) was first presented in 1995 (Choi, 2009). The author revealed that nanofluids offer improved thermal properties and are able to overcome the limitations posed by suspension with mili- or micro-sized particles. Comparison between suspension with nanoparticles and micro-sized particles is shown in Table 2.1. From Table 2.1, it is found that nanoparticles offer greater advantages compared to the micro particles.

Table 2.1 Comparison between micro and nanoparticles (Sarit et al., 2008)

	Micro particles	Nanoparticles
Stability	Settle	Stable
Surface/volume ratio	1	1000 times higher than microparticles
Conductivity (same volume fraction)	Low	High
Clog in micro channel	Yes	No
Erosion	Yes	No
Pumping power	Large	Small
Nanoscale phenomena	No	Yes

2.3 Preparation of nanofluids

Rapid development in nanotechnology has made it possible to produce materials in nano dimension (nanoparticles). Nanoparticles are usually available in the form of powder and have higher thermal conductivity than fluid. Being in nano scale, nanoparticles exhibit unique and enhanced physical and chemical characteristics compared to that of bulk materials (Murshed et al., 2008a; Yu et al., 2007). Nanofluid is not just a simple mixture of nanoparticles and base fluids. The nanofluid must be a stable and durable suspension, with no chemical reaction and minimum particles agglomeration (Wang and Mujumdar, 2007). A stable nanoparticle suspension is necessary to produce nanofluids with an optimum or enhanced thermal properties (Keblinski et al., 2005; Ghadimi et al., 2011).

Nanofluids can be produced through a two-step or single-step method. In two-step method, nanoparticle dry powders are produced either by physical or chemical synthesis. Then, it will be dispersed into the base fluid using ultrasonic disruptor (Murshed et al., 2005; Hwang et al., 2006; Duangthongsuk and Wongwises, 2009) or high pressure homogenizer (Hwang et al., 2008). The limitations and disadvantages of this method are sedimentation, clustering and aggregation of nanoparticles with respect to length of time. Nanoparticles are prone to agglomeration due to the attractive force between them known as van der Waals attractive force. Typical transmission electron

microscopy (TEM) images of nanoparticles in water base fluid are shown in Figure 2.1. From Figure 2.1, it is observed that there is slight particle agglomeration existent in the base fluid suspension.

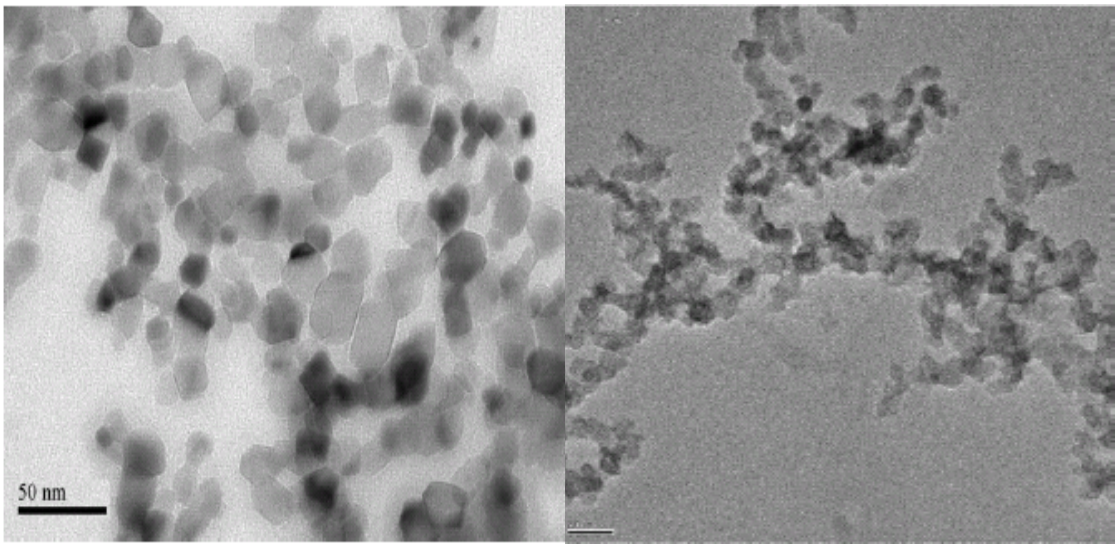

(a)TiO_2/water (b) Carbon black/water

Figure 2.1 (a) Typical Transmission electron microscopy (TEM) image of titanium dioxide/water nanofluids (Duangthongsuk and Wongwises, 2009) (b) carbon black/ water nanofluids (Hwang et al., 2008)

A stabilizer agent which is able to provide repulsive force is needed to overcome the attractive force. Apart from that, two-step method is preferable for oxide type nanoparticles compared to that of metallic type (Mahbubul et al., 2012; Ghadimi et al., 2011; Wang and Mujumdar, 2007). Sarit et al., (2008) emphasized that two-step method is not an effective approach for metal nanoparticles such as copper. Figure 2.2 shows the typical nanofluids subjected to ultrasonication process.

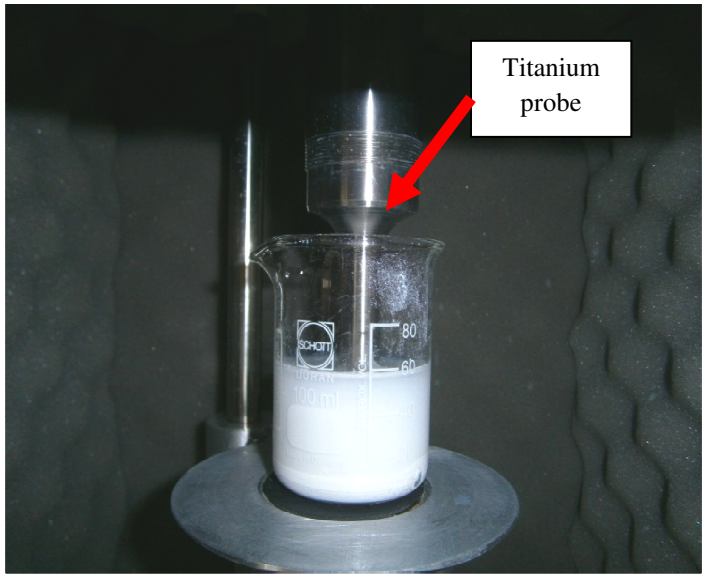

Figure 2.2 Ultrasonication process of nanofluids

Single-step method is a technique where fabrication of nanoparticles and nanofluids synthesis is done in a same single process. In this method, direct evaporation technique condenses the nanoparticles vapour directly to the lower vapour pressure base fluid in a vacuum chamber. Argonne laboratory used this method in preparing ethylene glycol based copper nanofluids (Eastman et al., 2001). Advantages of this method is the capability of reducing the nanoparticle agglomeration (Murshed et al., 2008a), and prevention of nanoparticles oxidation (Yu et al., 2007). However, two-step method is preferred due to its low cost nature, therefore it is potential for bulk production. Table 2.2 summarizes synthesis methods used in nanofluid research. This can be concluded that two-step method is widely used in nanofluid research.

Table 2.2 Synthesis method in nanofluids formulation

Base fluid	Nanoparticles	Synthesis method	References
Water	Alumina(15-50nm)	Two-steps	Zhu et al., (2009)
Ethylene glycol	titanate nanotube (10nm,Length =~100nm)	Two-steps	Chen et al., (2009)
Water	Alumina(<30 ± 5 nm)	Two-steps	Do et al., (2010)
60%Ethylene glycol,40% Water	Alumina,silicon dioxide, Copper(I)oxide	Two-steps	Vajjha et al., (2010)
Ethylene glycol	Copper	Two-steps	Yu et al., (2010)
Ethylene glycol	Diamond	Two-steps	Yu et al., (2011)
De-ionized water	Alumina (10-30nm)	Two-steps	Lin et al., (2011)
Water	Silver	Single step	Paul et al., (2012)
De-ionized water	Alumina (43nm); copper oxide (30nm)	Two-steps	Suresh et al., (2012)
De-ionized water	Alumina, titanium dioxide, zinc oxide	Two-steps	Putra et al., (2012)
Ethylene glycol	Copper	Single step	De Roberties et al., (2012)

2.4 Thermal conductivity of nanofluids

Nanofluids' thermal conductivity represents the ability of the heat to flow. It is the most important characteristic used to justify the suitability of nanofluids as a heat transfer fluid. Substantial studies have been conducted to investigate the factors affecting the thermal conductivity of nanofluids. Summary of nanofluids thermal conductivity related studies is depicted in Table 2.3.

Table 2.3 Nanofluids thermal conductivity related studies

Reference	Base fluid	Particle	Study related to				
			Temp	Shape / size	Vol.% /Wt.%	Surfactant / pH	Particle
Eastman et al., (2011)	Ethylene glycol	Cu			√	√	
Murshed et al., (2005)	Deionized water	TiO_2		√	√		
Liu et al., (2006)	Water	Cu		√	√		
Yoo et al., (2007)	Water, ethylene glycol	TiO_2,Al_2O_3, Fe,WO_3		√	√		√
Zhang et al., (2007)	Toluene,water	Au,Al_2O_3, TiO_2,CuO, CNT	√	√	√		√
Beck et al., (2007)	Ethylene glycol	Al_2O_3	√		√		
Lee et al., (2008)	Deionized water	Al_2O_3			√		
Li et al., (2008)	Water	Cu			√	√	
Duangthongsuk and Wongwises, (2009)	Water	TiO_2	√		√		
Mintsa et al., (2009)	Distilled Water	CuO,TiO_2	√	√	√		√
Zhu et al., (2009)	Water	Al_2O_3			√	√	
Yu et al., (2009)	Ethylene glycol	ZnO	√		√		
Chandrasekar et al., (2010)	Water	Al_2O_3			√		
Yu et al., (2010)	Ethylene glycol	Cu	√		√	√	
Teng et al., (2010)	Water	Al_2O_3	√	√	√		
Lee et al., (2011)	Deionized water	SiO			√	√	
Lin et al., (2011)	De-ionized water	Al_2O_3	√			√	

2.4.1 Experimental study of nanofluids' thermal conductivity

There are several factors that affect the thermal conductivity of nanofluids. The factors are particle volume fraction, particle size and shape, temperature, surfactant and pH. The following sub-sections will describe all these factors in detail.

2.4.1.1 Effect of particle volume fractions

The distinguished research of Eastman et al.,(2001) which draws great interest and attention of thermal scientists and engineers reported that thermal conductivity of ethylene glycol based copper (<10nm) nanofluids with 0.3 vol.% was enhanced up to 40% compared to that of base fluid. Study found that the metallic-based nanofluids provide higher thermal conductivity than oxide type of nanofluids. This is attributed to higher intrinsic thermal conductivity of Cu nanoparticle compared to that of Al_2O_3 and CuO. Another reason is that the Cu particle used in this study was four times smaller than oxide particle. Same type of nanofluids was investigated by Yu et al., (2010). In contrast to the Eastman's result, only 11% enhancement was obtained for the same particle loading. This discrepancy may be due to different synthesis methods of nanofluid preparation and type of dispersant used in both studies. In another research, Liu et al. (2006) found that water containing only 0.1 vol % of Cu nanoparticles exhibited 23.8% improvement in thermal conductivity. The nanofluids in their study were produced through one step chemical reduction method.

Up to now, most of the studies implied that the thermal conductivity increases with respect to particles volume fractions. Some researchers indicated that a linear thermal conductivity with respect to particle's loading relationship was discovered. However, there are researchers that observed a non-linear thermal conductivity trend. Chandrasekar et al., (2010) studied thermal conductivity of water based Al_2O_3 nanofluids and concluded linear dependency on the particle volume fractions. For the lower range of Al_2O_3 volume fractions (0.01 to 0.3 vol.%), Lee et al., (2008) showed that thermal conductivity increased linearly with particle volume fractions. However, in another studies, non-linear relationship was observed for nanofluids thermal conductivity with low concentration. Murshed et al., (2005) found that, thermal conductivity of TiO_2 nanofluid showed non-linear relationship for volume fractions less

than 2%. This could be due to the addition of cetyltrimethylammonium bromide (CTAB) surfactant into the base fluid in their study. Non linear relationship was also discovered for nanofluids containing up to 5 vol. % of ZnO particle (Yu et al.,2009). The slope of the thermal conductivity enhancement with respect to particle volume fraction was higher at lower volume fractions (about 0.2 to 0.7 vol. %) compared to the slope at higher volume fractions (1 to 5vol.%). Authors explained that this was due to the larger increase of nanofluids viscosity compared to thermal conductivity enhancement.

Two types of nanofluids that are commonly used in researches are Al_2O_3 and TiO_2 nanofluids. Murshed et al., (2005) experimentally showed that thermal conductivity of water based TiO_2 nanofluids correlates with particle volume fractions. With only 5 vol.%, of TiO_2 nanoparticles, 29.7% and 32.8% thermal conductivity enhancement were observed for nanofluids with TiO_2 of Ø15nm and Ø10nm × 40nm, respectively. Comparison between water based Al_2O_3 and TiO_2 nanofluids were carried out by Yoo et al., (2007). Study revealed that by adding 1% nanoparticle volume fraction, thermal conductivity enhancement of Al_2O_3 (4% enhancement) was lower than TiO_2 (14.4% enhancement) although it is known that Al_2O_3 has higher bulk thermal conductivity than TiO_2. This shows that particle's thermal conductivity is not the major factor to improve nanofluids thermal conductivity. The same study also found that ceramic type nanofluids have lower thermal conductivity than metallic type nanofluids under the same concentration. Beck et al., (2007) demonstrated the dependence of Al_2O_3 nanofluids thermal conductivity on particle volume fractions. Duangthongsuk and Wongwises (2009) performed research on TiO_2/ water nanofluids with respect to volume fraction up to 2%.

Another study done by Mintsa et al., (2009) covered a larger range of nanoparticle volume fraction (up to 18%). Similar to the previous studies, these authors

experimentally pointed out that the nanofluids (Al_2O_3, CuO) thermal conductivity was relatively higher than base fluid. The drawback of the addition of higher particle volume fractions is the stability issue. Wu et al., (2009) revealed nanoparticles tend to agglomerate at higher volume component. There are also studies focused on nanofluids containing carbon nanotube. Hwang et al., (2006) highlighted that 11.3% enhancement was achieved with addition of 1% of MWCNT into water. It has the highest thermal conductivity improvement compared to that of CuO/water, SiO_2/water and CuO/EG nanofluids. Thermal conductivity of water containing 3wt.% MWCNT enhanced about 13% which is higher than predicted value from Maxwell correlation (Lee et al., 2011).

2.4.1.2 Effect of particle size and shape

Most of the researchers found that thermal conductivity of nanofluids with smaller nanoparticle sizes tend to produce higher values compared to larger particles. Chon and Kihm (2005) investigated the thermal conductivity of three different sizes of Al_2O_3 nanofluids. Thermal conductivity of nanofluids with 11nm Al_2O_3 particles was the highest compared to 47 and 150 nm alumina nanofluids. Smaller nanoparticle increases the surface area and number of particles interactions. Sarit et al., (2008) added that the heat transfer process happens on the surface of the particles thus higher thermal conductivity of nanofluids is observed.

Another researcher, Yoo et al., (2007) revealed that particle size is the main factor in affecting thermal conductivity compared to particle thermal conductivity. Smaller particle sizes provide larger surface to volume ratios which facilitates nanofluids heat transfer process. In their study, it was identified that nanofluids with smaller TiO_2 exhibited higher thermal conductivity than the bigger Al_2O_3 nanoparticles. Vajjha and Das (2009) noted that effective thermal conductivity for ethylene glycol/water mixture based ZnO (29nm) was 3% higher than nanofluids with ZnO

(77nm) for 2% volume fraction concentration. However, Mintsa et al., (2009) reported that particle sizes of nanofluid have substantial effect on thermal conductivity only at high operating temperatures. At ambient temperature, particle size has limited influence on thermal conductivity. Murshed at al., (2005) found that thermal conductivity of nanofluids with cylindrical particles is higher than spherical shape particle.

2.4.1.3 Effect of temperature

Beck et al., (2007) measured the thermal conductivity of ethylene glycol based Al_2O_3 nanofluids at 298K to 411K. It was argued that, the thermal conductivity characteristics of nanofluids at higher temperatures are almost similar to the base fluid. This concludes that effect of Brownian motion only plays a minor role in nanofluids thermal conductivity enhancement.

In contrast to the previous research, Murshed at al., (2008b) highlighted the importance of Brownian motion of nanoparticles on nanofluids thermal conductivity. Higher operating temperature will intensify the effect of Brownian motion of nanoparticles which eventually contributes to formation of micro convection in the base fluid. Subsequently, thermal conductivity enhancement is observed. The selected nanofluids used in their study were Al_2O_3 nanoparticles with three different types of base fluids (ethylene glycol, water and engine oil).

Duangthongsuk and Wongwises (2009) tested TiO_2/ water-based nanofluids thermal conductivity at three different temperatures, 15^{o}C, 25^{o}C, 35^{o}C. It is conclusively found that thermal conductivity is a function of temperature. Yu et al., (2009) reiterated that thermal conductivity of ethylene glycol based ZnO nanofluids increases with temperature. The enhancement ratio is almost constant when the temperature increases. Similar conclusion is deduced by Lin et al., (2011) who investigated the water based Al_2O_3 nanofluids. However, Colangelo et al., (2011)

revealed that temperature has no effect on the diathermic oil nanofluids thermal conductivity.

2.4.1.4 Effect of surfactant and pH

Addition of surfactant is a common method to minimize the particles sedimentation and agglomeration. These are the two phenomena which determine the nanofluids' stability. The particles downward movement due to the nature of gravitational force is defined as sedimentation while agglomeration is referred to as the formation of cluster of particles (Bhattacharya, 2005). Surfactant is a long organic molecule which can be classified into few types: anionic (SDBS and SDS), cationic surfactant (CTAB) and non-ionic surfactant(PVP).According to Ghadimi et al., (2011), surfactant is capable of modifying the particles surface from hydrophobic to hydrophilic surface and vice versa. The surfactant molecules will attach to nanoparticle and create repulsive force. This force prevents the nanoparticles from getting closer to each another.

Li et al., (2008) studied the thermal conductivity of Cu/H_2O nanofluids under various loadings of SDBS surfactant. Authors reiterated that addition of surfactant increases the nanofluids thermal conductivity. However, thermal conductivity decreased when the loading exceeded the optimum concentration. Minzheng et al., (2012) investigated the influence of SDBS, PVP, SDS and CTAB on thermal conductivity of nanofluids. Similar to the previous study, it indicated that there is an optimum level of concentration for every type of surfactant. Other researchers who used surfactant in their experiments are Murshed et al., (2008a) (CTAB); Wang et al., (2009) (SDBS),Hwang et al., (2006) (SDS), Chen and Xie (2010) (Gemini)

The pH value is associated with the electrostatic charge around the nanoparticles. Zeta potential is a parameter usually used to quantify this surface charge.

To get a stable suspension, pH must be kept far from the iso-electric point (IEP). Iso-electric point refers to zero zeta potential. At this stage, the repulsive force is minimized; hence, there is a higher tendency for particles to agglomerate. If the pH deviates from IEP, the electric double layer (EDL) is strong enough to resist the particles from getting closer to each another (Lee et al., 2011). The authors successfully identified pH 6 as the IEP value for SiC/water nanofluids. Li et al., (2008b) showed that the thermal conductivity of Cu/water nanofluids is higher at pH 8.5-9.5. The authors explained that, the surface charge around the nanoparticles is the highest at this condition. Zhu et al., (2009) observed that Al_2O_3/water nanofluids have higher zeta potential value at 8-9 pH. This contributes to uniform distribution of nanoparticles in the suspension and leads to higher thermal conductivity.

2.4.2 Theoretical model of nanofluids' thermal conductivity

The models used to predict the nanofluids thermal conductivity are classified into two (2) categories. They are static and dynamic models. Typical static models are Maxwell and Hamilton Crosser models as depicted in Equations (2.1) and (2.2), respectively.

$$\frac{k_{eff}}{k_f} = \frac{k_p + 2k_f + 2\emptyset(k_p - k_f)}{k_p + 2k_f - \emptyset(k_p - k_f)} \tag{2.1}$$

$$\frac{k_{eff}}{k_f} = \frac{k_p + (n-1)k_f - (n-1)\emptyset - (k_f - k_p)}{k_p + (n-1)k_f + \emptyset(k_f - k_p)} \tag{2.2}$$

where k = thermal conductivity; *eff* = effective, p = particle; $\emptyset$ = particle volume fraction and n = shape factor

Maxwell model is based on the concept of conduction heat transfer through a stagnant suspension of the spherical particles (Khanafer and Vafai, 2011). Both models are function of particle volume fractions and thermal conductivity of particle and base

fluid. However, Maxwell model is only valid for spherical particle. Hamilton Crosser model is applicable for both spherical and cylindrical particles due to the introduction of shape factor, *n* in this model.

Several researchers have further improved these classical models by incorporating the effect of interfacial layer (Yu and Choi, 2003; Yu and Choi, 2004; Leong et al., 2006). It is presumed that each particle is surrounded by an ordered layer. Inclusion of ordered layer increases the volume fraction of nanoparticles. Yu and Choi (2004) improved the Hamilton-Crosser model to accommodate the non-spherical nanoparticles. In this model, the interface is described as a confocal ellipsoid with a solid particle.

Thermal conductivity model which incorporates particles Brownian motion is started by Jang and Choi (2004). Authors proposed that Brownian motion is an important factor for heat transport of nanoparticles suspended in a base fluid. This contradicts with the classical approach which assumes the discrete particles are stagnant and motionless. The proposed model is developed based on several mechanisms such as collision between base fluid molecules, thermal diffusion of nanoparticles, collision between nanoparticles due to Brownian motion and thermal interaction of dynamic nanoparticles with base fluid molecule.

Another well known model based on Brownian motion is developed by Prasher et al., (2006). The proposed model considers the effect of interfacial thermal resistance between the nanoparticles and liquid. Authors proposed that the thermal conductivity enhancement of nanofluids is due to localized convection caused by nanoparticles' Brownian motion. The proposed model is a combination of Maxwell-Garnett (MG) conduction and convection models.

Although numerous models have been developed, at present there are no model available to predict the nanofluids thermal conductivity accurately (Khanafer and Vafai,

2011). Thus, Corcione (2011) and Khanafer and Vafai (2011) developed empirical models based on the experimental data available in the literatures. For instance, the model constructed by Khanafer and Vafai is valid and suitable for water based Al_2O_3 and CuO -based nanofluids.

2.5 Viscosity of nanofluids

Viscosity of nanofluids is influenced by several factors. The main factors are particle volume fraction and operating temperature and rheology behaviour of nanofluid which are discussed in sub-section 2.5.1. Sub-section 2.5.2 discusses the theoretical model of nanofluids viscosity.

2.5.1 Experimental study of nanofluids' viscosity

Earlier works on nanofluid were mainly focused on its thermal conductivity and convective heat transfer performance. However, nanofluids viscosity characteristics also deserve the same attention. Addition of nanoparticles increases nanofluids viscosity. Viscosity represents the resistance of fluid to flow and it is associated with the amount of pressure drop. There are two important issues concerning nanofluids viscosity characteristics. Firstly, common factors such as particle volume fractions and size, surfactant and operating temperature affecting the nanofluids viscosity. The second issue is whether nanofluids are classified as Newtonian or non-Newtonian fluid. The Newtonian fluids have a constant viscosity with respect to different values of shear rate. The shear stress of a Newtonian fluid is proportional with shear rate.

Most of the researchers found that nanofluids viscosity increases with augmentation of nanoparticle volume fractions (Nguyen et al., 2008; Duangthongsuk and Wongwises, 2009; Kole and Dey, 2010; Corcione, 2011; Mahbubul et al., 2012). Addition of nanoparticles creates higher internal force in the base fluid (Kole and Dey,

2010). Phuoc and Massoudi (2009) proposed that nanoparticles tend to form a structure in base fluid. The motion of the fluids were restricted which resulted in increase of viscosity. Murshed et al., (2008b) added, the increase of nanofluids viscosity could be attributed to nanoparticles clustering and surface adsorption. It is followed by the increase of particles hydrodynamic diameter that leads to augmentation of viscosity. Namburu et al., (2007) found that viscosity of water and ethylene glycol mixture based CuO nanofluids increases along with particle loading. Lee et al., (2008) revealed that non linear relation between Al_2O_3/water nanofluids viscosity increment and nanoparticle concentration ranged from 0.01-0.3vol.% Author pointed out that the non linear relation was resulted from longer sonication time (5 hours) which produced uniform dispersed nanoparticles. It augmented the particle-particle interaction and surface area of the well-dispersed nanoparticles. Consequently, hydrodynamic force which acted on the particles in the fluid was also affected.

Nanofluids viscosity depends on the fluid operating temperature. Interparticle forces tend to be weakened when temperature increases. The fluid can move freely when the particles motion is not restricted. Chen et al., (2007) measured the rheological behaviours of ethylene glycol based TiO_2 nanofluids up to 8wt.% for temperature range of 20^{o}C to 60^{o}C. Viscosity of low volume fraction Al_2O_3 (0.01 to 0.3 vol.%)/ water - based nanofluids was studied by Lee et al., (2008). In this study, the author considered temperature range of 21^{o}C to 39^{o}C. Duangthongsuk and Wongwises (2009) studied the TiO_2/water-based nanofluids at three different temperatures, 15^{o}C, 25^{o}C and 35^{o}C. All these studies concluded that nanofluids viscosity decreases with the increasing of fluid temperature. Kulkarni et al., (2009) extended the nanofluids viscosity to very low temperature to test the suitability of nanofluids in the cold climate countries. Varying the temperature from -35^{o}C to 50^{o}C in the study showed that the viscosity of nanofluids is higher at low temperatures.

There are considerable researches focused on the rheological behaviour of nanofluids. Newtonian and non-Newtonian fluids have completely different characteristics. Phuoc and Massoudi (2009) discovered that Fe_2O_3–deionized water nanofluids rheological behaviour depends on the particle volume fraction. Addition of 0.2% (by weight) PVP surfactant, these nanofluids still exhibit shear thinning non-Newtonian behaviour with 2% particle volume fraction. Similar trend was observed for the same nanofluids with addition of 0.2% (by weight) PEO. Yu et al., (2009) revealed that ZnO-ethylene glycol nanofluids demonstrate shear thinning non-Newtonian behaviours when particle volume fraction exceeds 3%. Chen et al., (2008) found that shear thinning behaviour is more obvious for higher weighted percentages of titanate nanotubes/ water nanofluids. Kulkarni et al., (2009) found that water/ethylene glycol mixture with 6.12% volume fraction of CuO shows Newtonian behaviour at -35^{o}C.

Chen et al., (2007) found that a nanofluid with higher base fluid viscosity (ethylene glycol) tends to have Newtonian characteristics. The authors measured the rheological behaviours of ethylene glycol based TiO_2 nanofluids up to 8% wt. for temperature range of 20^{o}C to 60^{o}C. However, Kole and Dey (2010) concluded that addition of small amount of Al_2O_3 nanoparticles into engine coolant base fluid transforms its behaviour from Newtonian to non-Newtonian. In the most recent study by Bobbo et al.,(2012) it was concluded that water based SWCNH and TiO_2 nanofluids exhibit Newtonian behaviour.

2.5.2 Theoretical model of nanofluids' viscosity

There are a few analytical models available to estimate the viscosity behaviour of nanofluids. It is interesting to find that most of the models are originated from Einstein's pioneering work. His model is based on the linearly viscous fluid containing dilute spherical particles ($\emptyset < 2\%$). The proposed formulation is shown in Equation (2.3)

$$\frac{\mu_{nf}}{\mu_f} = (1 + 2.5\emptyset) \quad (2.3)$$

The limitations of this formula are: it only considers non-interacting particle and negligible inertia force in the fluid. Since then, many researchers have introduced new models to overcome the mentioned limitations of Einstein's model. An extended Einstein's model for higher particle volume concentrations was developed by Brinkman (1952) as shown in Equation (2.4)

$$\mu_{nf} = \frac{1}{(1-\emptyset)^{2.5}}\mu_f \quad (2.4)$$

Another researcher, Batchelor (1977) focused on the hydrodynamic and Brownian effect of spherical particle as shown in Equation (2.5)

$$\frac{\mu_{nf}}{\mu_f} = (1 + 2.5\emptyset + 6.2\emptyset^2) \quad (2.5)$$

Lundgren (1972) developed a Taylor series formulation as shown in Equation (2.6)

$$\frac{\mu_{eff}}{\mu_f} = \frac{1}{(1-2.5\emptyset)} = (1 + 2.5\emptyset + 6.25\emptyset^2 + \ldots\ldots) \quad (2.6)$$

Nguyen et al. (2007) presented viscosity correlation for water based copper oxide (CuO) and alumina (Al_2O_3) nanofluid as shown in Equations. (2.7 – 2.9)

$$\frac{\mu_{nf}}{\mu_f} = (1.475 - 0.319\emptyset + 0.051\emptyset^2 + 0.009\emptyset^3) \text{ for CuO} \quad (2.7)$$

$$\frac{\mu_{nf}}{\mu_f} = (1 + 0.025\emptyset + 0.015\emptyset^2) \text{ for 36nm } (Al_2O_3) \quad (2.8)$$

$$\frac{\mu_{nf}}{\mu_f} = 0.904e^{0.1483\emptyset} \text{ for 47nm } (Al_2O_3) \quad (2.9)$$

2.6 Density and specific heat of nanofluids

To the best of the author's knowledge, most researchers used single formulation to determine the density of nanofluids. The density formulation is shown in Equation (2.10).

$$\rho_{nf} = (1-\emptyset)\rho_f + \emptyset\rho_p \quad (2.10)$$

Similar formulation has also been used by other researchers (Namburu et al., 2009 and Kulkarni et al., 2009). From the formulation, it seems that the density of nanofluid tends to increase with the increase of particle volume fraction.

The common formulation for specific heat used by researchers is shown in Equation (2.11). Specific heat tends to reduce with particle volume fraction.

$$c_{p,nf} = \frac{(1-\emptyset)\rho_f c_{p,f} + \emptyset\rho_p c_{p,p}}{\rho_{nf}} \qquad (2.11)$$

2.7 Convective heat transfer coefficient of nanofluids

Zenaili et al., (2007) studied convective heat transfer performance of water based Al_2O_3 nanofluid in a circular tube under constant wall temperature. Findings implied that there is an augmentation of nanofluid convective heat transfer coefficient with the increase of nanoparticle volume fraction. The authors concluded that heat transfer coefficient is much higher than the predicted value from single phase heat transfer correlation. Ding et al., (2007) observed that aqueous-based carbon nanofluid offers the highest enhancement of convective heat transfer compared to that of aqueous-based titanate and aqueous-based titania nanofluids. Bianco et al., (2009) employed single and two-phase models in the analysis of nanofluids' characteristics in a uniformly heated circular tube. The authors found that the heat transfer performance of the base fluid increases with the increase of particle volume fractions. However, this is accompanied by the higher wall shear stress. The selected heat transfer fluid applied in this study is water based Al_2O_3 nanofluids.

He et al., (2009) concluded that convective heat transfer coefficient has its maximum value at the entrance region. The authors added that this property is highly affected by nanofluid thermal conductivity. Other factors such as viscosity, Brownian, lift and thermophoretic forces have minor effect on convective heat transfer coefficient of nanofluids. Jung et al., (2009) studied the convective heat transfer of Al_2O_3 in

rectangular micro channels. It was observed that convective heat transfer coefficient of 1.8% Al_2O_3 nanofluid in laminar flow increases to about 32% compared to distilled water. Kim et al., (2009) investigated the effect of convective heat transfer coefficients derived from thermal conductivity. His study found that thermal conductivity enhancement has a key role in nanofluids convection. However, an amorphous carbonic nanofluid with similar thermal conductivity value as pure water did not show any convection improvement at the turbulent flow. Vajjha et al., (2010) studied convective heat transfer and pressure loss characteristics of nanofluids in turbulent flow.

Ebrahimnia-Bajestan et al., (2011) conducted the numerical investigation on the heat transfer and pressure drop performance of several types of nanofluids flowing in a circular tube subjected with constant heat flux. Analysis was done by using custom-made FORTRAN language. For simplication and ease of analysis, single phase thermo-physical properties models were used. Study revelead that, the heat transfer performance of nanofluids are more accurately predicted by using particle dynamic based thermal conductivity model compared to that of static based model. This shows that particle's Brownian motion play significant role in nanofluids' thermal performance.

Duangthongsuk and Wongwises (2012) used Einstein-Strokes's model to investigate the heat transfer coefficient of water based TiO_2 nanofluids. Authors stated that heat transfer coefficient of nanofluids increases with the increase of fluid's Reynolds number and particle volume fractions. In another hand, this performance decreases when the tube length is increasing. Huminic and Huminic (2013) applied three dimensional CFD analyses to evaluate the thermal performance of flattened tube operated with nanofluids. Ethylene glycol based CuO nanofluids were applied in this study. Similar with the previous studies, authors found that heat transfer performance improved with particle volume fractions.

2.8 Entropy generation

Optimum design of a thermal system is achieved when the entropy generation is minimized (Bejan, 1996; Sahin, 1998). Entropy generation and irreversibility are reduced when there is a heat transfer improvement; however, higher pressure drop due to fluid friction causes exergy loss in a thermal system (Moghaddami et al., 2011). Numerous studies have been conducted to investigate the entropy generation of a thermal system. Sahin (1998) analysed the entropy generation of several cross sectional duct geometries under a constant wall temperature. The author found that circular duct is favourable for high Reynolds numbers. Dagtekin et al., (2005) have applied this concept on the circular duct with different shapes of longitudinal fins (longitudinal thin, triangular and V-shape) using laminar flow. They revealed that the length, angle and number of fins affect the entropy generation of a circular duct under constant wall temperature. Ko (2006) obtained the optimal Reynolds number, using laminar flow in a double sine duct with various wall heat fluxes using the same approach. Ko and Wu (2009) conducted numerical study on entropy generation induced by turbulent forced convection in a curved rectangular duct exposed to heat flux. Yilmaz (2009) found that the temperature difference between fluid inlet and wall has an optimum value as it minimizes entropy generation of a circular duct with constant wall temperature. Overall, the above studies utilized conventional working fluids such as water and air.

Recently, there have been few studies which focused on the entropy generation of nanofluids flow. Singh et al.,(2010) conducted an entropy generation investigation on nanofluid (alumina/water) flow in circular tubes with three different diameters under constant wall heat flux. The study indicates that nanofluids are suitable to be used in conventional channels with laminar flow conditions, microchannels with turbulent flow conditions and minichannels for both laminar and turbulent regimes. Moghaddami et al., (2011) obtained optimum Reynolds number which minimized entropy generation

for water- alumina and ethylene glycol- alumina nanofluids using a circular tube under constant heat flux. On the contrary to other researchers who focused on circular tube, Bianco et al., (2011) conducted a study on entropy generation in a square tube. Recently, Leong et al., (2012) conducted an entropy analysis on three types of heat exchangers. They found that shell and tube with 50^{o} helical baffles experiences the lowest entropy generation compared to heat exchanger with segmental baffles and 25^{o} helical baffles. Ethylene glycol-based fluid containing up to 2% volume fraction of copper nanoparticles were used in this study. Shalchi-Tabrizi and Seyf (2012) investigated entropy generation of Al_2O_3 nanofluids in a tangential micro heat sink. It is found that the total entropy generation decreases when the particles volume fraction or Reynolds number increases and particle size decreases. The particle volume fractions and sizes considered in the study were 0.01-0.04 and 29and 47nm.

2.9 Nanofluids in heat pipe and shell and tube heat exchangers

Heat pipe is regarded as one of the most efficient heat recovery exchanger. It is capable of transmitting a large amount of heat, although it provides a smaller heat transfer area (Liu et al., 2006). Shafahi et al. (2010) revealed that thermal resistance of a cylindrical heat pipe decreases as the particle concentration increases or the particle size decreases. Do et al., (2010) found that thermal resistance in the evaporator-adiabatic section of the circular screen mesh wick heat pipes is reduced to about 40% for a heat pipe operated with distilled water based 3.0 vol.% alumina nanofluid. The mechanism attributed to this enhancement is due to the formation of a nanoparticles coating layer at the evaporator section. It widens the evaporation surface; improves the surface wettability and the capillary working performance. Mousa (2011) agreed that nanoparticles tend to form a porous layer at the evaporation section which eventually increases the surface wettability. Do and Jang (2010) found that the thermal

performance of a heat pipe operated with water based alumina (<1 vol. %) nanofluids increased up to 100% at an optimum condition. The nanoparticle depositions on the evaporator and condenser surface are the main reasons of thermal performance enhancement or deterioration for oscillating heat pipe (Qu and Wu, 2011).

Shell and tube heat is another common type of heat exchanger. There is limited study focusing on the application of nanofluids in shell and tube heat exchanger. Farajollahi et al.,(2010) performed an investigation on water-water shell and tube heat exchanger. Nanofluids used in their study were α-Al_2O_3/water and TiO_2/water nanofluids. Study found existence of optimum concentration for both types of nanofluids. At lower concentrations, TiO_2/water exhibited better heat transfer coefficient than the α-Al_2O_3/water nanofluids. On the other hand, α-Al_2O_3/water performed better at higher particle loading. Recently, Lotfi et al., (2012) found that overall heat transfer coefficient of the shell and tube heat exchanger operating with water based MWCNT nanofluids is higher than the base fluid. From here, it can be noted that Kern and effective-NTU methods are rarely used in the nanofluids operated shell and tube heat exchanger analysis. Most of the studies emphasize on the experimental aspect rather than mathematical modeling.

2.10 Energy saving using nanofluids

Over the past few years, energy costs have been increased significantly. This is getting even worse by the depletion of fossil energy resources. There are several researches which indicate that application of nanofluids can reduce the need for energy and pumping power. Kulkarni et al., (2009) revealed that for the same heat transfer coefficient, there is the possibility to decrease the size of heating coil by employing nanofluids as heat transfer fluid. Smaller heating coil requires lower coolant mass flow rate and pump power. For instance, ethylene glycol/water mixture with 6 vol %

aluminium oxide nanoparticle needs only 7.1W power compared to 11.5W for heating coil operates with base fluid. Strandberg et al., (2010) studied the performance of a hydronic finned tube heating units operated with nanofluids. The required pumping power for nanofluid was also reduced compared to base fluid in this application. The authors stated this is attributed to the lower nanofluids velocity that is required for the same heating output. Firouzfar et al., (2011) compared the application of methanol-silver nanofluids and pure methanol in a thermosyphon heat exchanger of an air conditioning system. For cooling of supply air stream, about 8.8 to 31.5% energy saving was achieved for nanofluids compared to pure methanol. As for reheating the supply air process, 18 to 100% was observed for nanofluids application.

Liu et al., (2011) experimentally investigated the performance of chillers operated with MWCNT/water nanofluids. It was seen that, the power consumption was slighty lower (about 0.8%) for chiller operated with nanofluids compared to water base fluid. Recently, Zarifi et al., (2013) conducted a thermal-hydraulic modelling of application of nanofluids in a VVER-1000 reactor core. Similar to the previous studies, the authors suggested that the cooling process for reactor core with nanofluids requires lower coolant flow rate.

It is obvious that there are many studies that indicated nanofluids contribute to energy saving. But there are arguements that substitution of nanofluids as heat transfer fluid may involves large investment. However, the recent market survey on the nanoparticles shows that the average cost of the 100g nanoparticles is less than RM1,000. Saidur et al., (2010) revealed the cost of nanofluids and the paybacks period of nanofluids application are reasonable. The authors added that only small amount of nanoparticles is needed to produce large quantities of nanofluids. Moreover the two-step method is suitable for bulk production of nanofluids. The market price of the

nanoparticles is depicted in Table 2.4. It is found that oxide type nanoparticle is cheaper than the pure metallic type.

Table 2.4 Market price of the nanoparticles (Sigma Aldrich, 2013; US Research Nanomaterials, 2013)

Num	Particle	Company	Particle size (nm)	Purity (%)	RM/gram
1	Al_2O_3	Sigma Aldrich	13	99.8	725.01
2	γ -Al_2O_3	Sigma Aldrich	<50		740.02
3	TiO_2	Sigma Aldrich	21	≥99.5	650.02
4	Cu	US Research Nanomaterials, Inc	40	99.9	USD$296(RM964.96)
5	γ-Al_2O_3	US Research Nanomaterials, Inc	20	99+	USD$59 (RM192.34
6	TiO_2	US Research Nanomaterials, Inc	20nm	99+	USD$76(RM247.76)

2.11 Conclusion

This chapter summarizes the fundamental thermo-physical characteristics of nanofluid coolants, their preparation, convective heat transfer and entropy generation, application of nanofluids in heat pipe and shell and tube heat exchangers and energy savings using nanofluids. Most of the researchers found that nanofluids exhibit enhanced thermal conductivity and convective heat transfer coefficient compared to base fluids. From the nanofluids' applications point of view, it seems that favourable results are obtained. Application of nanofluids can enhance the heat recovery exchanger's thermalperformance. An effective heat recovery exchanger will lead to optimization of energy consumption in industrial sector. Optimization of energy use is the main concern nowadays, due to the depletion of fossil fuel based energy, escalating of fuel price and emission of green house gasses. Thus, a comprehensive study on this is important to adderess the mentioned issues.

CHAPTER 3 METHODOLOGY

3.1 Introduction

This chapter describes the methodology used to conduct the study. The methodology for thermal conductivity, viscosity and density measurements will be described in sub-section 3.2. Sub-section 3.3 explains the mathematical modelling of flue gas/hot gas heat recovery through shell and tube heat exchanger. In the last subsection 3.4, the mathematical modelling of a thermosyphon air-preheater heat exchanger is presented.

3.2 Thermal conductivity, viscosity and density measurements

This section covers the methodology used in thermo-physical properties measurement. The type of nanoparticle and base fluids used in the experiment, nanofluids' preparation, and instruments used to measure thermal conductivity, viscosity and density will be described in the subsequent sub-sections.

3.2.1 Preparation of Nanofluids

Two types of nanofluids are used in the present experimental. They are aluminium oxide, Al_2O_3 and TiO_2 based nanofluids. In order to investigate the particle size effect on the base fluid thermo-physical properties, two different sizes of Al_2O_3 are chosen: 13nm and particle size less than (<) 50nm. The selection of these sizes is adequate since there is a large gap between these sizes. Bigger size is not selected because it will limit the thermal conductivity of nanofluids. In another hand, the selected size for TiO_2 particle is 21nm. These particles are commonly used in nanofluids researches as they are easy and inexpensive to purchase in market. In this study, the nanoparticles were purchased from Sigma Aldrich. As for the base fluid, author selected water and water/ethylene glycol mixture (50:50). Water/ ethylene glycol

mixture is selected due to the limitation of the ultrasonic equipment available in the laboratory. High viscosity samples such as ethylene glycol is not suitable to be sonicated by this equipment. As stated in the manual, the manufacturer recommended that, samples with high viscosity to be diluted before the sonication process. This is to avoid damage to titanium horn (see Figure 3.1).

Two-step method is used for nanofluids preparation. This method is inexpensive and does not require high-end equipment as compared to single-step method. It is a common method in nanofluid research (Lee et al., 2011; Nasiri et al., 2011 and Suresh et al., 2012). Ultrasonic Cell Disruptor KS- 1200R with maximum power of 1200W and 20 kHz frequency as depicted in Figure 3.1 is used in the present study.

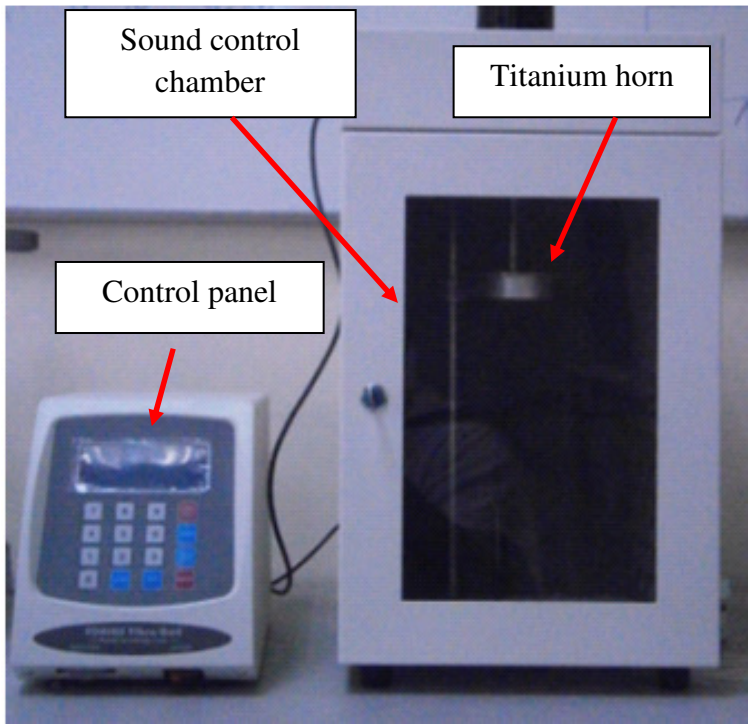

Figure 3.1 Ultrasonic cell disruptor KS-1200R

Each of the nanofluids is prepared in two different nanoparticle volume fractions (0.1vol. % and 0.5vol. %). Higher value is not preferable in the present study as it requires longer ultrasonication time. The preparation process of nanofluids is as

follows: the mass of nanoparticles is weighed using digital weighing balance (Denver Instrument SI-234, readability 0.0001g); the weighted nanoparticles are put into distilled water or ethylene glycol/water mixture, then the mixture is sonicated for the duration of 15 minutes. Ultrasonication process is able to produce stable and uniform nanofluids suspensions compared to suspensions without ultrasonication process (Lee et al., 2011).

3.2.2 Measurement of thermal conductivity

A hand-held thermal conductivity analyzer (KD2-Pro, Decagon) as shown in Figure 3.2 was used to measure nanofluids thermal conductivity. It uses the concept of transient line heat source to measure the thermal conductivity of nanofluids. There are three (3) types of sensors available with this instrument, however a sensor (Single-needle KS-1) with 6 cm length and 1.27 mm diameter is chosen since it is the best for fluid's thermal conductivity measurement. This needle has accuracy of ±5% W/mK for thermal conductivity range from 0.2 - 2 W/mK. It is capable of measuring thermal conductivity of fluid at -50^{o}C to 150^{o}C.

In order to obtain accurate results, average value from 5 measurements was taken in this study. Several precaution procedures were strictly followed to minimize the error during the measurement. They are:-

(a) The measurement is started only 15 minutes after the sensor is immersed in the fluid sample. This is to ensure that the fluid and sensor reach equilibrium temperature condition.

(b) The convection in the fluid is minimized or eliminated. This is done by preventing bench shakes during the measurement. Any vibration of the bench will create convection since the fluid will be moving.

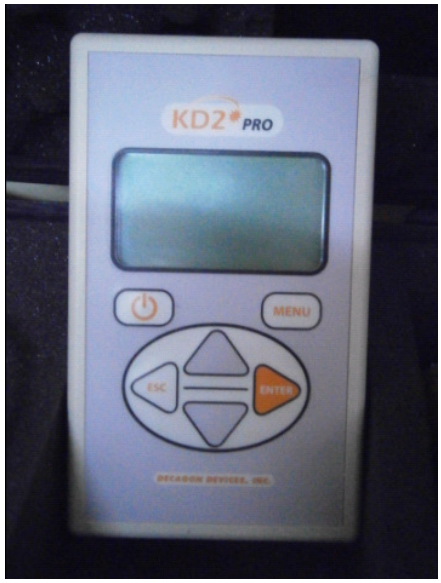

Figure 3.2 KD2 Pro Decagon

3.2.3 Measurement of viscosity

As mentioned in sub-section 3.2.1, two types of nanofluids based coolant were considered in this study. They are ethylene glycol/water mixtures and water-based nanofluids. Thus, sub-sections 3.2.3.1 and 3.2.3.2 will describe the instruments used to measure viscosity of the samples.

3.2.3.1 Ethylene glycol/water mixture-based nanofluids

The viscosity of the samples was measured using LVDV- III Ultra Brookfield Rheometer as illustrated in Figure 3.3. The accuracy of this instrument is ±1.0% and the revolution per minute (rpm) of the spindle, which will be immersed in the sample, can be set to maximum 250.

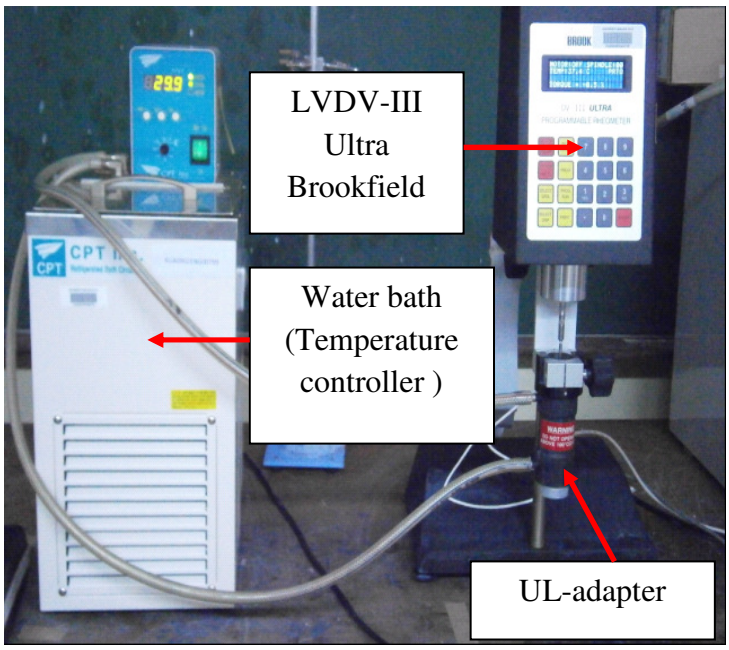

Figure 3.3 LVDV –III Ultra Brookfield Rheometer with water bath circulator

Spindle is driven by a motor through a calibrated spring as seen in Figure 3.4. The viscous drag of the fluid creates resistance against the spindle resulting in deflection of the spring. It will be then converted into viscosity value based on calibrated scale.

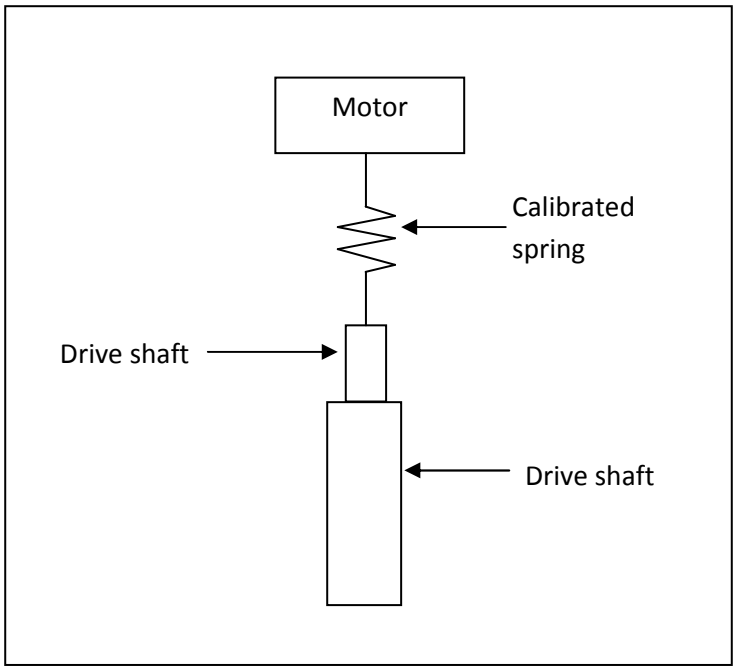

Figure 3.4 Viscosity measurement concept of LVDV-III Ultra Brookfield Rheometer

UL Adapter with spindle “00” is attached into this instrument since it is meant for low viscosity samples down to 1mPa.s. Refrigerated water bath is used to control the sample temperature.

3.2.3.2 Water-based nanofluids

The viscosity of water-based nanofluids was measured using Vibro viscometer SV–10 (Figure 3.5) instead of LVDV-III Ultra Brookfield. This is because the lowest measurement value for LVDV-III Ultra is only 1mPa.s. Water definitely has lower viscosity value. Viscometer (SV – 10) is capable of measuring sample with viscosity ranging 0.3 to 10,000 mPa.s. This instrument has high accuracy where it is capable of providing 1% of repeatability reading.

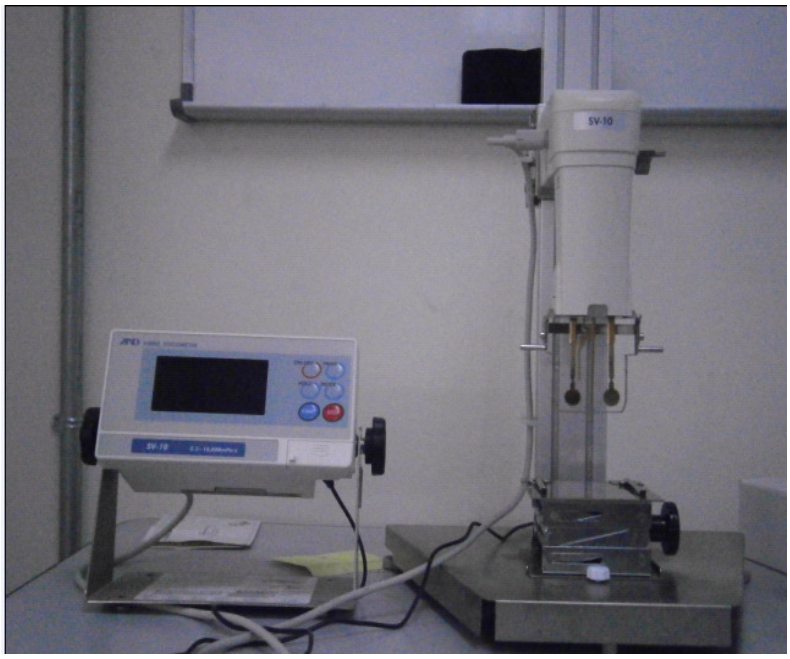

Figure 3.5 SV- 10 Viscometer

Figure 3.6 shows the major parts of the instrument.

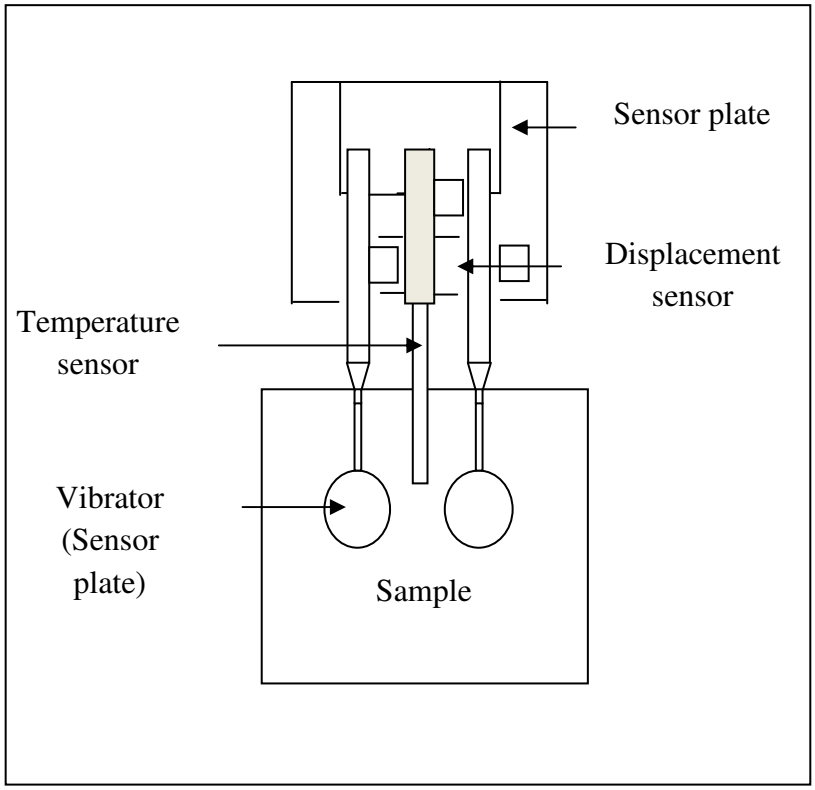

Figure 3.6 Major parts of SV- 10 Viscometer

There are two sensor plates (at the left and right) and a temperature sensor (middle) in this instrument. Temperature range that can be measured by the sensor is from 0^{o}C to 100^{o}C. The sensor plates that are immersed into a sample will vibrate with uniform frequency during the measurement process. The vibration of the sensor plates are control by the electromagnetic drive. The driving electric current to maintain the constant amplitude will be regarded as the viscidity between the sample and sensor plates.

3.2.4 Measurement of Density

The density of the ethylene glycol/ water mixture and water-based nanofluid is measured using density meter DA-130N from Kyoto Electronics. This instrument is able to measure sample density ranging from 0 to 2 g/cm^3. The accuracy of this instrument is ±0.001 g/cm^3 at temperatures within 0 to 40^{o}C. Similar to thermal

conductivity measurements, average value from 5 readings was taken for each sample. Figure 3.7 illustrates the density meter used in this study.

Figure 3.7 Density meter

3.3 Modelling of flue gas or hot gas waste heat recovery through shell and tube heat exchanger

Sub-section 3.3.1 presents methodology used in modelling of thermal and energy performance of a shell and tube heat recovery exchanger operated with nanofluids. Sub-section 3.3.2 covers the energy saving associated with size reduction of heat exchanger. In the sub-section 3.3.3, the entropy generation analysis of nanofluids flows through a circular tube is included.

3.3.1 Shell and tube heat exchanger and operating condition

This type of heat exchanger is commonly used as a pre-heater in power plant, steam generator in nuclear power plant and etc (Kakac and Liu,2002). It consists of two

sides namely; shell and tube sides. In the present study, necessary input data such as shell and tube heat exchanger specifications and operating characteristics were taken from the literatures. The composition of flue gas was obtained from Chen et al.,(2012) as shown in Table 3.1.

Table 3.1 Composition of flue gas from biomass heating plant

Type of gases	Percentage
CO_2	12.1
H_2O	24.4
O_2	3.2
N_2	60.3

The flue gas compositions are from biomass heating plant. The specifications of heat exchanger and operating conditions are shown in Table 3.2. Shell and tube heat exchanger is used to recover the waste heat available in the flue gas.

Table 3.2. Specifications of shell and tube heat exchanger and operating conditions for flue gas and nanofluids

Description	Type/Value
Type of heat exchanger	Single tube pass, type E shell and tube heat exchanger
Tube outside diameter, d_o(mm)	25.4
Tube inner diameter, d_i(mm)	22.9
Pitch, p_t/d_o	1.75
Total tube number, N	1024
Tube layout	Rotated square
Shell inner diameter, D_s(mm)	2090
Shell thickness, δ_s (mm)	14
Baffle type	Single-segmental
Baffle spacing, B(mm)	1776
Baffle cut	25%
Fluid mass flow rate (kg/s)	111.6
Flue gas mass flow rate (kg/s)	26.3
Fluid inlet temperature (^oC)	30
Flue gas temperature (^oC)	150

The length of tubing is assumed to be 5 meters. Thermal conductivity of ethylene glycol based copper and water -based nanofluid is obtained from Eastman et al., (2001) and Jang and Choi (2006) as shown in Fig. 3.8 and 3.9, respectively.

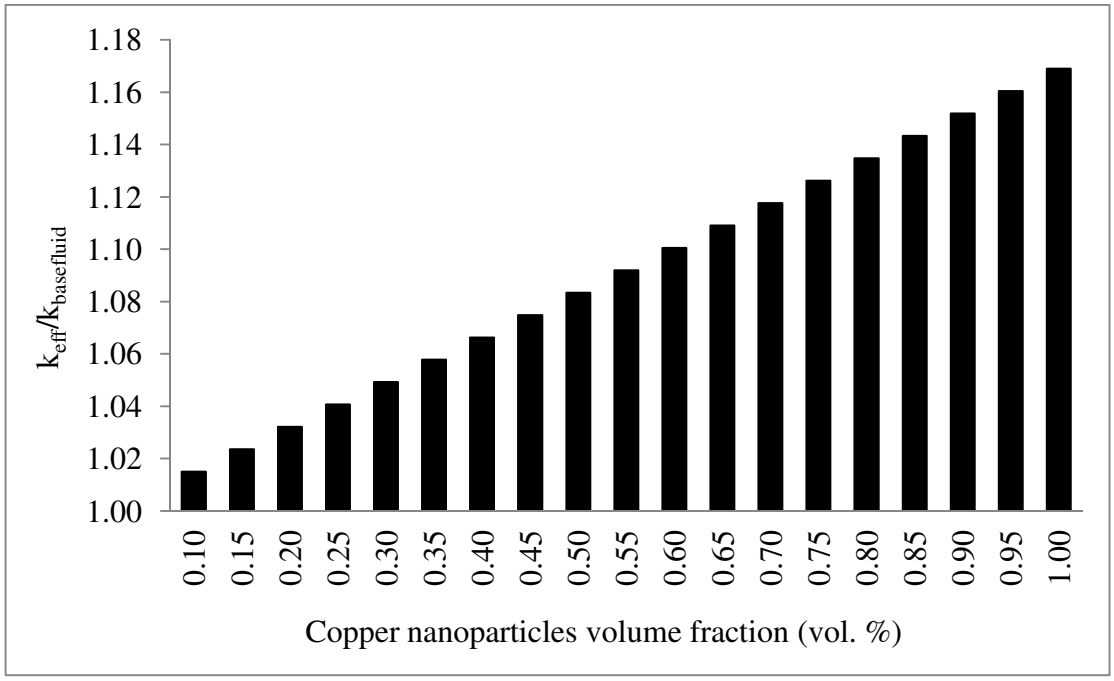

Figure 3.8. Thermal conductivity ratio of ethylene glycol based copper nanofluids (Eastman et al., 2001)

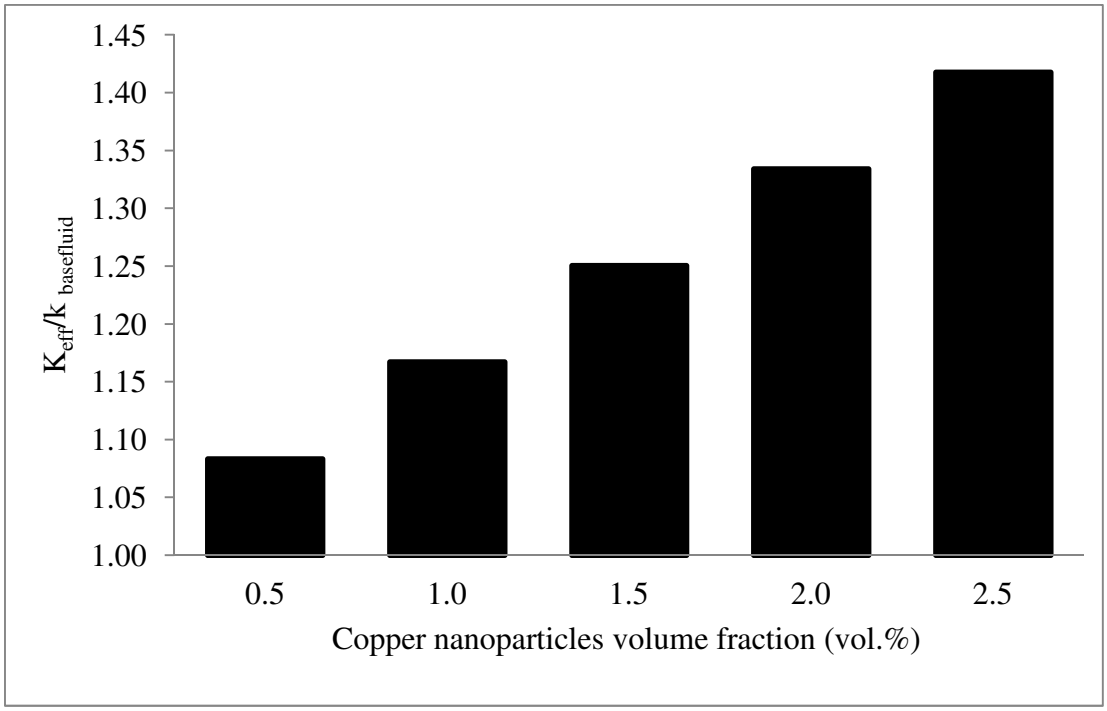

Figure 3.9 Thermal conductivity ratio of water based copper nanofluids (Jang and Choi, 2006)

Leong et al. (2010) used Eastman thermal conductivity data in their study on automotive radiator. Other thermo-physical properties such as density, specific heat and viscosity are calculated from correlations found from the literature. The obtained thermo-physical properties and stability of nanofluids are assumed to remain constant in the application of heat exchanger. On the other hand, the thermo-physical properties of the ethylene glycol/water, ethylene glycol/water based Al_2O_3 (particle size :13nm and <50nm) and TiO_2 (particle size:21nm) nanofluids were obtained from the present experiment as discussed in section 3.2. These properties were used in the mathematical modelling and analysis works. Thermo-physical properties of flue gas, ethylene glycol and water are also needed in calculation. These are depicted in Table 3.3.

Table 3.3. Thermo-physical properties of flue gas, ethylene glycol and water

Flue Gas thermo-physical properties (Increase Performance, 2011)			
Specific heat (kJ/kgK)	Thermal conductivity (W/mK)	Viscosity (Ns/m^2)	
1.148	2.9×10^{-5}	1.9×10^{-5}	
Thermo-physical properties ethylene glycol (Incropera et al., 2007)			
Thermal conductivity (W/mK)	Density (kg/m^3)	Dynamic viscosity (Ns/m^2)	Specific heat (kJ/kgK)
0.2613	1071.81	0.263	2.6958
Thermo-physical properties water (Incropera et al., 2007)			
Thermal conductivity (W/mK)	Density (kg/m^3)	Dynamic viscosity (Ns/m^2)	Specific heat (kJ/kgK)
674.9×10^{-3}	968.32	318.6×10^{-6}	4.2048

3.3.1.1 Theoretical derivation on heat transfer and energy performance of shell and tube heat recovery exchanger

This study intregrated Kern and effective-NTU methods to investigate the performance of shell and tube exchanger. On the shell side modelling, Kern method was selected due to its good estimation on the heat transfer coefficient in shell side (Sarit,

2009). Effective-NTU approach was applied in the tube side analysis. Combination of these two approaches are required to evaluate the heat transfer from the flue/hot gasses to the heat transfer fluid flows through the circular tubes. Single phase models were used in the analysis due to its simpler implementation. There has not been any study which uses these approaches in nanofluids operated shell and tube heat exchanger.

Mathematical modelling shown in this sub-section were taken from various references (Incropera et al., 2007; Ramesh and Dusan, 2003; Velagapudi et al., 2008; Kakac and Liu, 2002). The heat transfer and energy performance of shell and tube heat exchangers were analysed. The base fluids considered are ethylene glycol, water and ethylene glycol/water mixtures while the nanoparticles are Cu, Al_2O_3 and TiO_2. The mathematical modelling used in the analysis is divided into flue gas and base fluid or nanofluids calculations.

The mathematical modelling for flue gas side started with determining cross flow area and equivalent diameter of the shell side. These two values were needed to calculate the flue gas Reynolds number. Eventually, the flue gas Reynolds's number was used in the convective heat transfer coefficient formulation. The mathematical modelling used in this study is shown below.

(a) Crossflow area, A_{cf} can be determined by using Equation (3.1):

$$A_{cf} = (D_s - N_{TC} d_o) B \tag{3.1}$$

where

$$N_{TC} = \frac{D_s}{P_t}$$

(b) Equivalent diameter, D_e can be determined by using Equation (3.2):

$$D_e = \frac{4\left(P_t^2 - \frac{\pi d_o^2}{4}\right)}{\pi d_o} \tag{3.2}$$

(c) Flue gas Reynolds, Re_{fg} number can be determined by using Equation (3.3):

$$Re_{fg} = \left(\frac{\dot{m}_{fg}}{A_{cf}}\right)\frac{D_e}{\mu_{fg}} \tag{3.3}$$

(d) Flue gas convective heat transfer coefficient, h_{fg} can be determined by using Equation (3.4):

$$h_{fg} = \frac{0.36k}{D_e} Re_{fg}^{0.55} Pr_{fg}^{\frac{1}{3}} \tag{3.4}$$

Mathematical equations to calculate Prandtl number, specific heat, density and viscosity of nanofluids are shown in Equations (3.5) - (3.8).

(a) Nanofluids density, ρ_{nf} can be determined by using Equation (3.5)

$$\rho_{nf} = (1 - \emptyset)\rho_f + \emptyset\rho_p \tag{3.5}$$

(b) Nanofluids specific heat $c_{p,nf}$ can be determined by using Equation (3.6)

$$c_{p,nf} = \frac{(1 - \emptyset)\rho_f c_{p,f} + \emptyset\rho_p c_{p,p}}{\rho_{nf}} \tag{3.6}$$

(c) Nanofluids viscosity μ_{nf} can be determined by using Equation (3.7)

$$\frac{\mu_{nf}}{\mu_f} = \frac{1}{(1 - \emptyset)^{2.5}} \tag{3.7}$$

(d) Nanofluids Prandtl number, Pr_{nf} can be determined by using Equation (3.8)

$$Pr_{nf} = \frac{c_{p,nf}\mu_{nf}}{k_{nf}} \tag{3.8}$$

Mathematical equations used to calculate convective and overall heat transfer coefficient and heat transfer rate are expressed by Equations (3.9) to (3.22).

(a) Number of tubes per pass, $N_{t,p}$ can be determined by using Equation (3.9)

$$N_{t,p} = N_T \tag{3.9}$$

since single pass tube is considered

(b) Tube side flow area per pass, $A_{o,t}$ can be determined by using Equation (3.10)

$$A_{o,t} = \frac{\pi}{4} d_i^2 N_{t,p} \quad . \qquad (3.10)$$

(c) Nanofluids Reynolds number, Re_{nf} can be determined by using Equation (3.11)

$$Re_{nf} = \frac{\dot{m}_{nf} d_i}{A_{o,t} \mu_{nf}} \qquad (3.11)$$

(d) Nusselt number, Nu_{nf} can be determined by using Equations. (3.12) and (3.13)

$$Nu_{nf} = 3.66 \text{ for laminar flow} \qquad (3.12)$$

$$Nu_{nf} = 0.024 Re_{nf}^{0.8} Pr_{nf}^{0.4} \text{ for turbulent flow} \qquad (3.13)$$

(e) Nanofluids heat transfer coefficient, h_{nf} can be determined by using Equation (3.14)

$$h_{nf} = \frac{Nu_{nf} k_{nf}}{d_i} \qquad (3.14)$$

(f) Overall heat transfer coefficient, U_o can be determined by using Equation (3.15) where fouling factors are not considered in this analysis.

$$\frac{1}{U_o} = \frac{1}{h_{fg}} + \frac{d_o \ln\left(\frac{d_o}{d_i}\right)}{2k_w} + \frac{1}{h_{nf}} \frac{d_o}{d_i} \qquad (3.15)$$

where k_w is thermal conductivity of copper wall.

(g) Total tube outside heat transfer area, A_s can be determined by using Equation (3.16)

$$A_s = \pi L d_o N_t \qquad (3.16)$$

(h) Number of heat transfer units, NTU can be determined by using Equation (3.17)

$$NTU = \frac{U_o A_s}{C_{min}} \qquad (3.17)$$

where

$$C_{max} = \left(\dot{m} c_p\right)_{nf} \qquad (3.18)$$

$$C_{min} = \left(\dot{m} c_p\right)_{fg} \qquad (3.19)$$

(i) Heat exchanger effectiveness, ε can be determined by using Equation (3.20)

Assuming single pass, both fluids unmixed

$$\varepsilon = 1 - \exp\left[\left(\frac{1}{C^*}\right)(NTU)^{0.22}\{\exp[-C^*(NTU)^{0.78}] - 1\}\right] \quad (3.20)$$

where

$$C^* = \frac{C_{min}}{C_{max}} \quad (3.21)$$

(j) Heat transfer rate, q can be determined by using Equation. (3.22)

$$q = \varepsilon C_{min}\left(T_{fg,i} - T_{nf,i}\right) \quad (3.22)$$

Pressure drop and pumping power can be determined by using following formulations from Equations (3.23) - (3.27).

(a) Friction factor, F can be determined by using Equations. (3.23) and (3.24)

$$F = \frac{64}{Re_{nf}} \text{ for laminar} \quad (3.23)$$

$$F = (0.790 \ln Re_{nf} - 1.64)^{-2} \text{ for turbulent flow} \quad (3.24)$$

(b) Mean velocity of nanofluids, u_m can be determined by using Equation (3.25)

$$u_m = \frac{4\dot{m}_{nf}}{\rho_{nf}\pi d_i^2} \quad (3.25)$$

(c) Pressure drop, Δp of nanofluids can be determined by using Equation (3.26)

$$\Delta p = F\,\frac{\rho_{nf}u_m^2}{2d_i}\,L \quad (3.26)$$

(d) Pump power,P can be determined by using Equation (3.27)

$$P = V_{nf} \times \Delta p \quad (3.27)$$

The mathematical flow chart is depicted in Figure 3.10

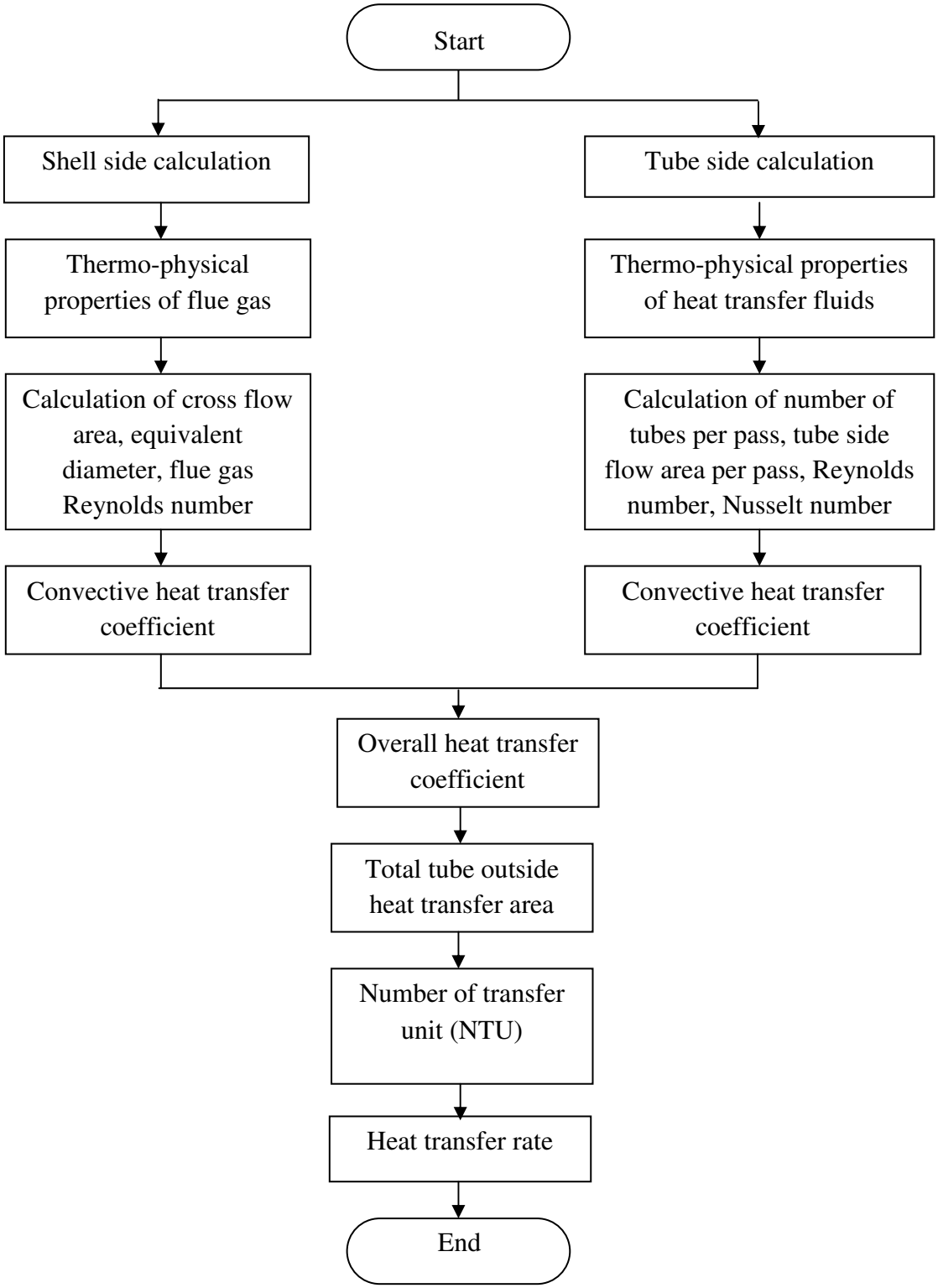

Figure 3.10 Mathematical flow chart (Thermal and energy performance of shell and tube heat exchanger)

3.3.1.2 Test procedures and conditions

The analysis in this study was conducted based on flue gas composition from the biomass heating plant, nanofluids and base fluid properties and operating conditions discussed in Sections 3.3.1. In this study, nanoparticle volume fraction, flue gas and nanofluids mass flow rate were varied to determine thermal and energy performance of the heat recovery exchanger. The test procedures and conditions in this study are shown below.

(a) Effect of nanoparticles volume fraction on thermal and energy performance of shell and tube heat recovery exchanger

In this analysis, flue gas and nanofluids mass flow rate were kept constant at 26.3kg/s and 111.6kg/s, respectively. These values are taken from Chen et al., (2012) which are based on actual mass flow rate values applied in the shell and tube exchanger. Nanoparticles volume fractions were augmented from 0 to 1% for ethylene glycol based copper nanofluids and from 0 to 2% for water based copper nanofluids. Nanofluids Reynolds number, convective and overall heat transfer coefficient and heat transfer rate were then determined. Other parameters such as pumping power as well as the nanofluids pressure drop were determined. Apart from that, analysis was also done on the overall heat transfer performance of the shell and tube heat recovery exchanger operated with ethylene glycol/water base fluid, ethylene glycol/water mixture-based aluminium oxide (particle size:13nm and <50nm) and titanium dioxide (particle size: 21nm). The nanoparticle volume fraction used for these nanofluids was 0.5%.

(b) Effect of flue gas mass flow rate on thermal performance of shell and tube heat exchanger

In this analysis, the flue gas mass flow rate was varied from 26.3kg/s to 42kg/s.

Reynolds number for flue gas was included. Nanofluids convective and overall heat transfer coefficient and heat transfer rate were also analyzed i. Nanofluid subjected to this study was ethylene glycol based copper nanofluids.

(c) Effect of coolant mass flow rate on thermal performance of shell and tube heat Exchanger

Coolant mass flow rate varied from 200 kg/s to 230 kg/s to create turbulent flow. Nanofluids convective and overall heat transfer coefficient and heat transfer rate were also analyzed in this section. Nanofluid subjected in this study was ethylene glycol based copper nanofluids.

3.3.2 Energy saving associated with size reduction of shell and tube heat exchanger

This section describes the method used to estimate the size reduction of shell and tube heat recovery exchanger operated with nanofluids based coolants and its associated energy saving.

3.3.2.1 Size estimation of shell and tube heat recovery exchanger

The specification of shell and tube heat exchanger (TEMA E type) is also taken from Chen et al., (2012) as described in Table 3.2. It is used to recover heat from flue gases emitted from biomass heating plant. From the study, it is implied that the flue gas inlet temperature of about 150^{o}C reduced to 35^{o}C with 26.3kg/s mass flow rate of flue gas. The flue gas thermo-physical properties are obtained from (Increase Performance, 2011) based on its composition given by Chen et al., (2012).

In the present study, the heat transfer fluid inlet temperature and mass flow rate are set as 30^{o}C and 60kg/s, respectively. However, the energy balance Equation (3.28)

is used to determine the heat transfer fluid outlet temperature since the specific heat changes with addition of nanoparticles. Similar to previous section, 5m tube length is considered in this study.

(a) Energy balance is expressed by the Equation (3.28):

$$\dot{m}_{fg} C_{p,fg} \left(T_{fg,in} - T_{fg,out} \right) = \dot{m}_{nf} C_{p,nf} \left(T_{nf,out} - T_{nf,in} \right) \quad (3.28)$$

Initially the convective heat transfer coefficients for flue gas and heat transfer fluid (coolant) are assumed in this analysis. The convective coefficient for the heat transfer fluid (coolant) is assumed to increase with the particle volume fraction due to substantial increase of nanofluids thermal conductivity (Wen and Ding, 2004). Nanoparticles movement which creates the thermal boundary disturbance also enhances convective heat transfer (Kim et al., 2009). Fouling factors are considered negligible in this study. The mathematical modellings used in this study are taken from different references (Incropera et al., 2007; Kakac and Liu,2002; Ramesh and Dusan, 2003; Velagapudi et al., 2008, Taborek, 1991).

(b) The required heat transfer area to perform the selected condition is expressed by the Equation (3.29)

$$A = \frac{Q}{LMTD \times U} \quad (3.29)$$

(c) LMTD constant is expressed by the Equation (3.30):

$$LMTD = \frac{\left(T_{fg,in} - T_{nf,out} \right) - \left(T_{fg,out} - T_{nf,in} \right)}{\ln \left(\frac{T_{fg,in} - T_{nf,out}}{T_{fg,out} - T_{nf,in}} \right)} \quad (3.30)$$

In this study, few similar parameters used by Chen et al. (2012) are taken into consideration as shown in Table 3.4

Table 3.4 Specification of shell and tube heat exchanger for size reduction estimation

Description	Value
Tube outside diameter (mm)	25.4
Tube inside diameter (mm)	22.9
Pitch ratio	1.75
Baffle length (mm)	1776

CTP constant was assumed to be 0.93 for one tube pass, while tube layout constant CL for 90^{o} is assumed to be 1 (Taborek, 1991).

(d) The overall shell diameter is expressed by the Equation (3.31):

$$D_s = 0.637\sqrt{\frac{CL}{CTP}}\left[\frac{(A)(PR)^2\left(d_{t,o}\right)}{L}\right]^{1/2} \tag{3.31}$$

(e) The required number of tubes is expressed by the Equation (3.32):

$$N_t = 0.785\left(\frac{CTP}{CL}\right)\frac{(D_s)^2}{(PR)^2(d_{to})^2} \tag{3.32}$$

Finally, the convective heat transfer of the heat exchanger with the calculated geometric values is compared with the initial assumption of convective heat transfer coefficient. This is to ensure that the calculated geometries value is capable to produce the same thermal performance.

3.3.2.2 Convective heat transfer coefficient of flue gas and nanofluids

Thermal conductivity, specific heat and viscosity of heat transfer fluids are required to calculate this convective heat transfer properties for the tube side. Two types of nanofluids are considered in this study namely; ethylene glycol and water based copper nanofluids. Both are taken from Eastman et al., (2001) (Figure 3.8) and Jang and Choi (2006) (Figure 3.9) respectively. It is noted that the thermal conductivity data

taken from Eastman et al., (2001) is measured from samples without addition of any surfactant. Flue gas and nanofluids convective heat transfer coefficient are calculated based on formulations listed in Section 3.3.1.1.

3.3.2.3 Energy savings

Mathematical formulations to calculate energy savings associated with the size reduction of heat exchanger are presented by Equations (3.33)-(3.36).

(a) Mass, m can be expressed by the Equation (3.33):

$$m = \rho \times v \tag{3.33}$$

(b) Energy consumption used for material processing , E can be expressed by the Equation (3.34):

$$E = \dot{e} \times m \tag{3.34}$$

Energy consumption for copper material processing is 1.17517kWh/kg copper (Yanjia and Chandler, 2010). Guo and Fu (2010) reported that energy consumption for steel is 0.45224 kWh/kg steel. Copper and steel are assumed as the materials for tube and shell, respectively.

(c) Mass reduction, m_{red} can be expressed by the Equation (3.35):

$$m_{red} = m_{bf} - m_{nf} \tag{3.35}$$

(d) Total energy savings for material processing, e_t can be expressed by the Equation (3.36)

$$e_{sav} = e_{bf} - e_{nf} \tag{3.36}$$

Figure 3.11 shows the mathematical flowchart of the size reduction and energy savings of shell and tube heat exchanger.

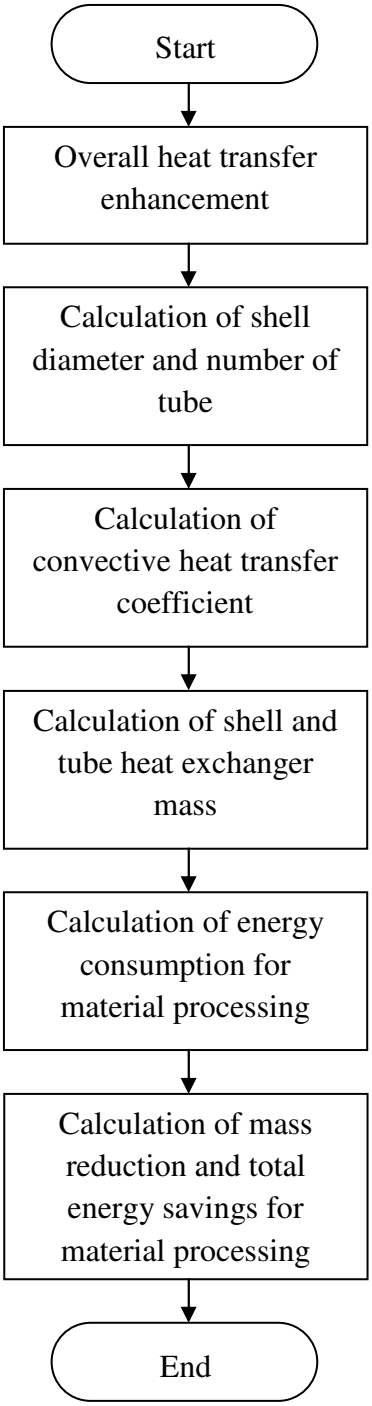

Figure 3.11 Mathematical flowchart of the size reduction and energy savings of shell and tube heat exchanger

3.3.3 Entropy generation of nanofluids flow through a circular tube subjected to constant wall temperature

The efficiency of nanofluids as a heat transfer fluid depends not only on the heat transfer enhancement but also on the pressure drop. Thus, entropy generation analysis was conducted in the present study. Circular tube is selected because this shape of tube is widely used in shell and tube heat exchangers. Sub-section 3.3.3.1 describes the geometry configuration and thermo-physical properties of nanofluids while the modelling used in the analysis is presented in the succeeding sub-section.

3.3.3.1 Geometry configuration of circular tube and thermo- physical properties of nanofluids

The schematic diagram of a circular tube subjected to entropy analysis is shown in Figure 3.12. In this figure, the circular tube is subjected to constant wall temperature due to heating process from flue gas/hot gas. The fluid that flows through the tube absorbs the heat from the circular tube's wall. The heat transfer rate of the fluid within the control volume can be determined using Newton's law of cooling as follows:

$$d\dot{Q} = \dot{m}c_p dT = h\pi(T_w - T)dx \qquad (3.37)$$

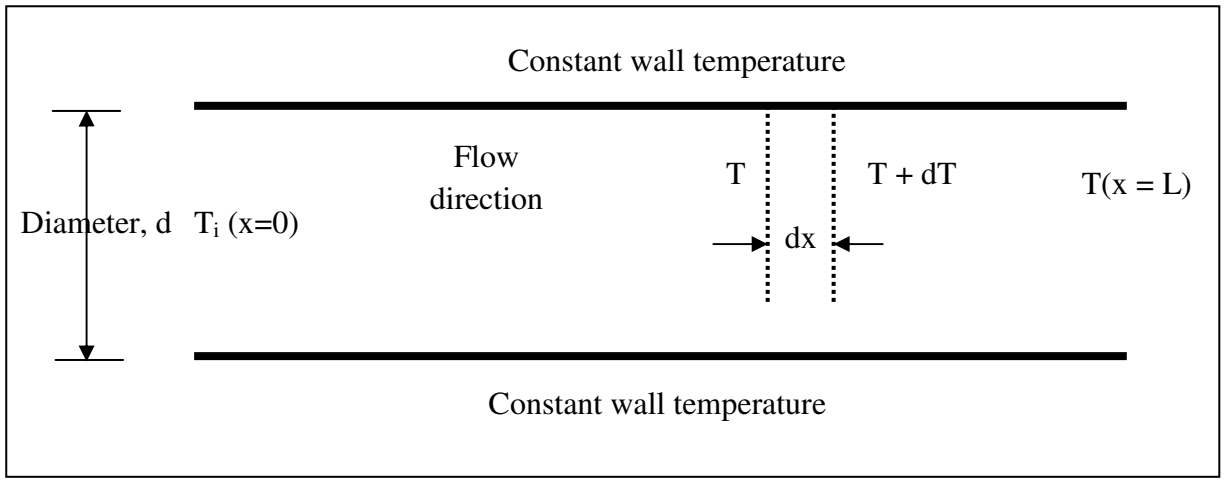

Figure 3.12 Circular tube under constant wall temperature (Sahin, 2000)

The specifications and operating characteristics are shown in Table 3.5.

Table 3.5 Specification and operating characteristic of circular tube

	Specification/ working condition	**Value/ Remark**
1	Diameter of circular tube, d (m)	0.01-0.03
2	Length of circular tube, l (m)	2-10
3	Temperature of heat transfer fluid , T_i(K)	300
4	Base fluid	Water
5	Nanoparticle volume fraction, $\emptyset$	Al_20_3 (0-7% volume fractions) and TiO_2(0-4% volume fractions)
6	Mass flow rate (kg/s)	Laminar (0.01-0.02), turbulent (0.1-0.2)
7	Dimensionless wall and fluid temperature different, τ	0.01-0.02

The thermal conductivity of water based Al_2O_3 nanofluids is obtained from Khanafer and Vafai (2011) as shown in Equation (3.38).

$$\frac{k_{eff}}{k_f} = 1.0 + 1.0112\emptyset_p + 2.4375\emptyset_p\left(\frac{47}{d_p(nm)}\right) - 0.0248\,\emptyset_p\left(\frac{k_p}{0.613}\right) \quad (3.38)$$

As for water based TiO_2 nanofluids, the thermal conductivity value is obtained from Murshed et al.,(2009) as shown in Figure 3.13.

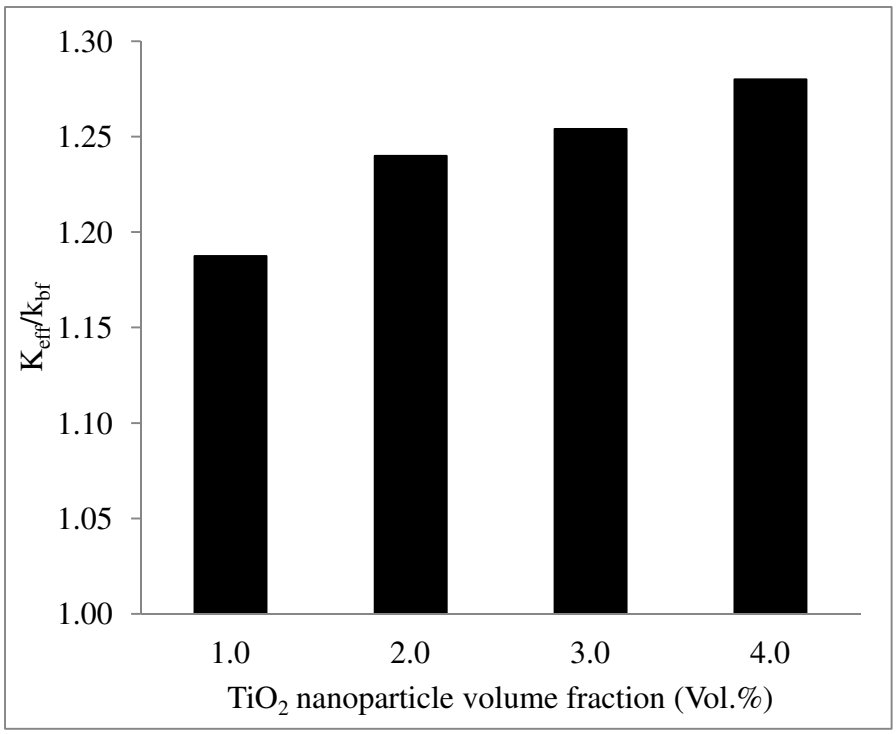

Figure 3.13 Thermal conductivity of water based TiO_2 nanofluids (Murshed et al., 2009)

Apart from the thermo-physical properties from literatures, the thermo-physcial properties of water based Al_2O_3 and TiO_2 nanofluids obtained from the present study, as described in section 3.2, were also used in the entropy generation analysis.

Generally, nanofluids thermal conductivity is affected by several factors, namely, particle size and shape, addition of surfactant, particle volume fractions and etc. Other thermo-physical properties are determined from Equations (3.5-3.7). The density formulation (Equation 3.5) is based on mixing rule while the dynamic viscosity (Equation 3.7) is originated from Einstein formulation. Thermo-physical properties of water, as base fluid, are obtained from Incropera et al., (2007). These are depicted in Table 3.6.

Table 3.6. Thermo-physical properties of water (Incropera et al., 2007)

Num	Thermo-physical properties	Value
1	Density, kg/m^3	997
2	Dynamic viscosity (Ns/m^2)	855×10^{-4}
3	Specific heat (J/kgK)	4179

3.3.3.2 Theoretical derivation on entropy generation of nanofluids flow through a circular tube subjected to constant wall temperature

The methodology used by Sahin (2000) is adopted in this present study. It is defined that the total entropy generation of the fluid flow through a circular tube is represented as follows:

$$\dot{S}_{gen} = \dot{m}c_p\left[\ln\left[\frac{1-\tau e^{-4St\lambda}}{1-\tau}\right] - \tau\left(1-e^{-4St\lambda}\right) + \frac{1}{8}f\frac{Ec}{St}\ln\left[\frac{e^{4St\lambda}-\tau}{1-\tau}\right]\right] \quad (3.39)$$

The overall heat transfer rate from the wall to the fluid can be obtained by integrating Equation (3.37) along the tube length as follows:

$$\dot{Q} = \dot{m}c_p(T_w - T_i)\left(1-e^{-4St\lambda}\right) \quad (3.40)$$

For simplification of analysis, the entropy entropy generation can be presented in dimensionless form as depicted indicated as follows:

$$\psi = \frac{\dot{S}_{gen}}{\dot{Q}/(T_w - T_i)} \tag{3.41}$$

Substitution of Equations (3.39) and (3.40) into Equation (3.41), the total dimensionless entropy generation can be written as follows:

$\Psi =$

$$\frac{1}{1 - e^{-4St\lambda}}\left\{\ln\left[\frac{1 - \tau e^{-4St\lambda}}{1 - \tau}\right] - \tau\left(1 - e^{-4st\lambda}\right) + \frac{1}{8} f \frac{Ec}{St} \ln\left[\frac{e^{4st\lambda} - \tau}{1 - \tau}\right]\right\} \tag{3.42}$$

where

$$\pi_1 = St\,\lambda \tag{3.43}$$

$$\pi_2 = f\frac{Ec}{St} \tag{3.44}$$

This formulation consists of entropy generation contributed by heat transfer and friction loss. Optimum condition for a thermal system or flow is achieved when this value is minimized. Equations. (3.45-3.56) are obtained from references (Sahin, 2000; Incropera et al.,2007; Ramesh and Dusan, 2003).

The friction factor, f of the fluid flow can be determined as follows:

$$f = \frac{64}{Re} \text{ for laminar flow} \tag{3.45}$$

$$f = (0.79 \ln Re - 1.64)^{-2} \text{ for turbulent flow} \tag{3.46}$$

The pumping power plays a significant role in a thermal system. It is known that, higher pumping power is required for fluid flow with higher pressure drop. The fluid pressure drop can be determined as follows:

$$d_p = \frac{f\rho_{nf}u^2}{2d_h} dx \tag{3.47}$$

The Reynolds number can be expressed as:

$$\mathrm{Re_{nf}} = \frac{4\dot{m}_{nf}}{\pi d_h \mu_{nf}} \tag{3.48}$$

The fluid velocity could be indicated by:

$$u_{nf} = \frac{\dot{m}}{\rho_{nf} A_c} \tag{3.49}$$

Stanton number, St is needed for total dimensionless entropy generation calculation as given in Eq. (3.50). St can be calculated as follows:

$$\mathrm{St} = \frac{h_{nf}}{\rho_{nf} u_{nf} c_{p,nf}} \tag{3.50}$$

Convective heat transfer can be determined as follows:

$$h_{nf} = \frac{\mathrm{Nuk_{nf}}}{d_h} \tag{3.51}$$

Nusselt number can be determined as follows:

$\mathrm{Nu} = 3.66$ for laminar flow (3.52)

$\mathrm{Nu} = 0.024\ \mathrm{Re_{nf}^{0.8}} \mathrm{Pr_{nf}^{0.4}}$ for turbulent flow (3.53)

The Eckert number can be obtained using the following relation:

$$\mathrm{Ec} = \frac{u_{nf}^2}{C_{p,nf} T_w} \tag{3.54}$$

The dimensionless wall and fluid temperature difference is expressed as follows:

$$\tau = \frac{T_w - T_i}{T_w} \tag{3.55}$$

The dimensionless length of a circular tube is defined as:

$$\lambda = \frac{L}{D} \tag{3.56}$$

The methodology used in the present analysis is validated with the results obtained from Sahin (2000). The Figure 3.14 shows the mathematical flowchart of the size reduction and energy savings of shell and tube heat exchanger.

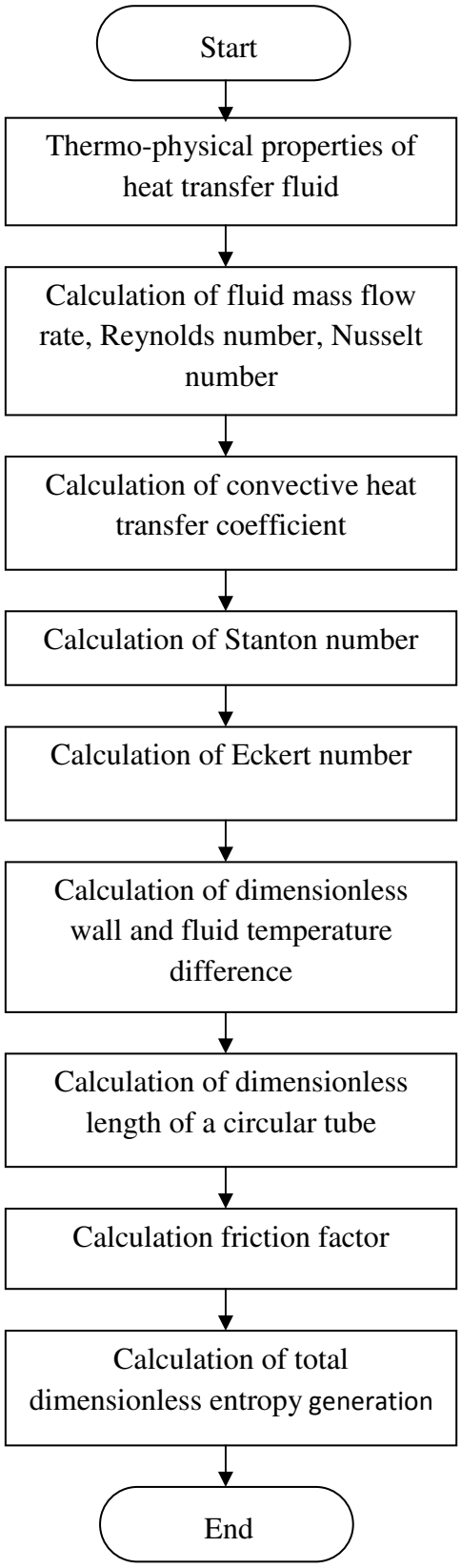

Figure 3.14 Mathematical flowchart of the size reduction and energy savings of shell and tube heat exchanger.

3.4 Modelling of hot gas waste heat recovery through thermosyphon air preheater

Beside from shell and tube heat exchanger, thermosyphon heat exchanger also can be used to recover the waste heat from the flue gass/hot gass. Therefore, this section describes the methodology used for performance investigation of thermosyphon air preheater. It covers the modelling characteristic, input data, mathematical modeling and test characteristics.

3.4.1 Modelling characteristics and input data

The specification of an air to air thermosyphon heat recovery exchanger is taken from Noie (2006). In their study, authors used water as the thermosyphon's working fluid. As mentioned in Chapter 2, nanofluids offer better thermal properties than water. Thus, the present study investigated the performance of the same thermosyphon but operated with nanofluids. The specification and schematic diagram of thermosyphon are shown in Table 3.7 and Figure. 3.15.

Table 3.7 Specifications of an air preheater (Noie, 2006)

Description	Value
Dimension of heat exchanger (m)	1.3 (H) × 0.43 (L) × 0.27 (W)
Dimension of each thermosyphon (mm)	d_o = 15, d_i=14, L_{tubes}=1300
Type and dimension of fins (mm)	Aluminium plate fin, thickness = 0.4mm Number of fins per meter = 300, Spacing,f_s =10mm
Thermosyphon arrangement	Staggered, s_l = 30mm , s_t=30mm
Number of rows	n_l = 6 , n_t= 15
Total number of the thermosyphons	N=90
Thermosyphon materials/ working fluid	Copper/ water

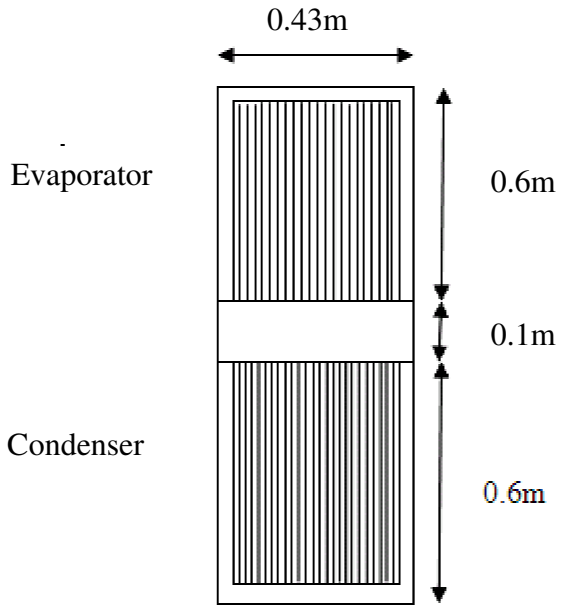

Figure 3.15 Schematic diagram of an air preheater (Noie, 2006)

The operating temperature for hot air ranges from 100°C to 240°C while the cold air is assumed to be 25°C. Thermo-physical properties of air at these temperatures are taken from Incropera et al., (2007). Nanofluids used in the present study are water based Al_2O_3 and water based TiO_2. These are commonly used in nanofluid researches.

3.4.2 Theoretical derivation of heat transfer and energy performance in thermosyphon air preheater

The formulations used for modelling analysis in this section are divided into: thermal resistance of air sides, wall, working fluids, overall effectiveness, outlet temperatures and energy performance.

3.4.2.1 Thermal resistance of air side

Nuntaphan et al. (2002) have used a formulation from Webb (1994) to calculate the convective heat transfer coefficient of air at the evaporator side, . It can be represented by Equation (3.57)

$$h_{air,eva} = \frac{j\,\rho_{air} u_{max} C_{p,air}}{Pr_{air}^{2/3}} \tag{3.57}$$

where j is Colburn factor which can be represented by the following equation:

$$j = 0.14 Re^{-0.328} \left(\frac{S_t}{S_l}\right)^{-0.502} \left(\frac{f_s}{d_o}\right)^{0.031} \tag{3.58}$$

It is a formulation to cater for plain finned tubes. The tubes are arranged in the staggered array. Incropera et al., (2007) used the following equation to determine the maximum velocity, u_{max} for the staggered configuration:

$$u_{max} = \frac{S_t}{2(S_d - d_o)} u \tag{3.59}$$

Maximum Reynolds number can be represented by the following equation:

$$Re_{D,max} = \frac{\rho_{air} u_{max} d_o}{\mu_{air}} \tag{3.60}$$

Mass flow rate,$\dot{m}$ can be represented by the following equation:

$$\dot{m} = \rho_{air} u A_{duct} \tag{3.61}$$

Air side thermal resistance at the evaporator can be expressed in the following equation:

$$R_{air,eva} = \frac{1}{h_{air,eva}\,\eta_o} \tag{3.62}$$

where $\eta_o$is the total surface temperature effectiveness. It can be represented by the following equation:

$$\eta_o = 1.0 - (1.0 - \eta_f) \times \frac{A_f}{A_t} \tag{3.63}$$

where η_f is the fin efficiency. It can be represented by the following equation:

$$\eta_f = \frac{\tanh ml}{ml} \tag{3.64}$$

where,

$$m = \sqrt{\frac{2h_{air,eva}}{k_{fin}\, f_{thickness}}} \tag{3.65}$$

Same formulations (Equations 3.57-3.65) are used to determine thermal resistance of air at the condenser side.

3.4.2.2 Thermal resistance of thermosyphon wall

The wall thermal resistances at both sides; evaporator and condenser are negligible. This is because wall thickness is only 1 mm. Moreover, in the present study, the thermosyphon heat exchanger is made of copper. Copper exhibits 401W/mK thermal conductivity at 300K. This material is known as one of the best heat conductors available in the market.

3.4.2.3Thermal resistance of working fluid at evaporator

Nanofluids considered in this study are similar with the previous nanofluids used in entropy generation analysis. The heat transfer coefficient of the working fluid in an evaporator is determined from Hewitt et al., (1993). Therefore, nanofluids heat transfer coefficient at the evaporator side of thermosyphon ($h_{nf,eva}$) can be represented by the following equation:

$$\frac{h_{nf,eva}}{k_{nf}}\left(\frac{\mu_{nf}^2}{\rho_{nf,l}\left(\rho_{nf,l}-\rho_{nf,g}\right)g}\right)^{1/3}=\left(\frac{4}{3}\right)^{\frac{1}{3}}\frac{1}{Re_{nf}^{1/3}} \tag{3.66}$$

Reynolds number for the nanofluid is assumed to be 30 in this study since the heat transfer fluid containing nanoparticles has higher viscosity. Thus, the fluid flow is restricted in this condition. Hagens et al., (2007) used Reynolds number ranging from 30 to100 in their experimental and analytical study of long heat pipes. Thermal resistance of nanofluids at an evaporator can be represented by the following equation:

$$R_{nf,eva}=\frac{1}{\left(\frac{\alpha_{nf}}{\alpha_{air}}\right)h_{nf,eva}} \tag{3.67}$$

3.4.2.4 Thermal resistance of working fluid at condenser

Same formulations from Equations (3.66-3.67) were used to calculate thermal resistance of working fluid in the condenser section. However, Equation (3.66) is replaced with Equation (3.68) since condensation process is taking place at the condenser section. This formulation is obtained from Hewitt et al. (1993):

$$\frac{h_{nf,cond}}{k_{nf}}\left(\frac{\mu_{nf}^2}{\rho_{nf,l}\left(\rho_{nf,l}-\rho_{nf,g}\right)g}\right)^{1/3} = \frac{4}{3}\left(\frac{4}{3Re_{nf}}\right)^{\frac{1}{3}} \tag{3.68}$$

3.4.2.5 Overall effectiveness of thermosyphon air preheater

The overall heat transfer coefficient is represented by the following equation:

$$U_o = U_{eva} + U_{cond} \tag{3.69}$$

Noie (2006) used Equations (3.70-3.79) in his analysis of thermosyphon air preheater operated with water as working fluid. The effectiveness for a single row heat pipe is represented by the following equations:

$$\varepsilon_{eva,single} = 1 - \exp\left(-NTU\right)_{eva} \tag{3.70}$$

$$\varepsilon_{cond,single} = 1 - \exp\left(-NTU\right)_{cond} \tag{3.71}$$

Number of transfer unit (NTU) for both evaporator and condenser section are shown as follows.

$$NTU_{eva} = \frac{(UA)_{eva}}{C_{eva}} \tag{3.72}$$

where

$$C_{eva} = \left(\dot{m}_{air}c_{p,air}\right)_{eva} \tag{3.73}$$

$$NTU_{cond} = \frac{(UA)_{cond}}{C_{cond}} \tag{3.74}$$

where

$$C_{cond} = \left(\dot{m}_{air}c_{p,air}\right)_{cond} \tag{3.75}$$

The effectiveness of thermosyphon with n rows of heat pipes is represented by the following equations:

$$\varepsilon_{eva,n} = 1 - \left(1 - \varepsilon_{eva,single}\right)^{n} \tag{3.76}$$

$$\varepsilon_{cond,n} = 1 - \left(1 - \varepsilon_{cond,single}\right)^{n} \tag{3.77}$$

Overall effectiveness of the thermosyphon , ε_t is represented by the following equations:

$$\varepsilon_t = \left(\frac{1}{\varepsilon_{cond,n}} + \frac{C_{air,cond}/C_{air,eva}}{\varepsilon_{eva,n}} \right)^{-1} \quad \text{if } C_{eva} > C_{cond} \tag{3.78}$$

$$\varepsilon_t = \left(\frac{1}{\varepsilon_{eva,n}} + \frac{C_{air,eva}/C_{air,cond}}{\varepsilon_{cond,n}} \right)^{-1} \quad \text{if } C_{cond} > C_{eva} \tag{3.79}$$

3.4.2.6 Outlet temperature at evaporator and condenser

The outlet temperatures at condenser and evaporator sections are represented by the following equations (Noie, 2006).

$$T_{eva,out} = T_{eva,in} - \varepsilon_t \frac{\left(\dot{m}_{air} c_{p,air}\right)_{min}}{\left(\dot{m}_{air} c_{p,air}\right)_{eva}} \left(T_{eva,in} - T_{cond,in}\right) \tag{3.80}$$

$$T_{cond,out} = T_{cond,in} + \varepsilon_t \frac{\left(\dot{m}_{air} c_{p,air}\right)_{min}}{\left(\dot{m}_{air} c_{p,air}\right)_{cond}} \left(T_{eva,in} - T_{cond,in}\right) \tag{3.81}$$

3.4.2.7 Energy performance

The absorbed energy at the evaporator and condenser sections of a heat pipe heat exchanger are represented by the following equations:

$$Q_{eva} = C_{eva} \times \left(T_{eva,in} - T_{eva,out}\right) \quad (3.82)$$

$$Q_{cond} = C_{cond} \times \left(T_{cond,out} - T_{cond,in}\right) \quad (3.83)$$

Figure 3.16 shows the mathematical flow chart of the thermpsyphon air reheater analysis

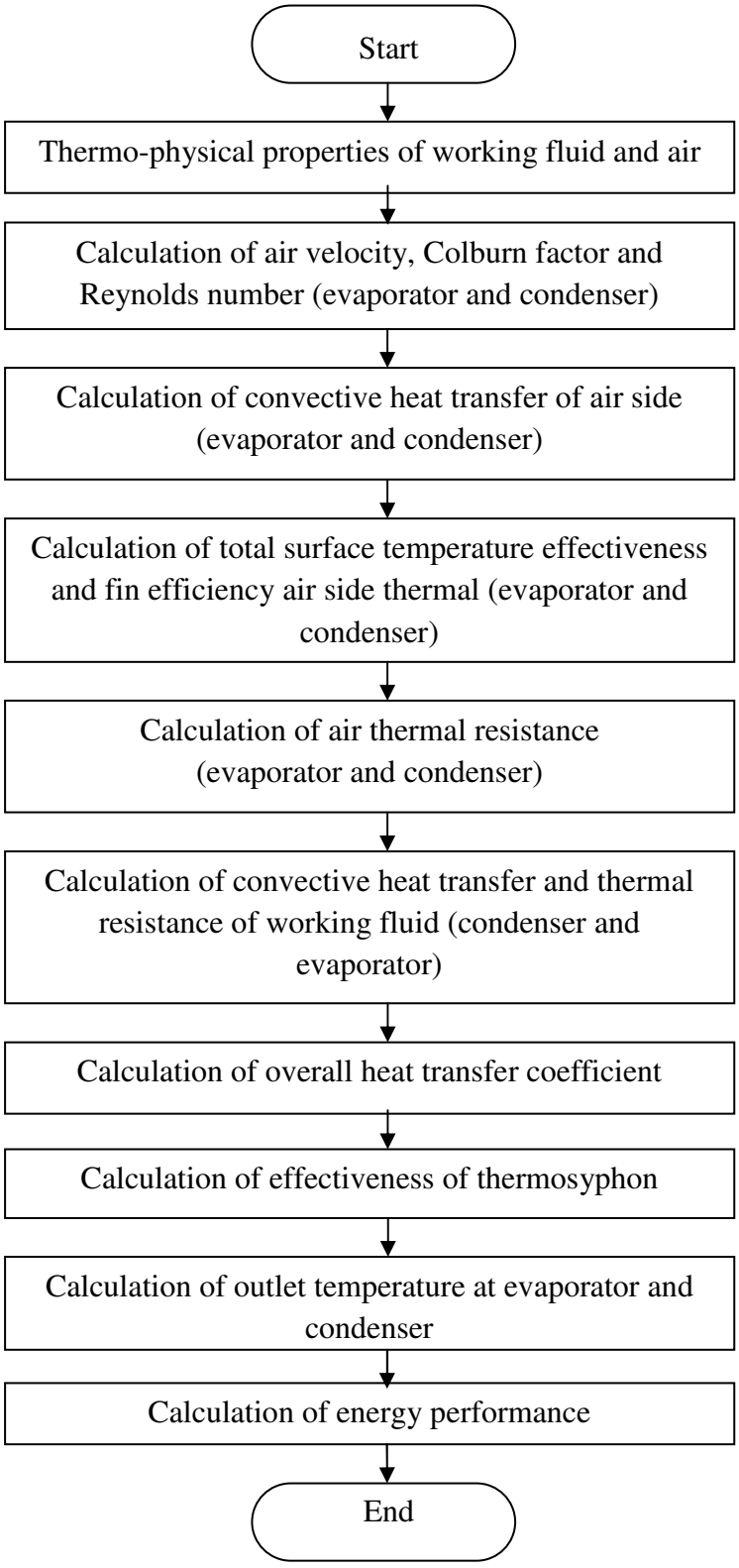

Figure 3.16 Mathematical flowchart of the thermosyphon air-preheater analysis

3.4.2.8 Test characteristics

The test characteristics considered in this study are presented in this section. It includes the operating condition used in the comparative studies and nanofluids analysis.

(a) Comparative studies

This sub-section describes the method used to validate the model in this study. The influence of hot air inlet temperature on the hot air outlet temperature was analyzed in this section. The obtained results were compared with results obtained from Noie (2006). The hot air temperature was varied from 100^{o}C to 240^{o}C. However, cold air inlet temperature was fixed at 25^{o}C. The analysis was conducted at three difference hot air velocities, which are 2.5, 4.0 and 4.75 m/s while, cold air velocity was kept constant at 3 m/s. These values are similar with the experimental conditions used by Noie (2006). Water was used as heat pipe working fluid in this study.

(b) Influence of particle volume fraction on thermal and energy performance of thermosyphon heat exchanger

Water based Al_2O_3 and TiO_2 nanofluids were used as the thermosyphon heat exchanger working fluid. The parameters that were kept constant in this section are hot air inlet temperature (100^{o}C), cold air velocity (3 m/s) and cold air inlet temperature (25^{o}C). Similar to the previous section, the analysis were conducted with three different hot air velocities. The effects of the particle volume fractions on overall heat transfer coefficient and cold air outlet temperature were analyzed in this part. In addition, the energy required to heat the combustion air was also estimated.

3.5 Conclusion

This chapter discusses the methodology used in the present study. Three types of thermo-physical experiments were conducted namely thermal conductivity, viscosity and density. For the thermal and energy performance of heat recovery exchanger's analysis, mathematical equations were presented. The relevant formulations are obtained from literatures and text book. The methodology discussed covers shell and tube heat exchanger and thermosyphon air preheater heat exchangers. Entropy generation formulations are also presented in this chapter. The next chapter will discuss the findings obtained from the present study.

CHAPTER 4 RESULTS AND DISCUSSION

4.1 Introduction

This chapter deals with results and discussions on thermo-physical properties of nanofluids. The thermal and energy performance of the heat exchangers used to recover the flue gas/ hot gas are included as well.

4.2 Thermal conductivity characteristic of nanofluid based coolants

Thermal conductivity of heat transfer fluids was measured using a KD2-Pro thermal analyzer. The accuracy of the instrument was tested by comparing the reference values (Incropera et al., 2007) and (ASHRAE, 2001) with the experimental values. This is shown in Figure 4.1. The deviation between the reference and experiment values for ethylene glycol/water mixture is 2.0% only. As for water, the recorded deviation is 6.3%. These values are acceptable and, it shows that the KD2-Pro thermal analyzer is reliable and provides accurate results.

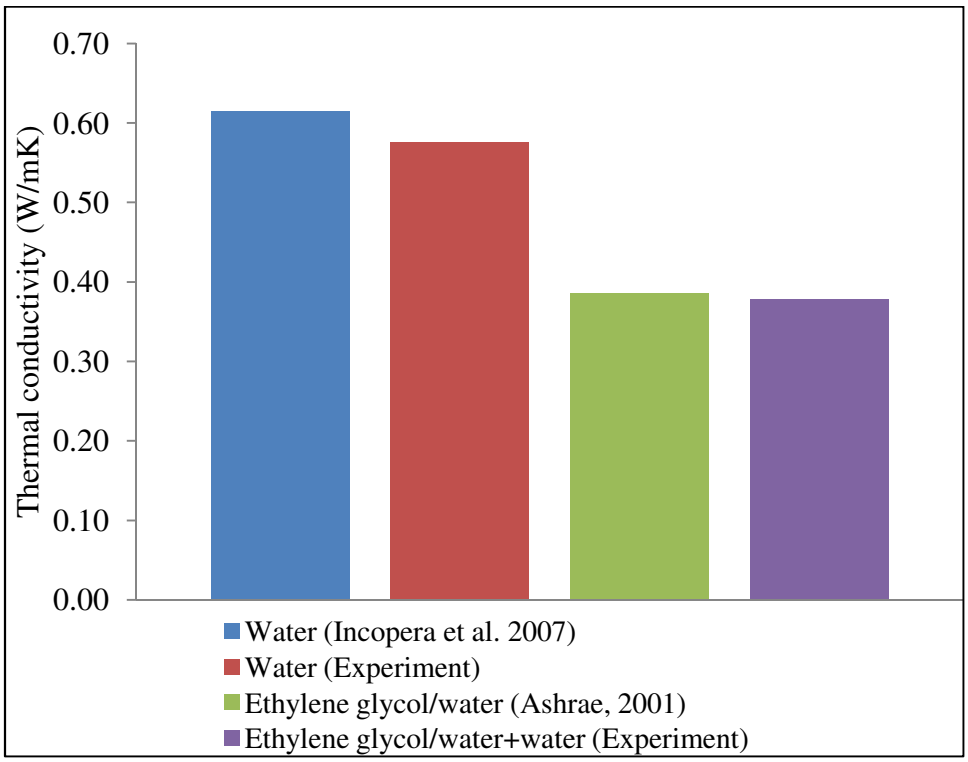

Figure 4.1 Validation of KD2-Pro thermal conductivity analyzer (~ 28^{o}C)

Thermal conductivity of various types of ethylene glycol/water and water-based nanofluid is shown in Figure 4.2.

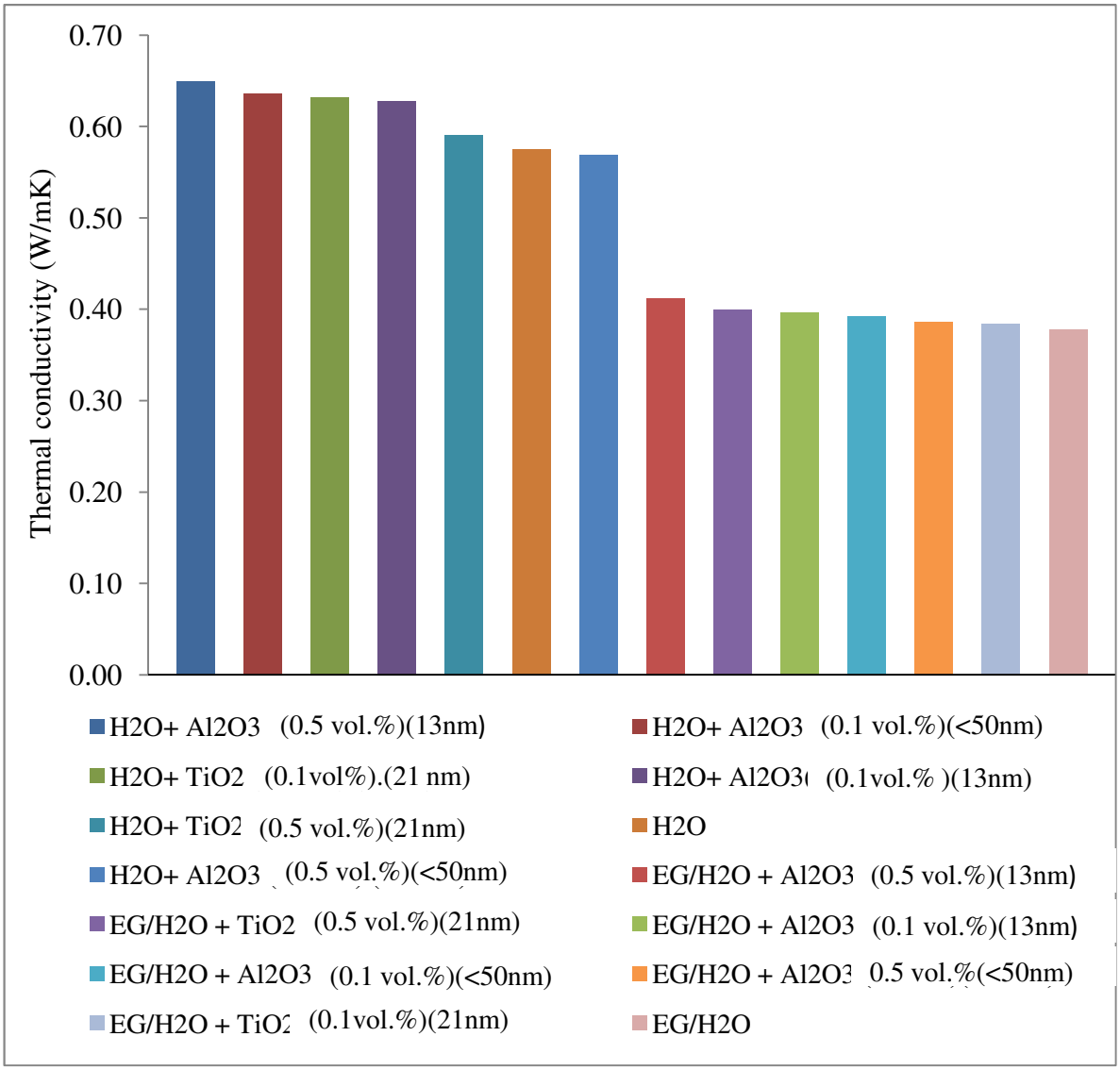

Figure 4.2. Comparison of thermal conductivity between various water and ethylene glycol/water-based nanofluid and base fluid (~ 28^{o}C)

The particles used in this study were TiO_2 (particle size: 21nm) and Al_2O_3 (particle size: 13nm and <50nm). It is found that thermal conductivity of ethylene glycol/water-based nanofluids is higher than ethylene glycol/water mixture. For instance, 8.9% thermal conductivity augmentation is observed for ethylene glycol/water mixture containing 0.5vol. % of Al_2O_3 (particle size: 13nm) compared to ethylene

glycol base fluid. This percentage of thermal conductivity enhancement is calculated based on formula show in Appendix G. On the other hand, addition of 0.5 vol. % of TiO_2 into ethylene glycol/water would increase the thermal conductivity of ethylene glycol/water about 5.6%. The increase of thermal conductivity could be due to formation of nanolayer around the particle. It is believed that the base fluid molecules tend to form an ordered layer around solid particles. This layering is much more ordered than the bulk fluid, thus, it would have higher thermal conductivity compared to the bulk fluid (Murshed et al., 2008b). Several other mechanisms contributing to the thermal conductivity enhancement of nanofluids have been discussed by various researchers (Keblinski et al., 2002; Keblinski et al., 2005; Murshed et al., 2008a; Choi, 2009). These mechanisms include Brownian motion, nature of heat transport in nanoparticles, nanoparticles clustering and etc.

Apart from that, the thermal conductivity of ethylene glycol/water based nanofluids increases with the increase of nanoparticle volume fraction except for Al_2O_3(particle size: <50nm). Nanoparticle might agglomerate in ethylene glycol/water containing 0.5vol. % of Al_2O_3 (particle size:<50nm). This hinders its thermal conductivity enhancement compared to 0.1vol. %. Shima et al., (2010) reported that particle agglomeration is the main reason for the thermal conductivity decrement of nanofluids. Another researcher, Hong et al., 2006) explained that nanoparticles are closer to each other for higher particle loadings; thus, they can agglomerate easily. They added that the decrease of nanofluids thermal conductivity is directly linked to the particle agglomeration.

The present experiment shows that nanofluids with smaller particle size exhibit higher thermal conductivity. For instance, thermal conductivity of ethylene glycol/ water based Al_2O_3 (particle size:13nm) nanofluids is higher than Al_2O_3 (particle size: <50nm) nanofluids irrespective of particle volume fraction. This is agreed by Teng et

al., (2010). These authors considered three types of particle size; 20, 50 and 100nm of Al_2O_3 in water base fluid. They concluded that nanofluids with smaller nanoparticles exhibit higher thermal conductivity enhancement especially at high temperatures. Chon and Kihm (2005) also reported that smaller nanoparticles give higher surface area and particles interaction which leads to thermal conductivity augmentation. In another research, Mintsa et al., (2009) added nanofluids with smaller nanoparticles for the same particle volume fraction create more contact area between the solid and fluid.

Thermal conductivity of various water -based nanofluids is also depicted in Figure 4.2. From this figure, it is shown that most nanofluids exhibit higher thermal conductivity compared to water base fluid. Water containing 0.5 vol.% of Al_2O_3 (particle size:13nm) offers 12.9% augmentation compared to water base fluid. This is higher than augmentation offered by the ethylene glycol/ water-based nanofluids containing the same type and particle concentration. However, nanoparticles might be not uniformly dispersed in water base fluid compared to the ethylene glycol/ water base fluid. This could be the reason why the thermal conductivity of water base fluid with 0.5 vol.% of TiO_2 and Al_2O_3 (particle size:13nm) is lower than 0.1 vol.% nanofluids. Nanoparticles agglomeration might be high in these samples. It is known that ethylene glycol/ water has higher viscosity compared to water base fluid.

4.3 Density characteristic of nanofluid based coolants

The comparison between the reference and the measured values of density is presented in Figure 4.3. This is done in order to validate the accuracy of the density meter. From Figure 4.3, 0.8% deviation is observed for the ethylene glycol/water mixtures while water only accumulates 0.04% deviation. This shows that the selected density meter is accurate and reliable in performing measurements in this study.

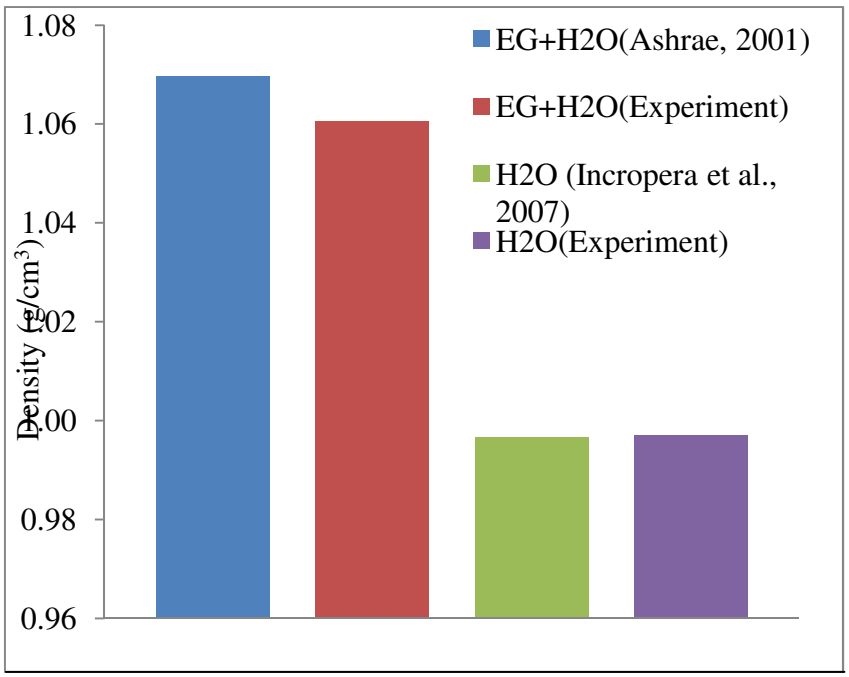

Figure 4.3 Validation of density meter (~28°C)

Comparison of the density of ethylene glycol/ water and water based nanofluids with base fluids is presented in Figure 4.4.

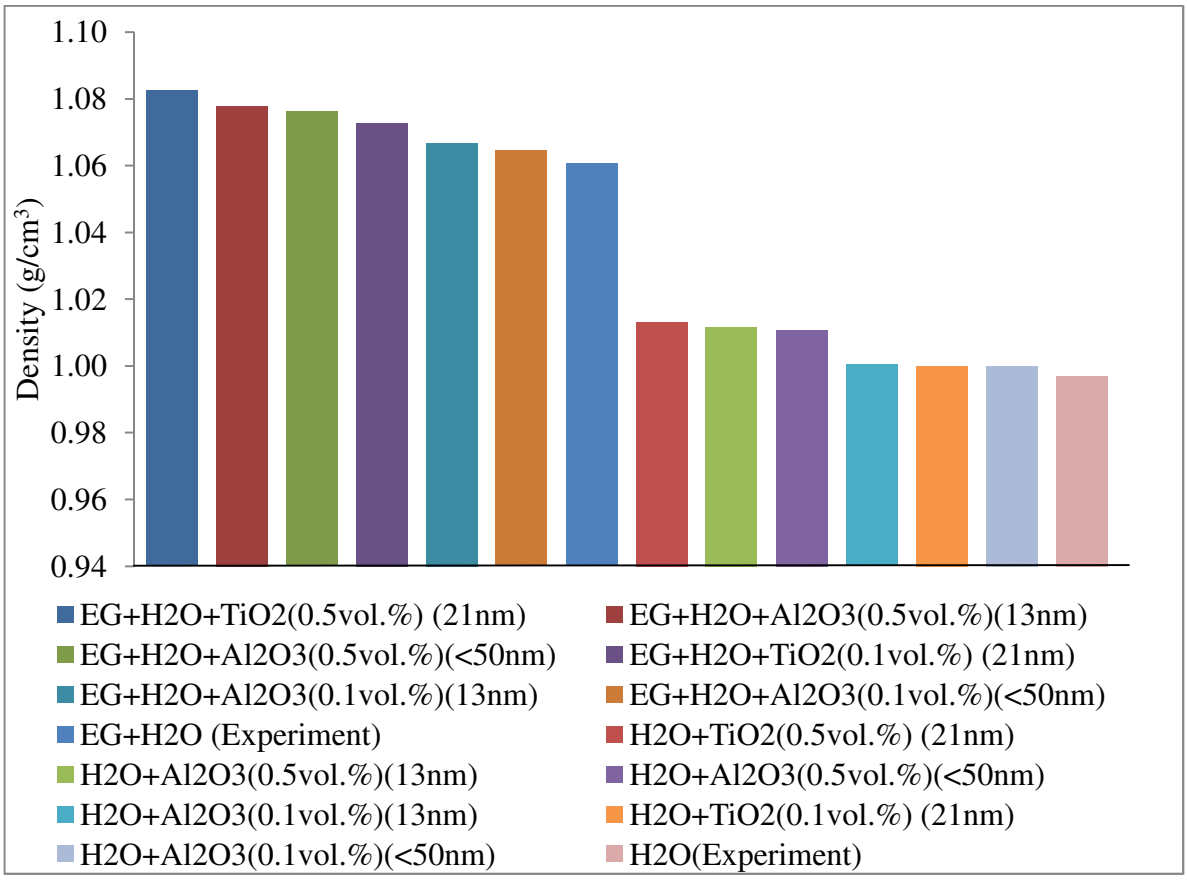

Figure 4.4 Density of ethylene glycol/water and water-based nanofluids and base fluid (~28°C)

As expected, the density of ethylene glycol-based nanofluids containing TiO_2 nanoparticles is higher than the Al_2O_3 nanofluids. This is attributed to the higher density of TiO_2 nanoparticles as compared to Al_2O_3. Incropera et al., (2007) stated that the density of TiO_2 and Al_2O_3 is 4157kg/m^3 and 3970 kg/m^3 respectively. Similar trend is also observed for water based nanofluids. This study shows that the particle type, rather than the size, plays a significant role in determining the density of nanofluids. Not much difference in density is observed for Al_2O_3 nanofluids at 13nm and <50nm particle sizes. Apart from that, density also increases with particle volume fractions.

4.4 Viscosity characteristic of nanofluid based coolants

As explained in Chapter 3, two types of instrument were used to measure viscosity of nanofluids. LVDV-III Ultra Brookfield was used to measure the viscosity of ethylene glycol/water-based nanofluids while a SV-10 viscometer was used for water-based nanofluids. Thus, the results and discussions on viscosity characteristic of nanofluids are divided into two sub-sections 4.4.1 and 4.4.2. Sub-section 4.4.1 covers the ethylene glycol/water based nanofluids while water-based nanofluids is presented in sub-section 4.4.2.

4.4.1 Viscosity of the ethylene glycol/ water -based nanofluids

Before adding nanoparticles into base fluid, the LVDV-III Ultra Brookfield rheometer was validated by measuring the viscosity of ethylene glycol and ethylene glycol/water mixture. The measured value is then compared with the values obtained from Incropera et al., (2007) and ASHRAE (2001). This is shown in Figure 4.5.

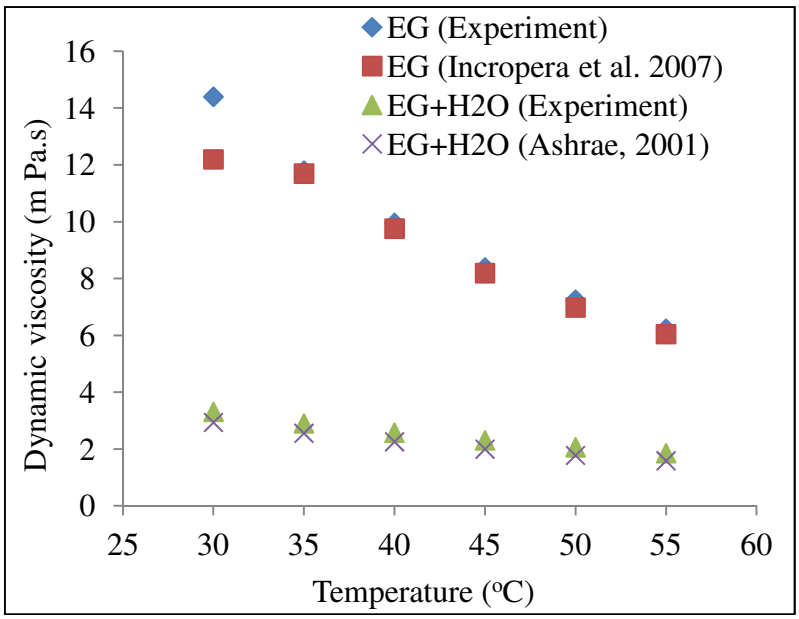

Figure 4.5 Theoretical and experimental viscosity of base fluids at different temperature

From Figure 4.5, it is deduced that there is a good agreement between the measured and standard values from text books. On the aspect of shear rate, it is successfully proved that the viscosity of ethylene glycol is independent of shear rate, thus, it is a Newtonian fluid. Figure 4.6 shows the effect of shear rate to the viscosity of ethylene glycol/water mixture at various temperatures. Ethylene glycol/water exhibits Newtonian characteristic from 30°C to 45°C.

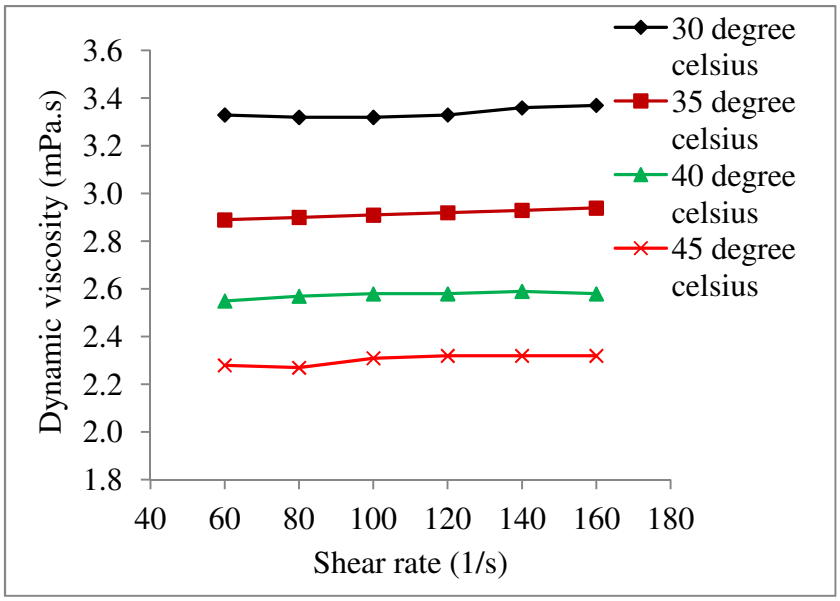

Figure 4.6 Dynamic viscosity of ethylene glycol/water mixture with respect to shear rate

Figure 4.7 shows the viscosity of ethylene glycol/ water-based nanofluids at various nanoparticle volume fractions as a function of temperature.

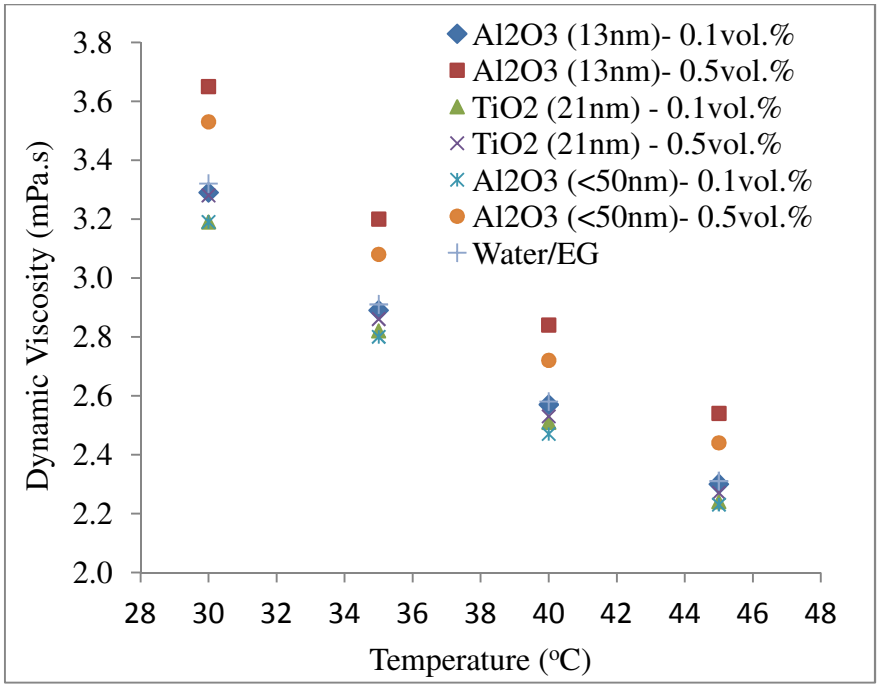

Figure 4.7. Effect of the particle volume fractions and temperature on the ethylene glycol/ water -based nanofluids

Generally, Al_2O_3 (0.5vol%. and particle size:13nm) nanofluids, demonstrate higher viscosities compared to base fluid. At 30°C, nanofluids containing 0.5vol% Al_2O_3 (particle size:13nm) experienced 9.9% augmentation compared to base fluid. This is in line with the results obtained by various researchers (Kole and Dey, 2010; Lee et al., 2011). Their results indicated that nanofluids viscosity tends to increase with the increase of nanoparticle volume fraction. Viscosity rises due to the mutual interference created by the nanoparticles as well as the interaction between the nanoparticles and base fluid. The internal shear stress also increases with nanoparticle concentration. These are supported by Yang et al., (2012) and Kole and Dey (2010). However, there are only slight differences observed for nanofluids at 0.1 vol.% loading. It is presumed that this concentration is too low to impose any effect on nanofluids viscosity. Apart from that, inclusion of TiO_2 nanoparticles into base fluid seems to give minimum effect

on viscosity for both 0.1% and 0.5% volume fractions. The TiO_2 particle size used in this study is 21nm. Particles in this suspension might be so well dispersed that agglomeration effect is minimized. Higher force is needed to overcome the nanoparticles structure due to agglomeration. Regarding the effect of temperature, it is obvious that inter-particles forces such as Van der Waals attractive force weaken with augmentation of temperature. Thus, the nanofluids viscosity is inversely proportional with temperature as shown in Figure 4.7. For instance, nanofluid viscosity irrespective of type declines approximately 30-31% when the operating temperature increases from 30 to 45^{o}C. Aside from that, Figure 4.7 also shows that nanoparticle size have effect on viscosity. For instance 3.3% increase is observed for nanofluid containing 0.1vol. % of Al_2O_3 (particle size:13nm) compared to the Al_2O_3 sizes less than 50nm at 30^{o}C. This increasing trend is also observed in the studies done by various researchers (Corcione, 2011; Duangthongsuk and Wongwises, 2009; Lu and Fan, 2008). Timofeeva et al.,(2010) explained that the total area of solid/liquid interface and the number of nanoparticles increases for the same concentration with smaller particle size. Thus it increases the electro-viscous effect due to the particle/liquid interfacial as well as the electrostatic interaction between the particles. Particles agglomeration and the flexibility of nanofluids motion depends on the electrostatic particles interaction. It becomes dominant when the particles are at smaller size, therefore, higher viscosity occurres. Lastly, Figures 4.8 and 4.9 show that all types of tested nanofluids exhibit Newtonian behaviour since they are independent of shear rate.

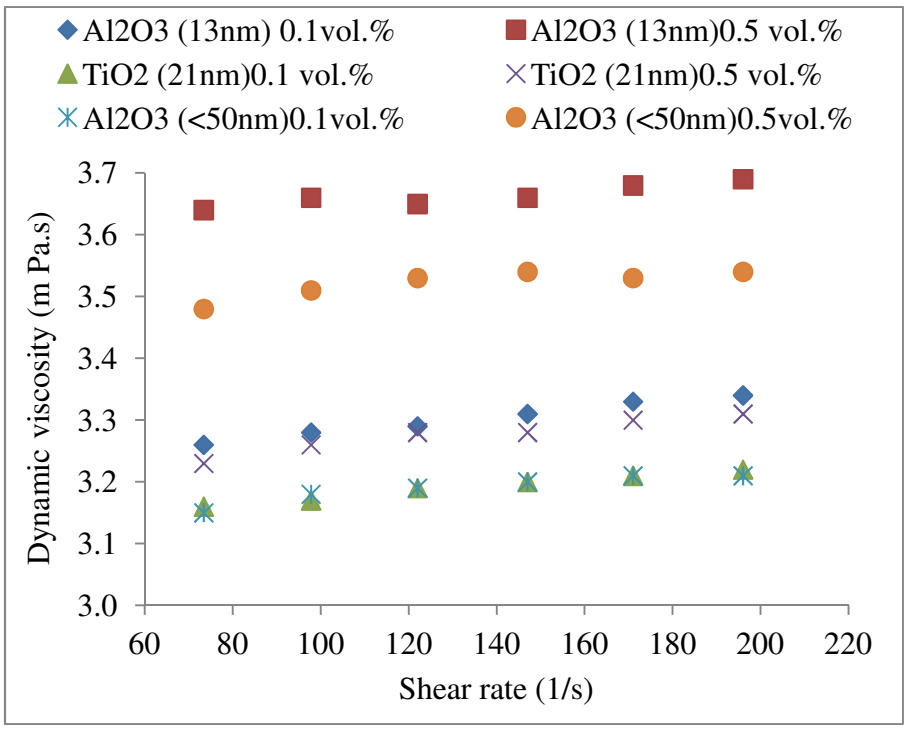

Figure 4.8 Viscosity of the ethylene glycol/water-based nanofluids with respect to shear rate at 30°C

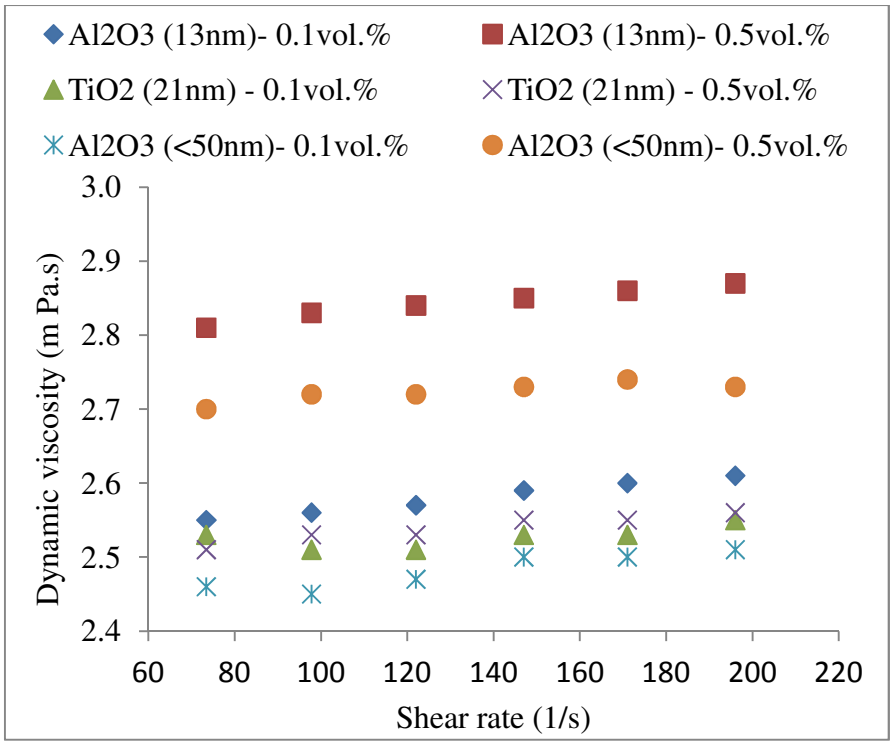

Figure 4.9. Viscosity of the ethylene /water-based nanofluids with respect to shear rate At 40°C

4.4.2 Viscosity of the water-based nanofluids

Figure 4.10 shows the comparison between measured and text book values of viscosity of water with respect to time. The maximum of 8.8% deviation is observed. Generally, both values show decreasing trend with function of temperature.

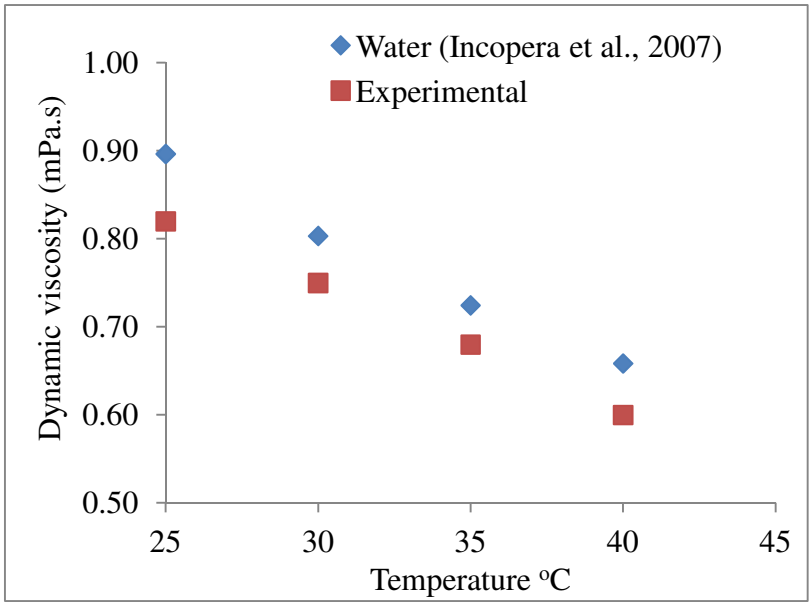

Figure 4.10 Viscosity of water (Experiment and reference values)

Figure 4.11 demonstrates the viscosity of various types of water-based nanofluids as a function of temperature. The viscosity of water-based nanofluids is definitely lower than ethylene glycol-based nanofluids. Again, it shows that viscosity decreases with the decrease of operating temperature. It is found that the heat transfer fluid's viscosity decreases when the operating temperature increases from 25°C to 40°C. Higher temperature is capable to break the van der Waals forces among the nanoparticles.

Water-based nanofluids containing 0.5vol.% Al_2O_3 (particle size: 13nm and <50nm) exhibit the highest viscosity compared to 0.1vol.% Al_2O_3 loading. Similar to previous sub-section 4.4.1, TiO_2 nanofluids demonstrate only slight differences from

the water. It can be assumed that TiO_2 is well dispersed not only in the ethylene glycol/water mixture but also in the water

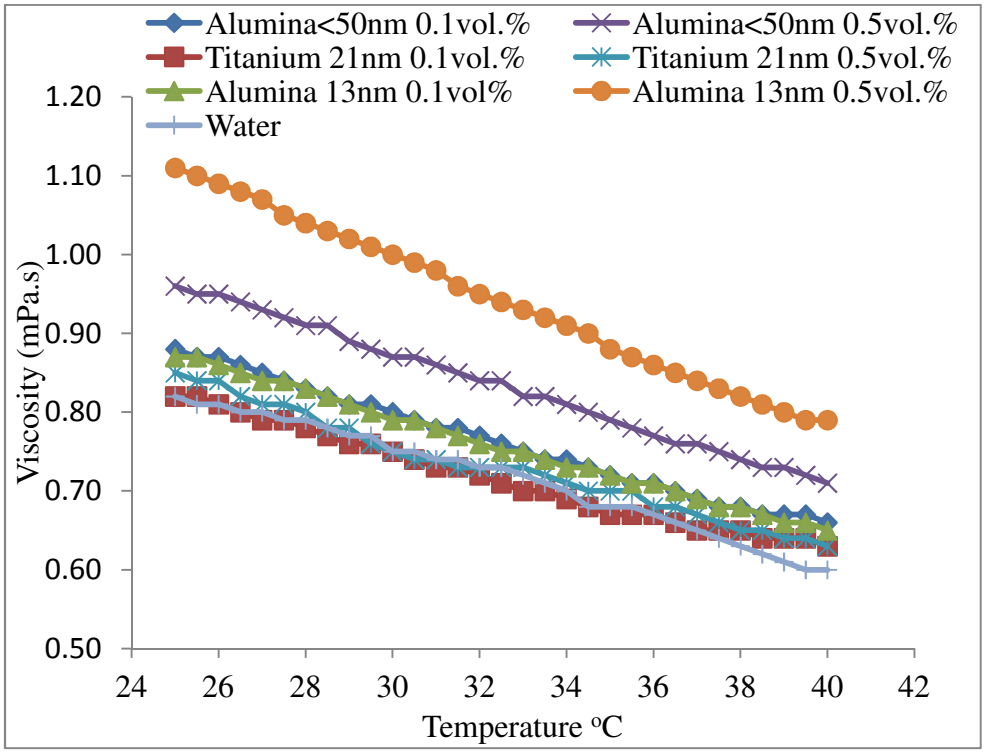

Figure 4.11. Viscosity of water-based nanofluids

4.5 Discussion on flue gas waste heat recovery through shell and tube heat exchanger

This section presents the results and discussion from modelling of shell and tube heat recovery exchanger operated with various types of nanofluids. Application of nanofluids in heat exchanger used to recover the waste heat from the flue gas. The analysis was done based on modelling as explained in sub-section 3.3.1.

4.5.1 Effect of nanoparticle volume fraction on thermal and energy performance of shell and tube heat recovery exchanger

Three types of nanofluids were used in the analysis. They are ethylene glycol based copper nanofluids, water based copper nanofluids and ethylene glycol/water based aluminium oxide and titanium dioxide nanofluids.

(a) Ethylene glycol based copper nanofluids

The effect of copper (Cu) nanoparticle volume fraction on thermal and energy performance of the heat recovery exchanger was carried out. In this analysis, the flue gas and coolant flow rate were kept constant at 26.3 kg/s and 111.6 kg/s, respectively. In this condition, the flue gas convective heat transfer coefficient was found to be 56.4W/m^{2}K. The sample calculation for flue gas convective heat transfer coefficient is shown in Appendix G. With the increase of the nanoparticle volume fractions, the coolant Reynolds's number decreases as shown in Figure 4.12.

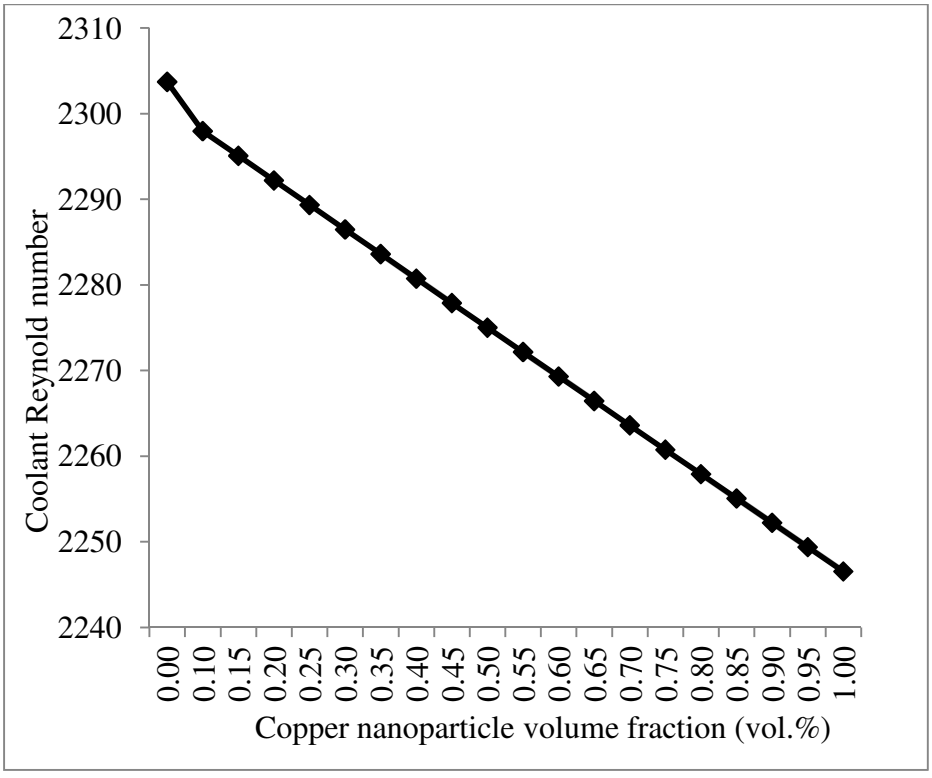

Figure 4.12 Effect of copper volume fraction to coolant Reynolds number at constant flue gas and coolant mass flow rate

In this analysis, all parameters except dynamic viscosity of coolant were kept constant. It is noted that, dynamic viscosity of coolant increases with nanoparticle volume fraction. Addition of nanoparticles increases the fluid shear stress associated with a higher dynamic viscosity. Substituting a higher value of this property into Equation (3.11) definitely decreases the coolant Reynolds number as shown in Figure 4.12. It is assumed that the flow is of laminar type.

Study found that the convective heat transfer coefficient for nanofluids is proportional with the nanoparticle volume fractions as depicted in Figure 4.13

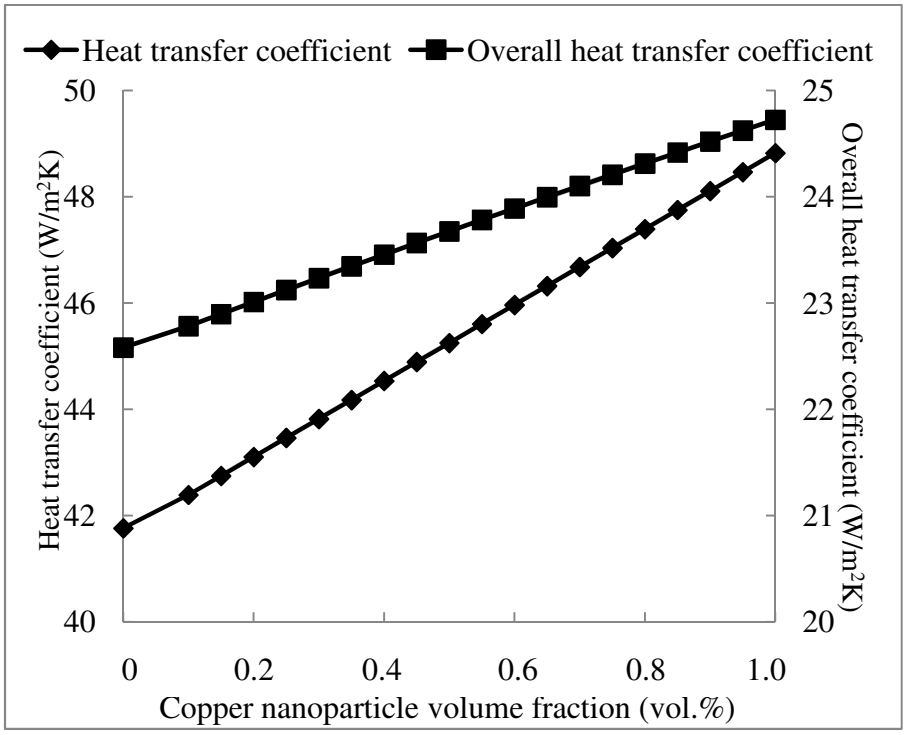

Figure 4.13 Effect of copper volume fraction to coolant convective heat transfer coefficient and overall heat transfer coefficient at constant flue gas and coolant mass flow rate.

In Equation (3.14), nanofluid heat transfer coefficient increases since it exhibits higher thermal conductivity with the increase of nanoparticle volume fraction. Figure 4.13 also depicts a higher overall heat transfer coefficient observed with copper nanoparticle volume fraction. About 9.5% augmentation was observed at 1vol.% copper nanoparticles compared to the base fluid. Typical calculation of the overall heat transfer

coefficient is shown in Appendix G. Heat transfer enhancement was observed with the particle volume fractions as shown in Figure 4.14.

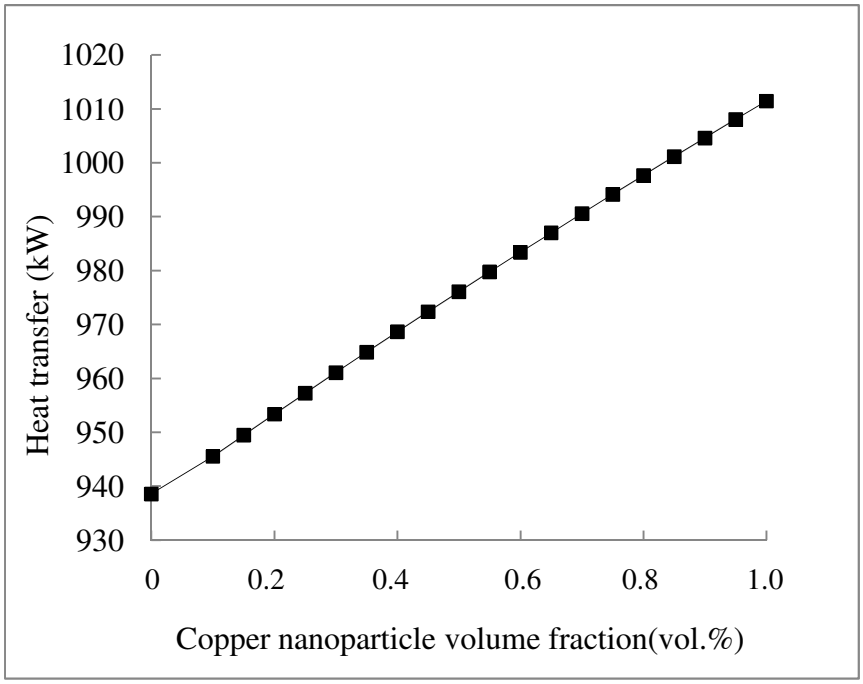

Figure 4.14 Effect copper volume fraction to heat transfer rate at constant flue gas (26.3kg/s) and coolant (111.6 kg/s) mass flow rate.

Heat transfer was calculated by using Equation (3.22). In this equation, the effectiveness of the heat recovery exchanger was found to increase with copper nanoparticle volume fraction. For instance, with an addition of 1vol. % copper nanoparticles in ethylene glycol-based fluid, 7.8% heat transfer enhancement was observed at 26.3 kg/s and 111.6 kg/s flue gas mass flow rate and coolant mass flow rate, respectively. Higher thermal conductivity of nanofluid probably is the main reason contributing to heat transfer enhancement. More heat can be absorbed and transferred with the application of nanofluids. The potential mechanism of thermal conductivity enhancement is due to the nanoparticles' heat transfer behavior as well as the formation of liquid-particle interface layer.

As for energy needed to pump the coolant, findings implied that the pressure drop decreased with copper nanoparticle volume fractions as shown in Figure 4.15.

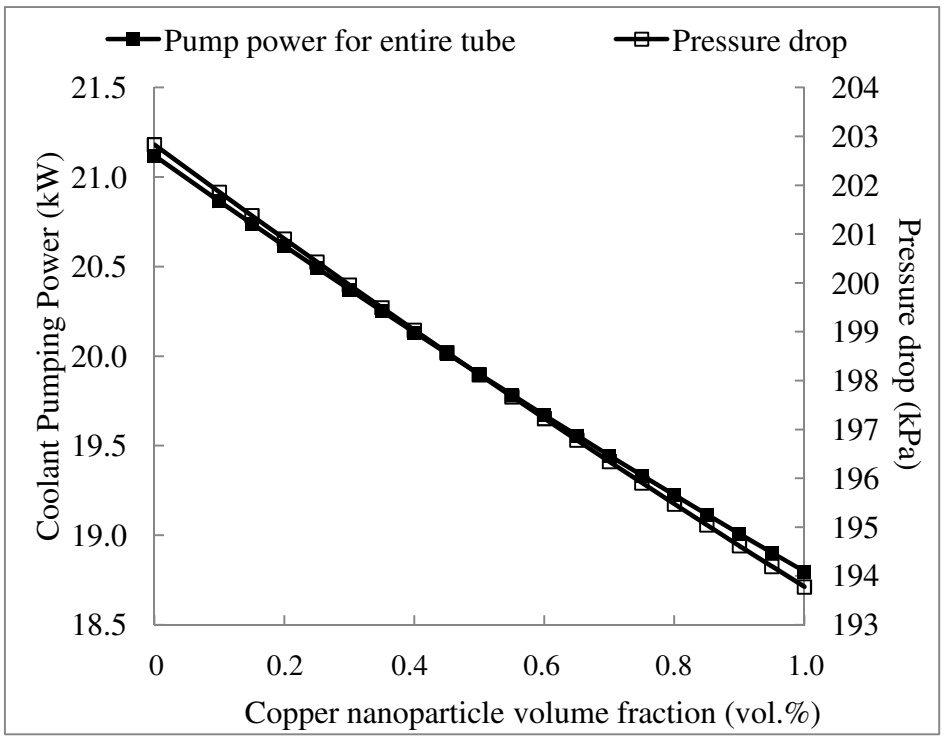

Figure 4.15 Effect copper volume fraction to coolant pressure drop and pump power at constant flue gas (26.3kg/s) and coolant (111.6 kg/s) mass flow rate.

Therefore, lower pumping power is needed when nanofluids is used in the heat recovery exchanger. About 10.99% less power or energy was observed at 1% nanoparticle volume fraction compared to ethylene glycol base fluid. In the present analysis, the coolant mass flow was kept constant. As a result, the coolant velocity decreases with particle volume fractions. Equation (3.25) shows that velocity decreases due to the increase of nanofluids density. Definitely, nanofluids density increases due to the higher density of nanoparticles. Nanofluids density can be determined based on rule of mixture as shown in Equation (3.5). The lower value of velocity decreases the pressure drop substantially.

(b) Water based copper nanofluids

Similar analysis was done on water based copper nanofluids. In this analysis, the coolant mass flow rate is fixed at 12 kg/s. Laminar flow was observed for this mass flow rate. Other parameters were the same as in the previous analysis. Table 4.1 depicts

the summary of thermal and energy performance enhancement of heat recovery exchanger operated with water based copper nanofluids compared to base fluid.

Table 4.1 Thermal and energy performance of water -based nanofluids containing 2% of copper nanoparticles compared to water base fluid at 12kg/s mass flow rate

Number	Description	Water based copper nanofluids
1	Coolant convective heat transfer enhancement	33.4%
2	Overall heat transfer coefficient enhancement	10.11%
3	Heat transfer enhancement	4.53%
4	Pump power (lesser)	22.5%

(c) Ethylene glycol/water based aluminium oxide and titanium dioxide nanofluids

Figure 4.16 depicts the overall heat transfer coefficient of the shell and tube heat recovery exchanger operated with ethylene glycol/water based Al_2O_3 and TiO_2 nanofluids. These nanofluids based coolants exhibit higher overall heat transfer coefficient compared to water. From this figure, it is observed that ethylene glycol/water based Al_2O_3 (particle size: 13nm) offers the highest overall heat transfer coefficient attributed to its highest thermal conductivity enhancement as described in sub-section 4.2.

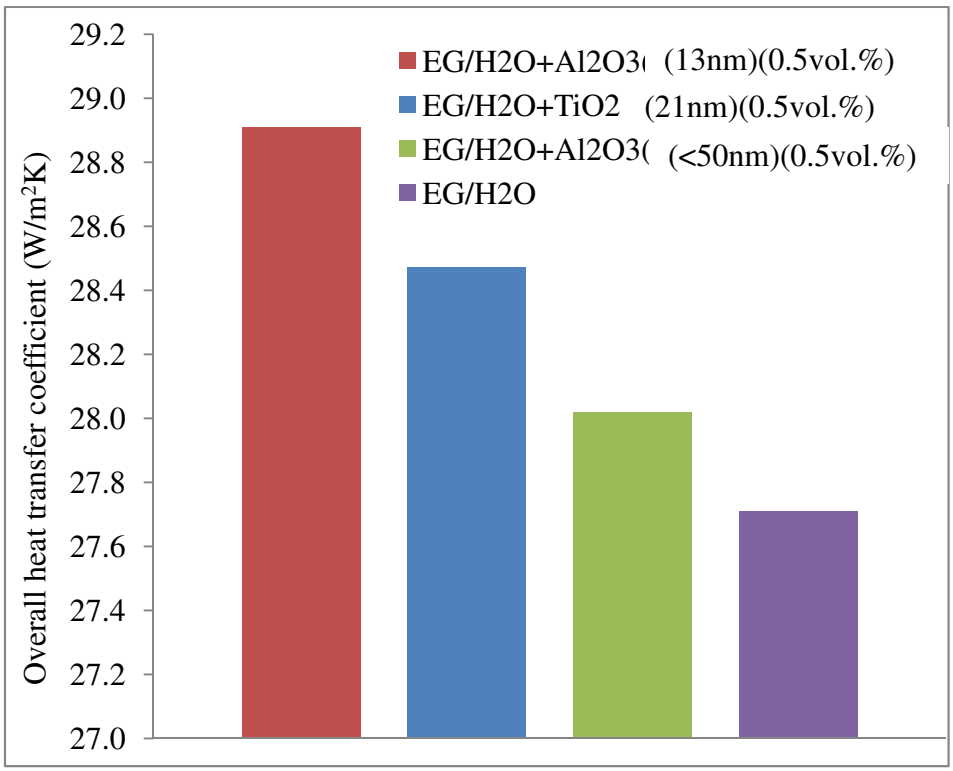

Figure 4.16 Overall heat transfer coefficient of shell and tube heat recovery exchanger operated with ethylene glycol/water -based nanofluids

4.5.2 Effect of flue gas mass flow rate on thermal performance of shell and tube heat recovery exchanger

This section discusses the influence of flue gas mass flow rate to thermal performance of heat recovery exchanger. The coolant mass flow rate was fixed at 111.6 kg/s. Flue gas Reynolds's number was found to increase with mass flow rate as calculated in Equation (3.3). In this equation, the cross flow area, equivalent diameter and flue gas dynamic viscosity were kept constant. Then, the higher value of flue gas convective heat transfer was calculated using Equation (3.4). In Equation (3.4), the Reynolds's number was increased with mass flow rate. Other parameters such as equivalent diameter and flue gas Prandtl number were kept constant. Hence, convective heat transfer coefficient of flue gas is proportional to mass flow rate as shown in Figure 4.17. It is due to the large number of random and bulk motion of flue gas molecules.

This value was substituted into Equation 3.15 to calculate the overall heat transfer coefficient which was found to be proportional to flue gas mass flow rate as depicted in Figure 4.18.

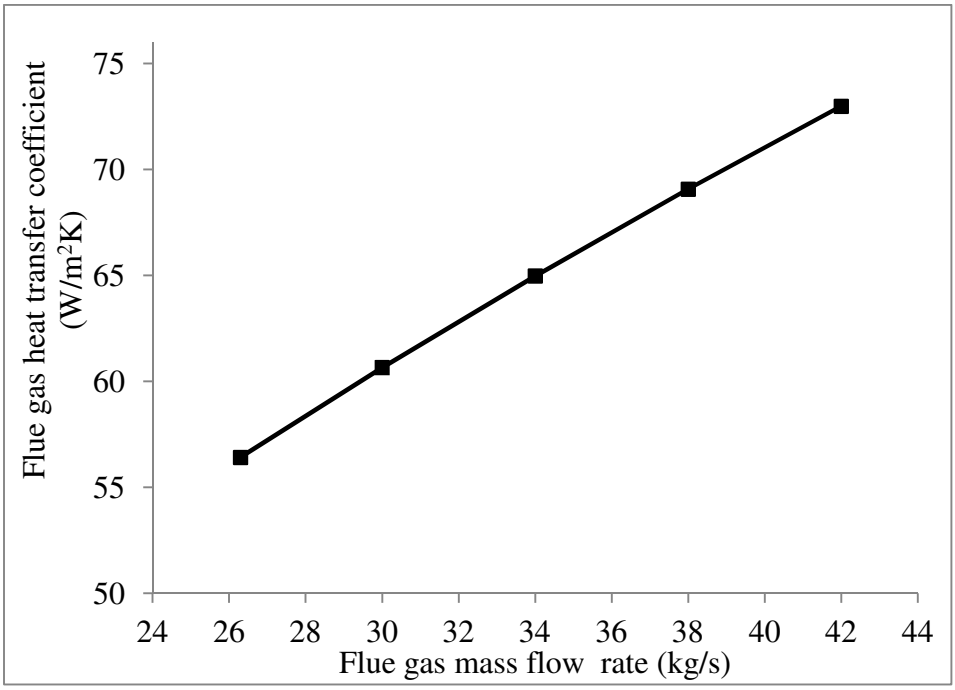

Figure 4.17 Effect of flue gas mass flow rate to flue gas convective heat transfer coefficient

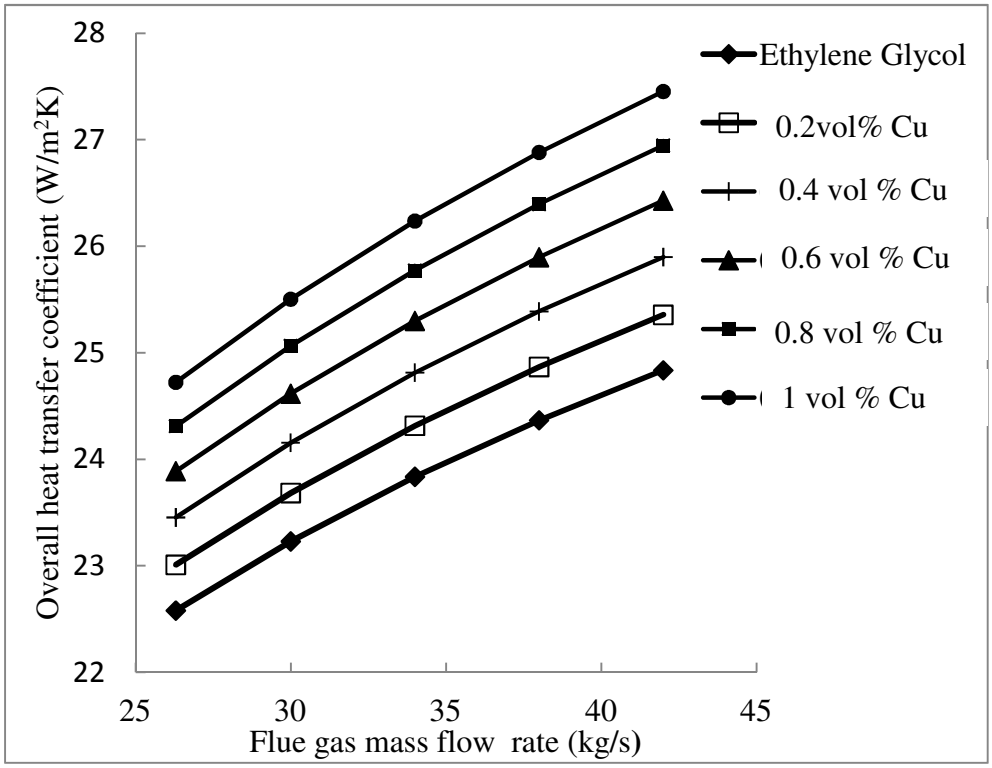

Figure 4.18. Effect of flue gas mass flow rate to overall heat transfer coefficient

As the flue gas mass flow rate increases, more energy can be transferred from the flue gas to the coolants due to the extensive random and bulk motion of flue gas molecules. Increase of flue gas mass flow rate will decrease the thermal resistance of flue gas. It also shows that overall heat transfer coefficient increases with the augmentation of particle volume fraction. Moreover, thermal conductivity of nanofluids increases with the particle volume fraction. Higher value of thermal conductivity leads to the higher amount of heat that can be transferred by the nanofluid. Figure 4.19 shows that the heat transfer rate of 1vol.% copper nanofluids is higher than of base fluid.

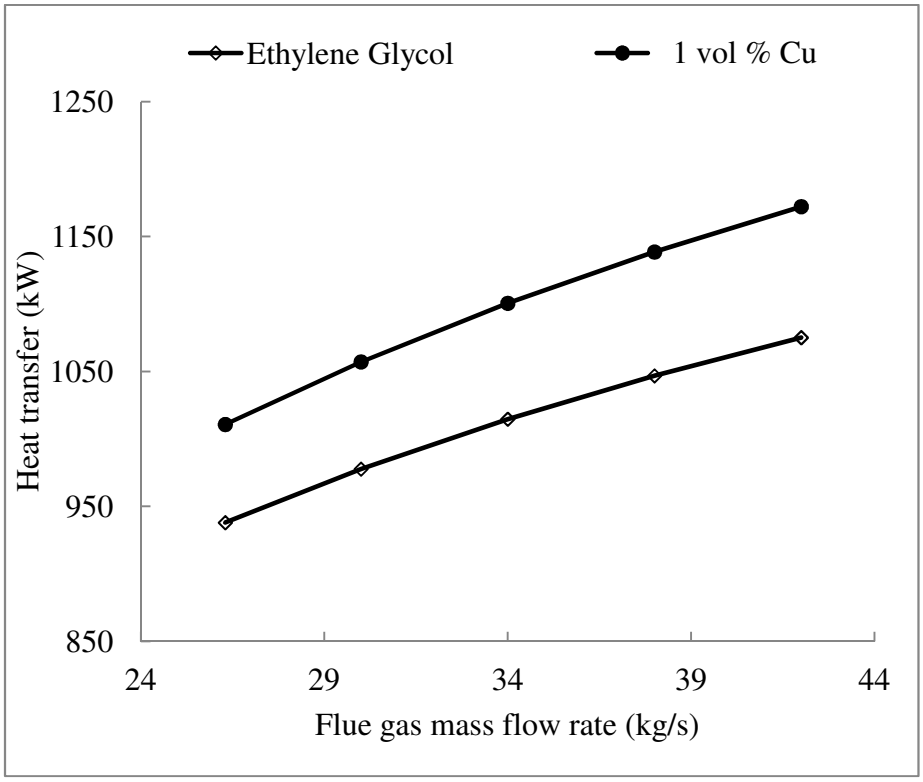

Figure 4.19. Effect of flue gas mass flow rate to heat transfer rate

At 1% of copper nanofluids, 15.97% heat transfer enhancement is observed when flue gas mass flow rate increased from 26.3 kg/s to 42 kg/s.

4.5.3 Effect of coolant mass flow rate on thermal performance of shell and tube heat recovery exchanger

This section presents the effect of coolant Reynolds number on the thermal performance of heat recovery exchanger. Based on Equation 3.11, it was found that coolant Reynolds number is proportional with mass flow rate at constant volume fraction of copper nanoparticle. With the increase of coolant's Reynolds number, Nusselt number was increased as calculated using Equation 3.13. Equation 3.13 was used since the calculated Reynolds number indicated that flow is of turbulent type. Substituting a higher value of Nusselt and nanofluids thermal conductivity, the convective heat transfer of coolants was higher than base fluid, which is obtained from Equation 3.14. The same happened for overall heat transfer coefficient which is depicted in Figure 4.20.

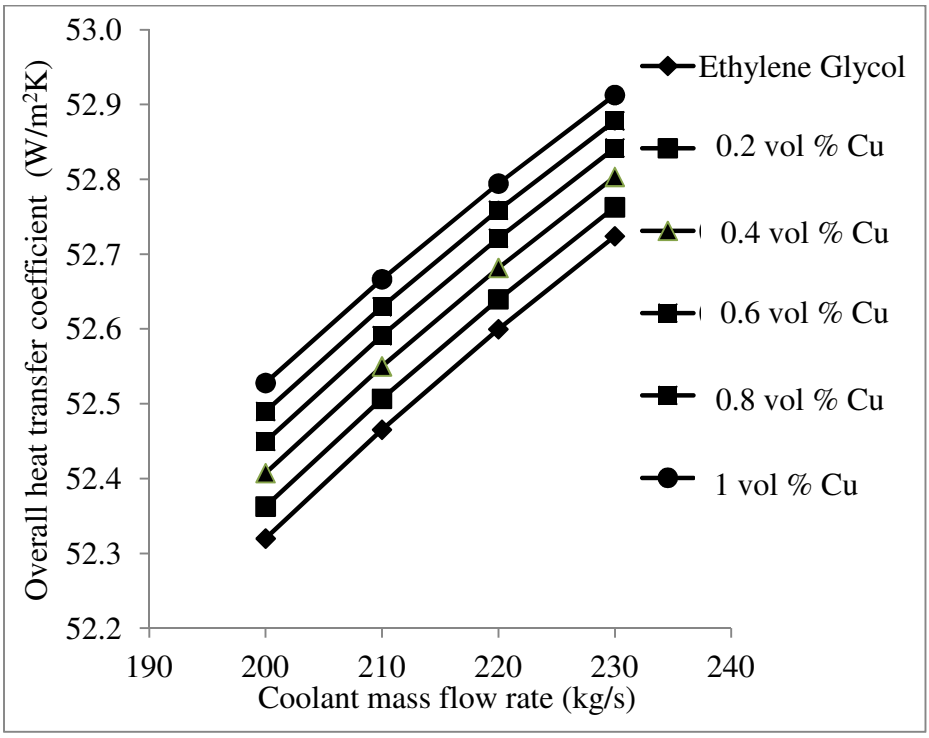

Figure 4.20. Effect of coolant mass flow rate to overall heat transfer coefficient

Similar to previous analysis, heat transfer rate is proportional to coolant mass flow rate as shown in Figure 4.21.

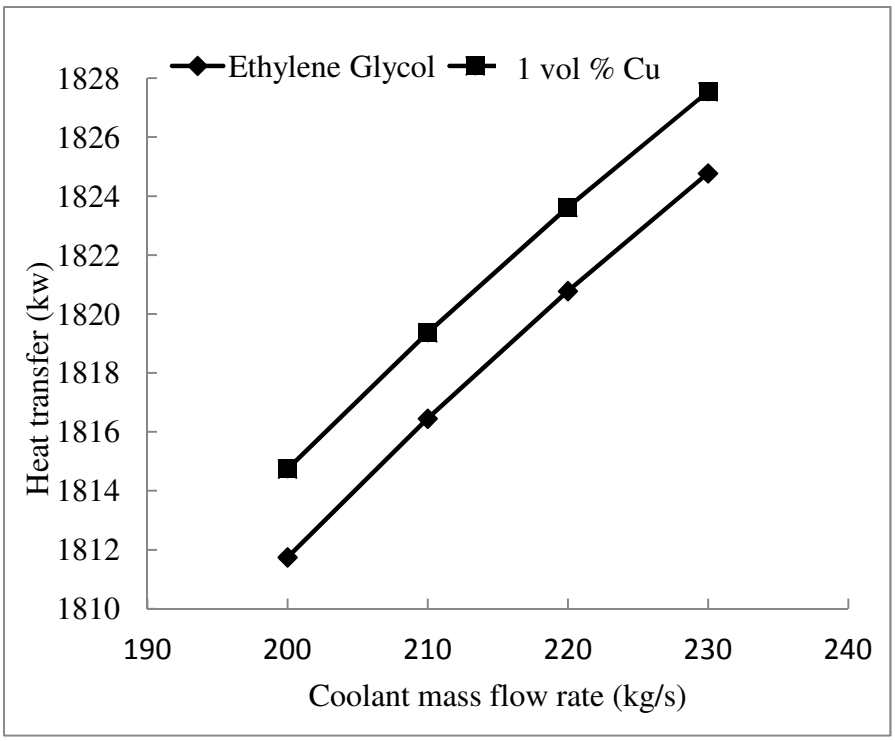

Figure 4.21. Effect of coolant mass flow rate to heat transfer rate

However, only 0.7% enhancement is observed when compared with 234kg/s and 200kg/s mass flow rate at 1vol.% of copper nanofluids. This indicates that the coolant mass flow rate only plays a minor role in enhancing the heat transfer rate compared to mass flow rate of flue gas.

4.5.4 Comparison of studies

Outcome of the previous section indicates that the overall heat transfer coefficient increases with the usage of nanofluids. This parameter depends on the convective heat transfer coefficient of nanofluids as shown in Equation (3.15). Overall heat transfer coefficient increases with convective heat transfer coefficient. Equation (3.14) also indicates that convective heat transfer coefficient is proportional to Nusselt number. Aside from the thermal conductivity, heat transfer coefficient of nanofluids plays a crucial role in determining the performance of a heat recovery system. To further strengthen the validity of the results of current study, comparisons have been

made with the study conducted by Hojjat et al. (2011). In that study, the authors investigated the thermal performance of a uniformly heated circular tube. The present study compares the Nusselt number of the nanofluid with deionized water in a circular tube. The higher value of Nusselt number definitely increases the heat transfer coefficient of the base fluid. Moreover, Ijam and Saidur (2012) revealed that convective heat transfer increases with fluid's thermal conductivity. The comparison result is shown in Figure 4.22.

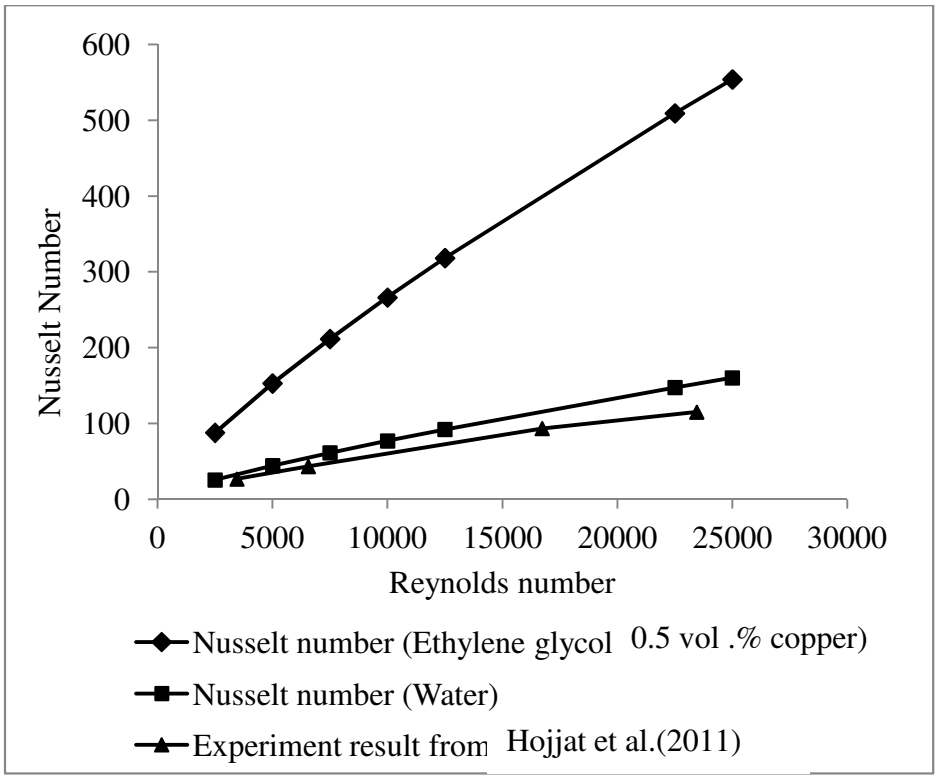

Figure 4.22. Comparison of studies

The Nusselt numbers for ethylene glycol based 0.5vol. % copper nanofluid and water has been calculated in the present study. It is found that Nusselt number for nanofluid is higher than deionized water determined by Hojjat et al., (2011). From this, it can be proved that the application of nanofluids is capable of improving the convective heat transfer coefficient of the base fluid. In addition, results from literatures also indicate that application of nanofluids improve the thermal performance of the heat exchanger. Kulkarni et al. (2008) found that superior performance of convective heat transfer

coefficient contributed by nanofluids leads to higher efficiency of waste heat recovery. It is also found that application of nanofluids in radiator increases the Nusselt number of the base fluid (Peyghambarzadeh et al., 2011a; Peyghambarzadeh et al., 2011b). As mentioned previously, Nusselt number is proportional to convective heat transfer coefficient. Thermal performance of shell and tube gas cooler in refrigeration system was improved with the application of nanofluids (Jahar, 2011). From these proven experimental results, there should be no doubt on the usefulness of nanofluids in heat exchangers, in particular shell and tube heat exchangers.

The following sub-section (4.6) will cover the size estimation of shell and tube heat recovery exchanger operated with nanofluids. It includes possible size reduction of shell diameter, number of tubes and etc.

4.6 Energy saving associated with size reduction of shell and tube heat recovery exchanger

The thermal performance enhancement of shell and tube heat recovery as explained in previous sub-section provides an opportunity to reduce the size of the heat exchanger without affecting its thermal performance. Smaller size of heat exchanger requires less material and energy for processing. The results obtained from this sub-section are based on mathematical modelling described in sub-sections 3.3.2.1-3.3.2.3.

4.6.1 Effect of ethylene glycol based copper nanofluids on geometries of shell and tube heat recovery exchanger

In this section, size reduction analysis of a heat exchanger is carried out. Figure 4.23 shows that 7.1% reduction of heat transfer area can be achieved with 1vol.% of copper nanoparticles.

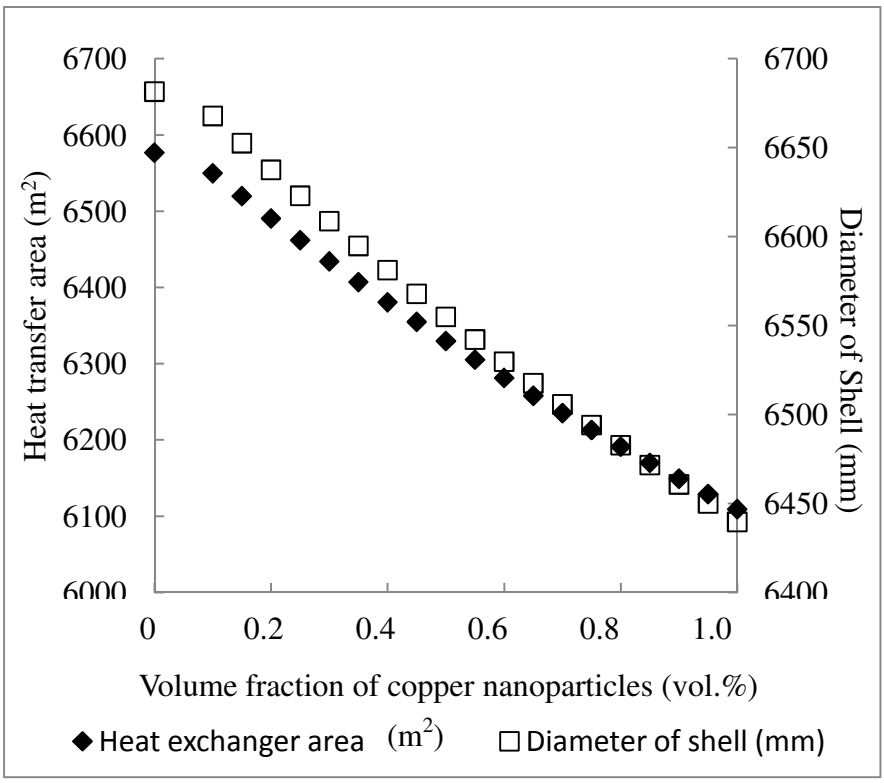

Figure 4.23. Effect of copper volume fraction to heat transfer area and shell diameter of shell and tube heat exchanger operated with ethylene glycol-based nanofluids

Inclusion of copper nanoparticles into base fluid increases the convective heat transfer coefficient and eventually the overall heat transfer coefficient of the heat exchanger due to enhancement of nanofluids thermal conductivity. Formation of solid and liquid interfacial nanolayer and Brownian motion contribute to higher thermal conductivity of nanofluids (Leong et al., 2010). Jung and Yoo (2009) suggested that, electric double layer produces interparticle interaction which contributes most significantly to the improvement of nanofluids thermal conductivity. Moreover, addition of nanoparticles will delay and create a disturbance of a thermal boundary layer which eventually improves the convective heat transfer. Substitution of higher value of overall heat transfer coefficient will decrease the required heat transfer area as shown in Equation (3.29). In this equation, the heat capacity, Q and log mean temperature difference values, LMTD are kept constant. Log mean temperature

difference is determined using Equation (3.30). Reduction of overall shell diameter is estimated using Equation (3.31) and depicted in Figure 4.23. It is found that volume fraction of copper nanoparticles is inversely proportional to the shell diameter. About 3.6% reduction of shell diameter is achieved using 1% of copper nanoparticles. In this equation, all the parameters were kept constant except the heat transfer area. Heat transfer area is determined based on Equation (3.29) while other parameters are determined based on the heat exchanger geometry as mentioned in sub-section 3.3.2.1. Substitution of lower heat transfer area will definitely decrease the overall shell diameter. Figure 4.24 shows that the volume fraction of nanoparticles is inversely proportional to the number of tubes.

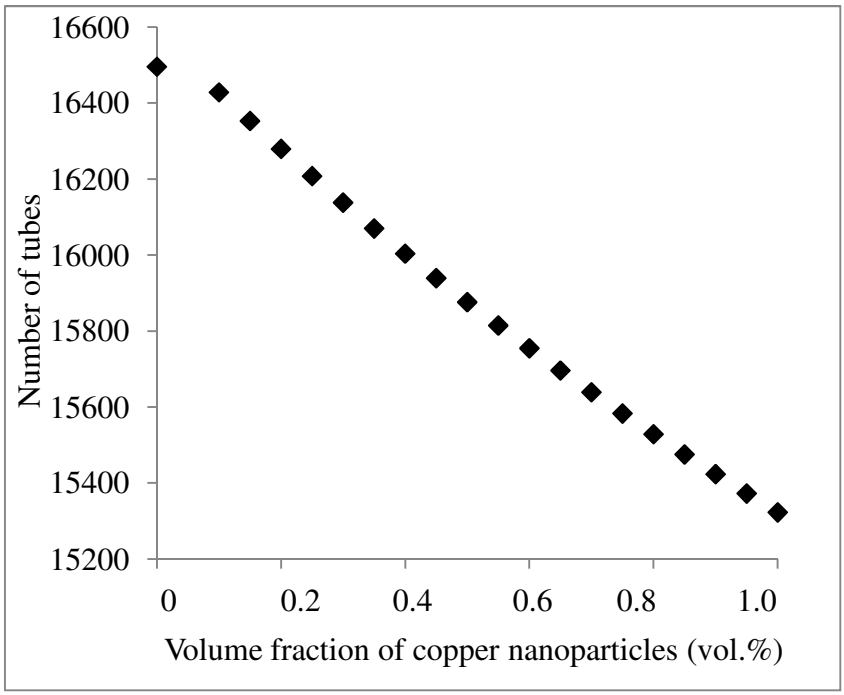

Figure 4.24 Effect of copper volume fraction to number of tubes in shell and tube heat exchanger operated with ethylene glycol-based nanofluids

The number of tube is obtained based on Equation (3.32). Geometry specifications of heat exchanger are kept constant except the diameter of the shell. Study found that number of tubes is decreased with the increase of copper nanoparticles. Figure 4.25 depicts the calculated convective heat transfer values for tube side. The calculated

convective heat transfer values are determined based on the obtained heat exchanger geometric values. The detail calculations are shown in Appendix G.

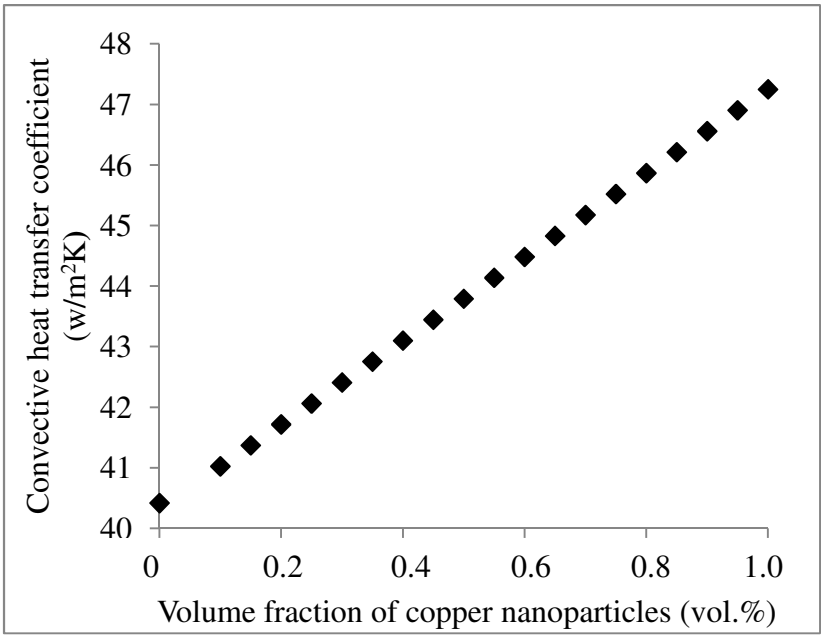

Figure 4.25 Calculated tube side heat transfer coefficient for shell and tube heat exchanger operated with ethylene glycol-based nanofluids

It is revealed that the convective heat transfer coefficient of tube side is increased although smaller size of heat exchanger is used. The convective heat transfer coefficient for tube side is calculated based on Equations (3.9)-(3.14).

4.6.2 Effect of water based copper nanofluids on the geometries of shell and heat recovery exchanger

About 4% area reduction is observed at 2.5 vol. % of copper nanoparticles. For the shell diameter, 2% reduction was observed. As for number of tubes, 4% reduction was observed. These results are shown in Figures 4.26 and 4.27.

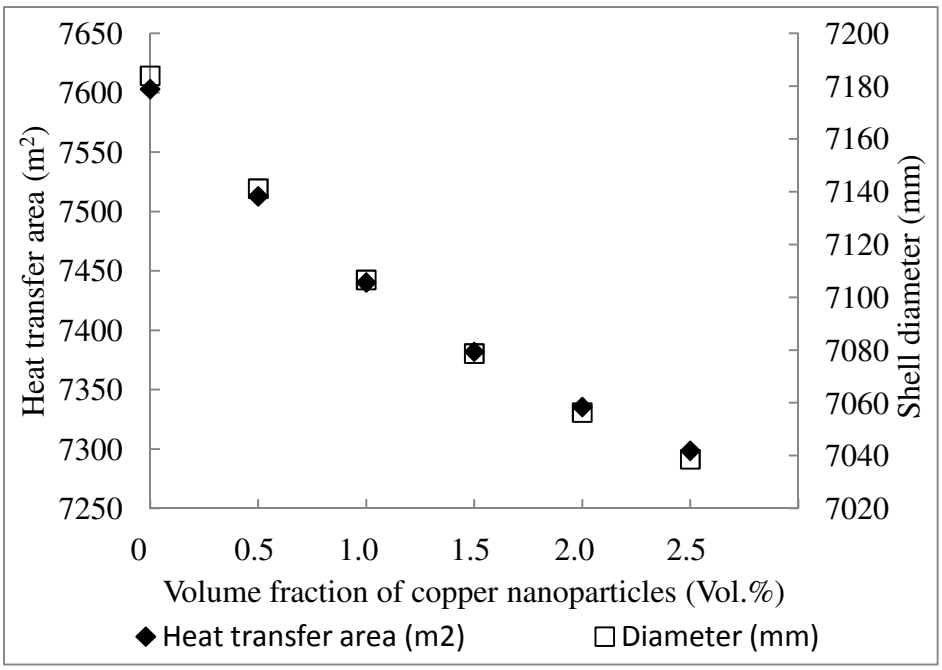

Figure 4.26 Effect of copper volume fraction to heat transfer area and shell diameter of shell and tube heat exchanger operated with water-based nanofluids

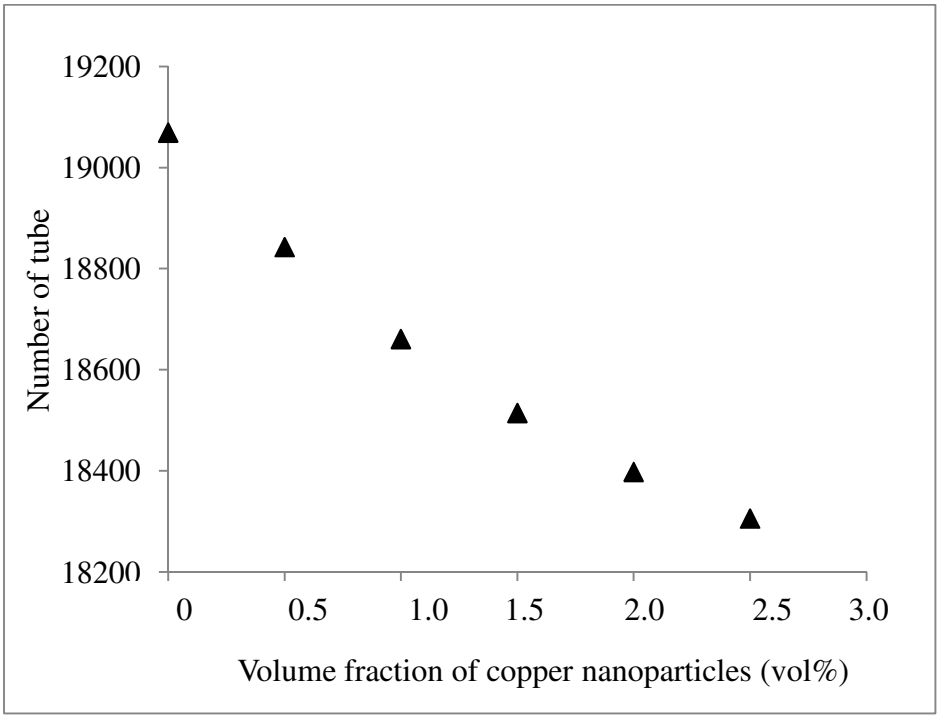

Figure 4.27 Effect of copper volume fraction to number of tubes in shell and tube heat exchanger operated with water-based nanofluids

The calculated convective heat transfer for tube side of heat exchanger is shown in Figure 4.28. Similar to the previous section, higher convective heat transfer coefficient is observed although smaller size of heat exchanger is used.

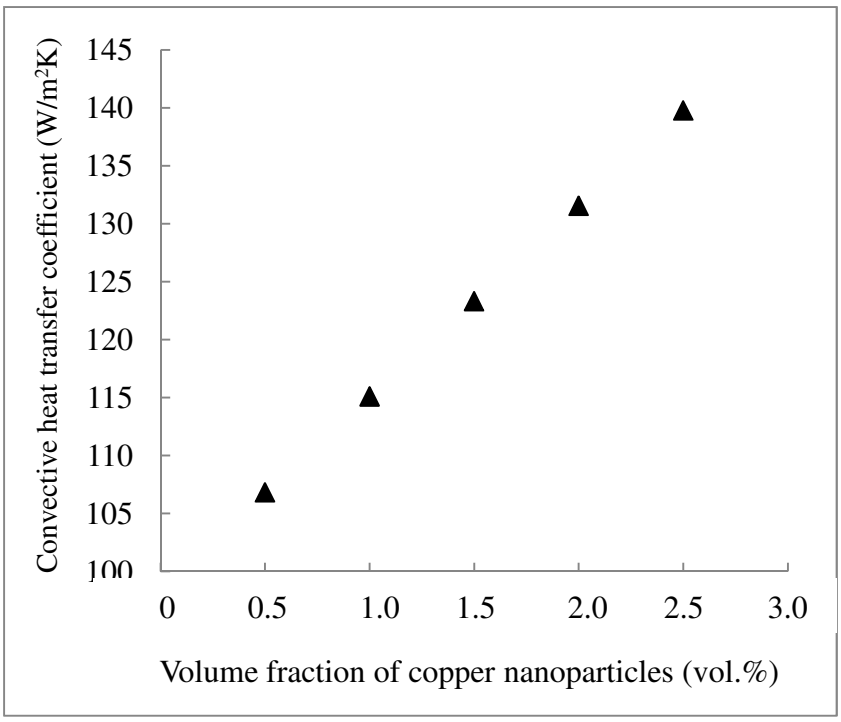

Figure 4.28. Calculated tube side convective heat transfer coefficient of shell and tube heat exchanger operated with water-based nanofluids

4.6.3 Energy savings

From section 4.6.1 and 4.6.2, it is implied that smaller heat exchanger with nanofluids is capable to produce similar thermal performance to the normal size heat exchanger without nanofluids. Hence, in this section the possibility of energy savings associated with size reduction is presented. Reduction of size is inclusive of the diameter of shell and number of tubes. In this study, it is presumed that the materials for shell and tube are steel and copper, respectively. Reduction of size is associated with energy savings for material processing as shown in Figures 4.29 and 4.30.

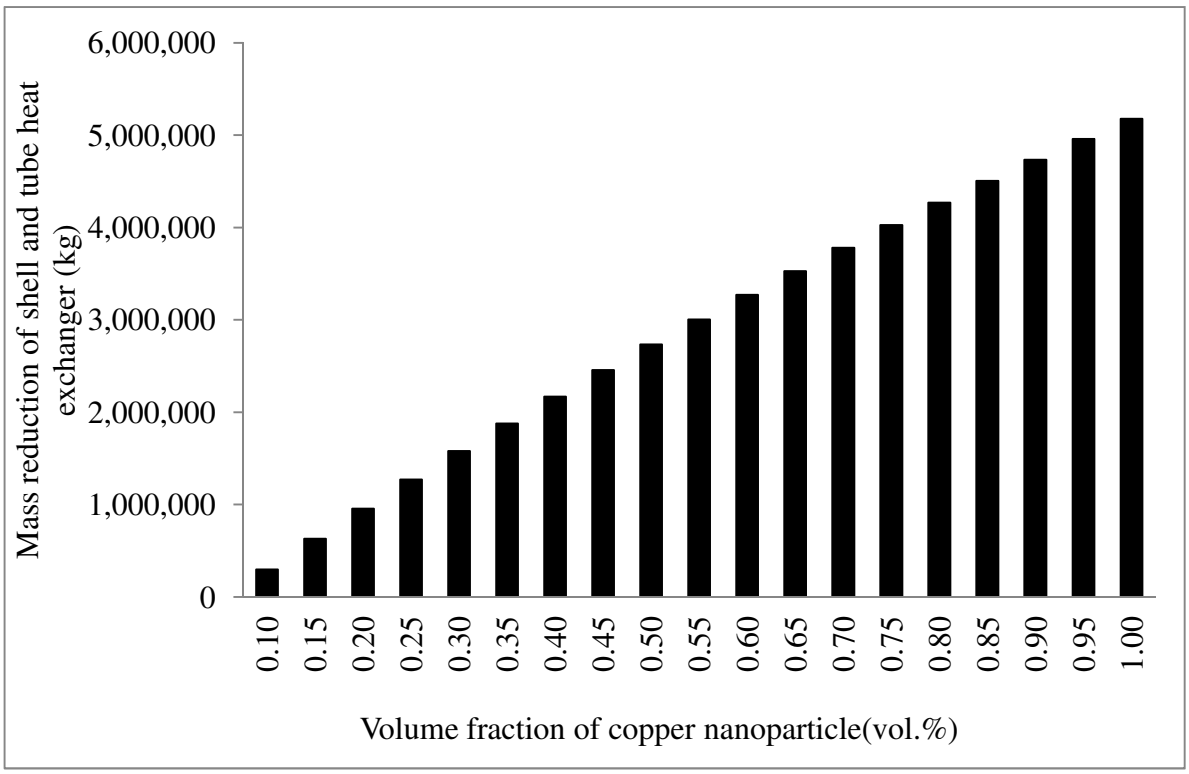

Figure 4.29 Mass reduction of shell and tube heat recovery exchanger operated with ethylene glycol-based copper nanofluids

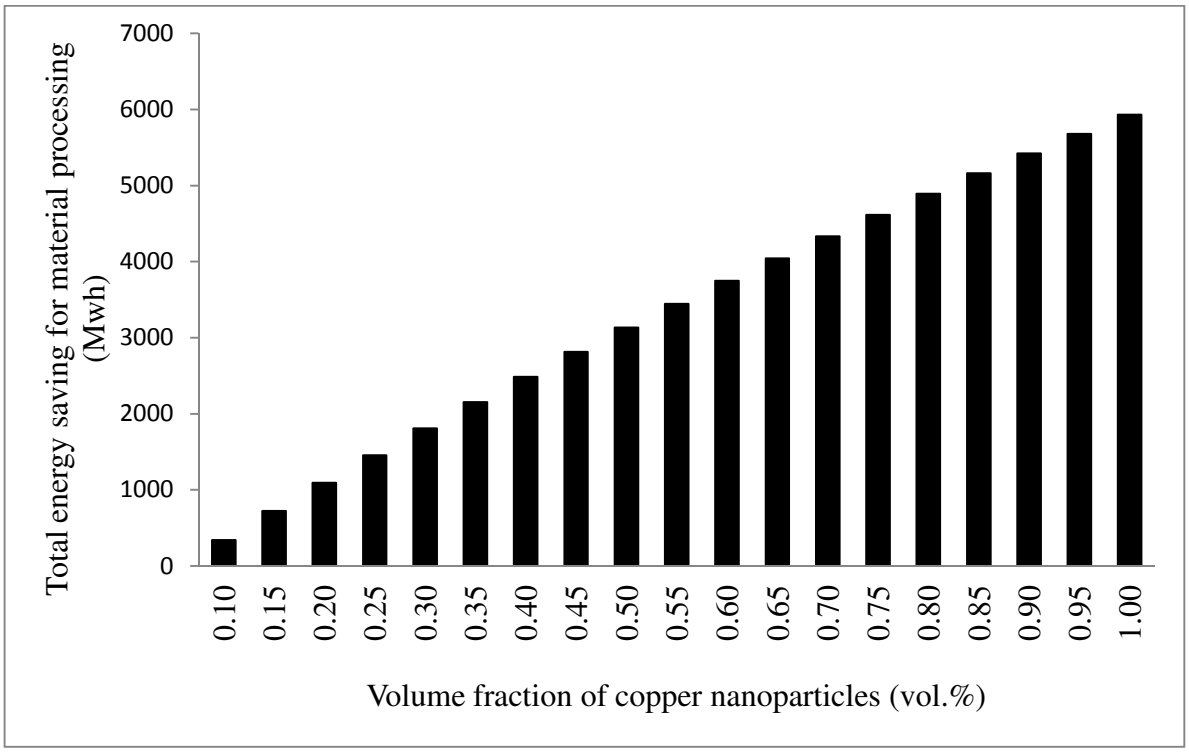

Figure 4.30 Energy saving of material processing of shell and tube heat recovery exchanger operated with ethylene glycol-based copper nanofluids

Observation of 5932.9MWh energy savings can be achieved at 1% copper volume fraction. This analysis is done on energy savings for a total of 1,000 shell and tube heat

recovery exchangers. Smaller size of heat exchanger requires fewer materials which will eventually decrease the energy needed for material processing. This can be explained by using Equations (3.33) - (3.34). Smaller size of heat exchanger definitely decreased the value of heat exchanger volume. Substitution of lower value of volume into Equation (3.33) will lead to fewer amounts (mass) of needed material. Finally, the energy required for material processing is determined using Equation (3.34). Equation (3.35) - (3.36) show the formulation used to calculate the mass reduction and energy savings of heat exchanger. Sample calculation of the energy saving is shown in Appendix G. Figure 4.31 and 4.32 show the energy savings associated with mass reduction of heat exchanger using water based copper nanofluids.

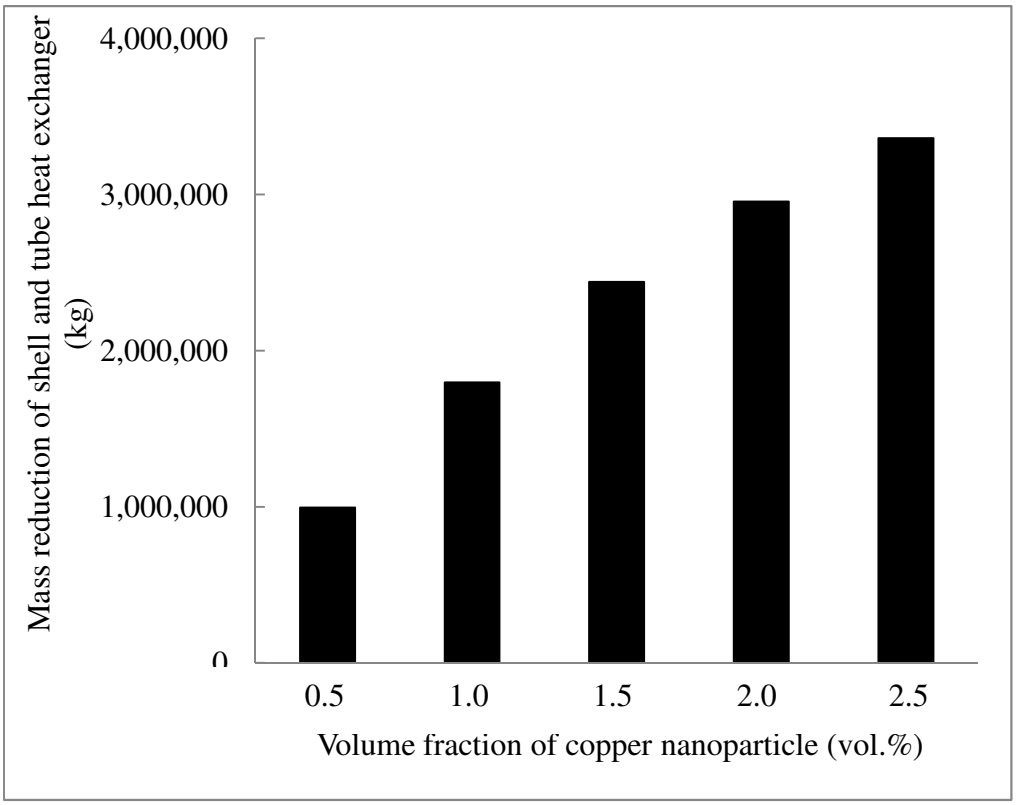

Figure 4.31 Mass reduction of shell and tube heat recovery exchanger operated with water- based copper nanofluids

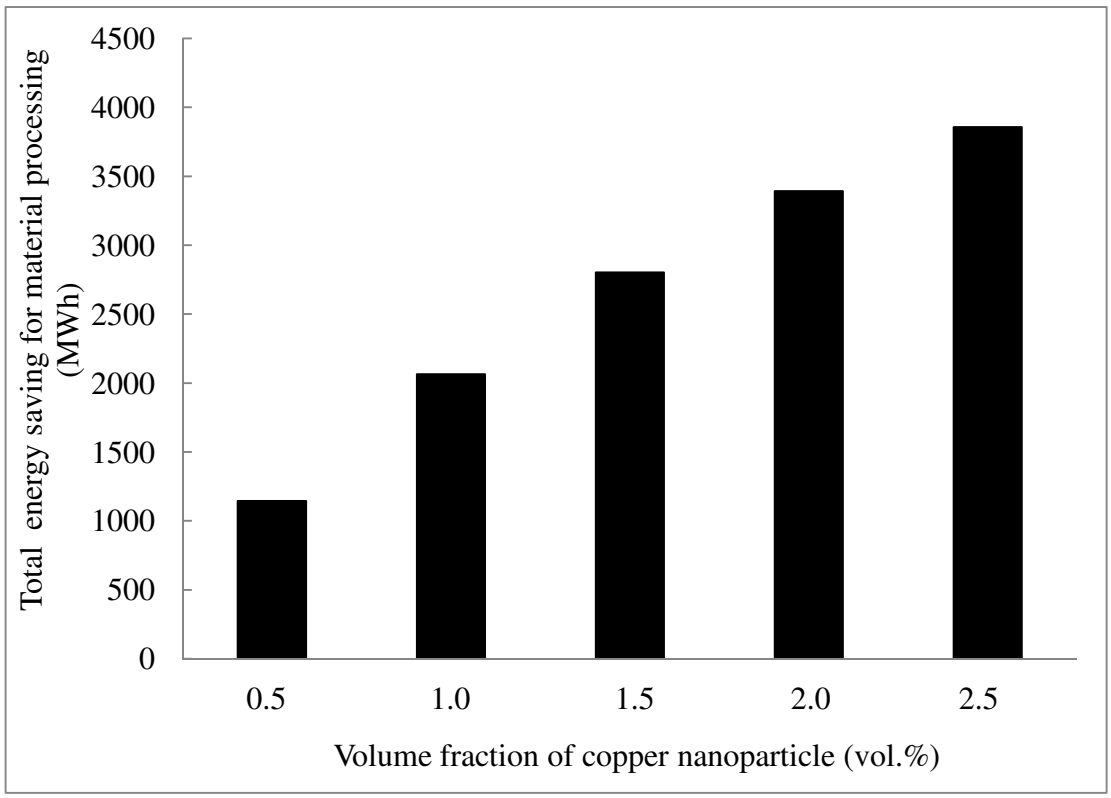

Figure 4.32 Energy saving of material processing of shell and tube heat recovery exchanger operated with water-based copper nanofluids

It is observed that 3857.9 MWh of energy can be saved at 2.5 vol. % of copper concentration into base fluid. Energy savings increase with increase of weight reduction. With this, it can be stated that, energy savings not only can save the cost but also reduces the amount of pollutant gasses. In the next sub-section, the findings on the entropy generation analysis of nanofluid flow in a circular tube subjected to constant wall temperature are elaborated.

4.7 Entropy generation analysis of nanofluid flow in a circular tube subjected to constant wall temperature

The comparative studies used to validate the proposed modelling will be discussed first in sub-section 4.7.1. The total dimensionless entropy generation of water-based nanofluids under different conditions and flows and the comparison between $Al_2O_3$and TiO_2 nanofluids will be described later in sub-sections 4.7.2 and 4.7.3.

4.7.1 Comparative studies

Figure 4.33 illustrates the total dimensionless entropy generation of water with respect to modified Stanton number, Π_1.

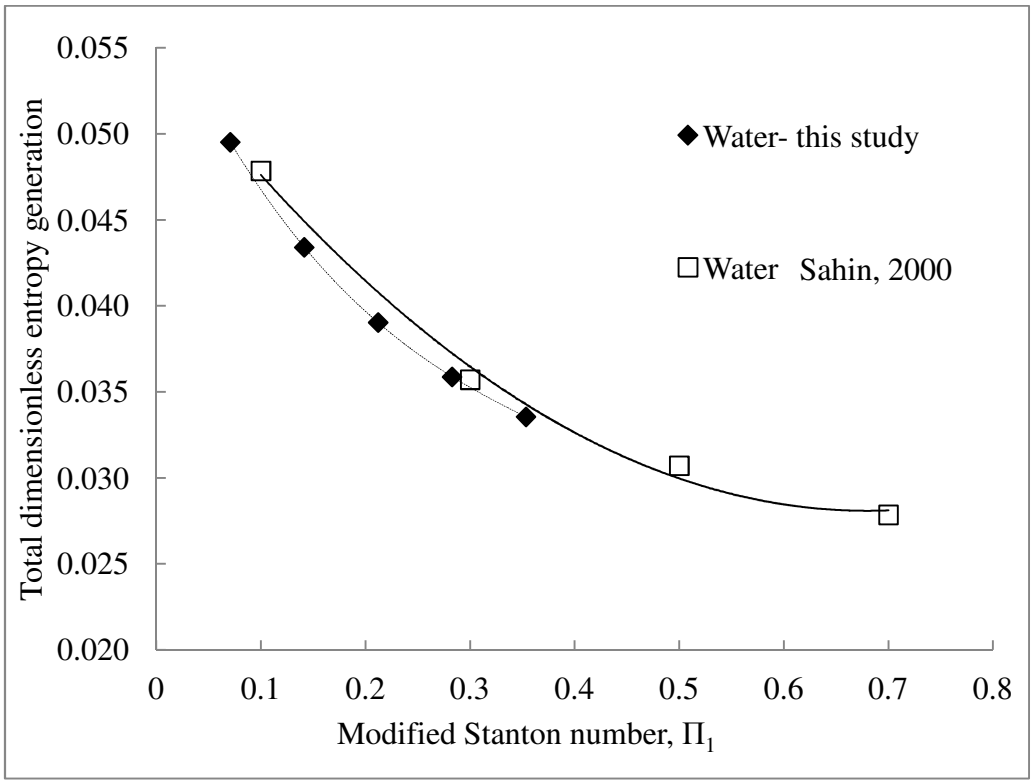

Figure 4.33. Comparative studies

Modified Stanton number, Π_1 is a product of Stanton number, St and dimensionless length, λ. Operating conditions for this analysis are fluid velocity (0.02 m/s), dimensionless wall and fluid temperature difference $\tau = 0.214$, tube diameter (0.1m) and fluid temperature (300K). There are slight differences in the results although both

studies use the same working fluid (water). One of the reasons for the discrepancies is the different thermo-physical properties of water. The present study used thermo-physical properties obtained from Incropera et al., (2007) which are different from those by Sahin (2000). Other contributing factors are the fluid temperature and Nusselt number correlation applied for turbulent flow. It is noted that, present study utilized Dittus-Boelter correlation but Sahin et al., (2000) used Nusselt number correlation from Gnielinski. This study also found that different properties of viscosity will result in different values for tube length in order to produce the same value of Π_1. Sahin (2000) used 9.93×10^{-4} Ns/m^2 while the current study used 8.55×10^{-4} Ns/m^2. The viscosity affects the Reynolds number of the fluid as shown in Equation 3.48. It is evident that the change in the Nusselt number (Equation (3.53)) due to Reynolds number will eventually change the convective heat transfer coefficient (Equation (3.51)). Substitution of different convective heat transfer coefficients into Equation (3.50) will definitely cause adjustment to the value of Stanton number. Therefore, length of tube needs to be changed to cater for the modification of Stanton number with production of the same value of Π_1. This is based on Equation (3.43). Overall, Figure 4.33 implies that the same trend is observed for both studies.

4.7.2 Water based aluminium oxide nanofluids

The following sub-section shows the entropy generation results for water based Al_2O_3 nanofluids. Factors such as nanoparticle loading, dimensionless wall and fluid temperature difference, type of flow and geometry configurations are presented as well.

4.7.2.1 Total dimensionless entropy generation using different aluminium oxide nanoparticles loading and dimensionless wall and fluid temperature different

In this analysis, the volume fractions of nanoparticle are set as variable parameter, ranging from 0 to 7%. Other parameters such as tube length, l (5m) and diameter, d (0.0229m), dimensionless wall and fluid temperature difference, τ (0.01), working fluid mass flow rate, $\dot{m}$ (0.01kg/s) and fluid temperature, T (300K) are fixed as constants. According to Figure 4.34, it is found that the total dimensionless entropy generation is reduced with nanoparticle volume fractions.

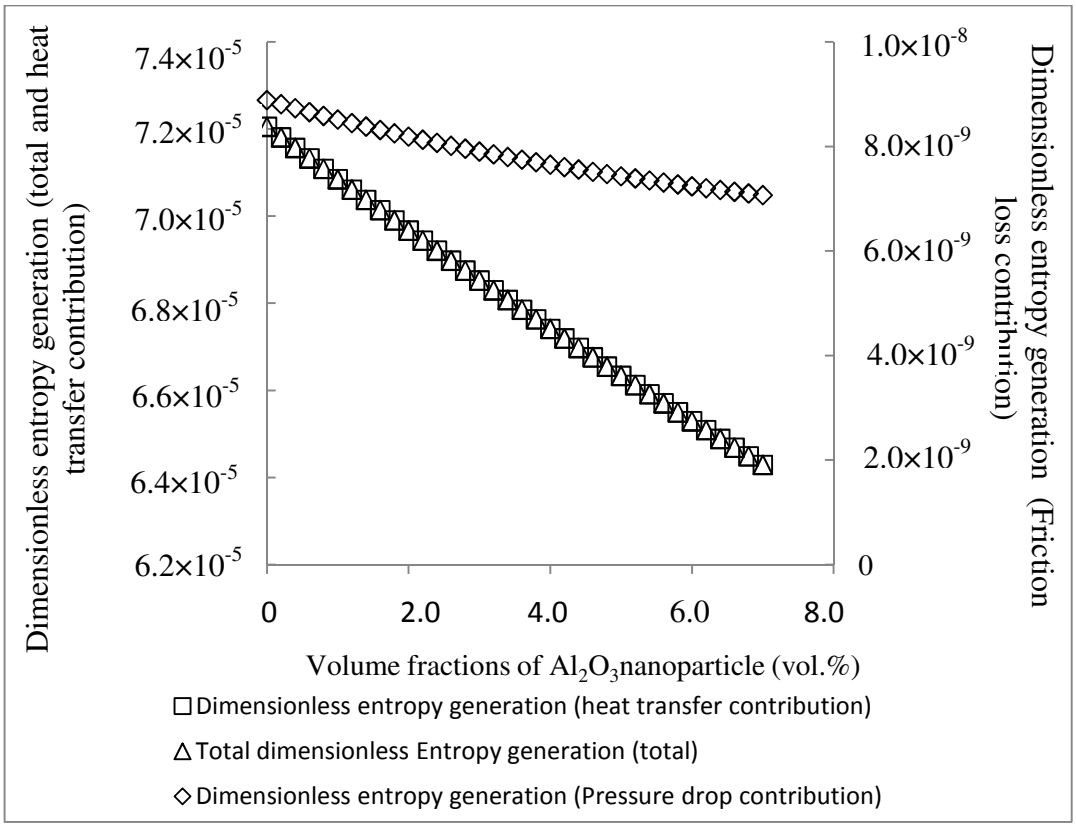

Figure 4.34 Contribution of heat transfer and fluid friction on the total dimensionless entropy generation

Total dimensionless entropy generation is calculated by Equation (3.38) which is comprised of heat transfer (first and second term in the parentheses) and fluid friction (third term). The entropy generation through the heat transfer enhancement process will be at reducing rate by the addition of nanoparticles. Addition of nanoparticles increases the thermal conductivity of nanofluids as depicted in Equation (3.38). At the same time, augmentation of convective heat transfer is observed since the thermal conductivity is proportional to convective heat transfer coefficient as shown in Equation (3.51). Thus, Stanton number as given in Equation (3.50) increases. Finally, the entropy generation due to heat transfer enhancement is minimized based on Equation (3.42).

The entropy generation is also created by the fluid friction which will eventually cause fluid pressure drop. Minimization trend can be explained by referring to pressure drop formulation (Equation (3.47)). There are three (3) variables in this equation namely friction factor, density and velocity of fluids. At constant mass flow rate, friction factor and density increases with particle volume fraction but velocity shows the other way. A close examination of this equation, it is noted that the decreasing effect of fluid velocity is more pronounced since it is in power of two. Thus, the slight decrease in pressure drop of the fluid is observed as given in Equation (3.47). However, this decreasing trend is only valid for lower particle volume fractions. At higher particle volume fractions, the pressure drop shows the opposing trend although the total dimensionless entropy generation due to fluid friction is still on a decreasing trend. This could be due to density effect, which is more pronounced for higher loading of nanoparticles. Density is determined using Equation (3.5). Sample calculation of the water based 1vol. % Al_2O_3 nanofluids can be obtained in Appendix G. Figure 4.35 demonstrates that total dimensionless entropy generation increases with τ.

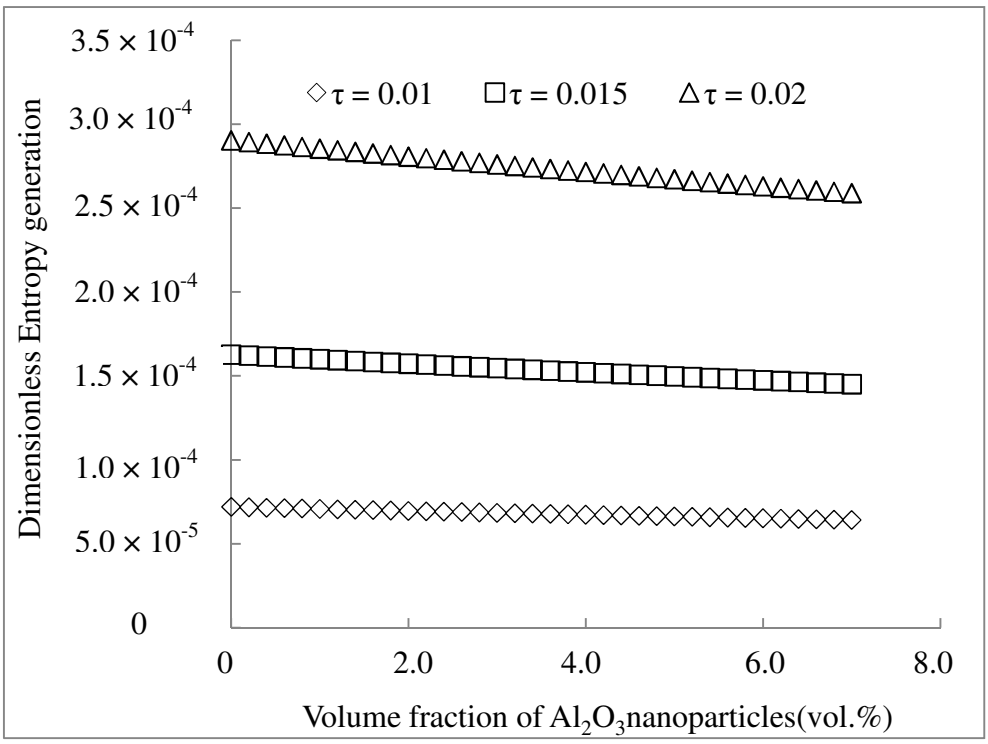

Figure 4.35 Effect of dimensionless temperature different on total dimensionless entropy generation of nanofluids flow

Total dimensionless entropy generation is defined by Equation (3.55). Similar result is found from the study conducted by Dagtekin et al. (2005). It is found that as τ increases, the total dimensionless entropy generation of the fluid increases (for circular duct with thin, triangular and V-shaped fins).

4.7.2.2 Total dimensionless entropy generation using laminar and turbulent flow

Figures 4.36 and 4.37 depict the effect of fluid mass flow rate on total dimensionless entropy generation of nanofluids for laminar and turbulent flows. Parameters that are fixed in this section include tube diameter, d (0.0229m), tube length, *l* (5m), dimensionless wall and fluid temperature different, τ (0.01). Laminar flow is produced from mass flow rate, $\dot{m}$ ranging from 0.01kg/s to 0.02 kg/s. Figure 4.36 shows that total dimensionless entropy generation increases with mass flow rate.

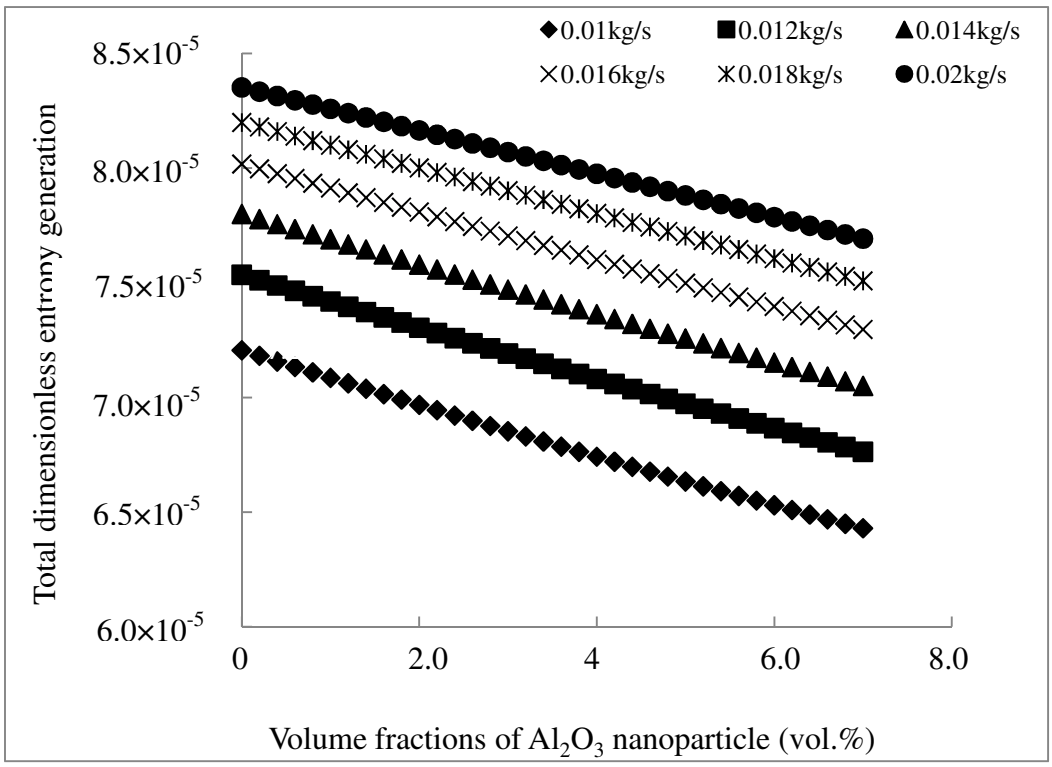

Figure 4.36 Total dimensionless entropy generation of nanofluids using laminar flow

Both entropy generations due to heat transfer and fluid friction are maximized when mass flow rate increases. Higher mass flow rate increases the fluid velocity as given in Equation (3.49). Stanton number which is determined from Equation (3.50) decreases due to the increase of fluid velocity. Inclusion of lower value of Stanton number will increase the entropy generation due to heat transfer process. Similar trend is observed for entropy generation contributed by fluid friction. Pressure drop tends to increase as the fluid velocity increases as depicted in Equation (3.47). Increase of pressure drop results in higher entropy generation. Similar trend is found for the turbulent flow as shown in Figure 4.37.

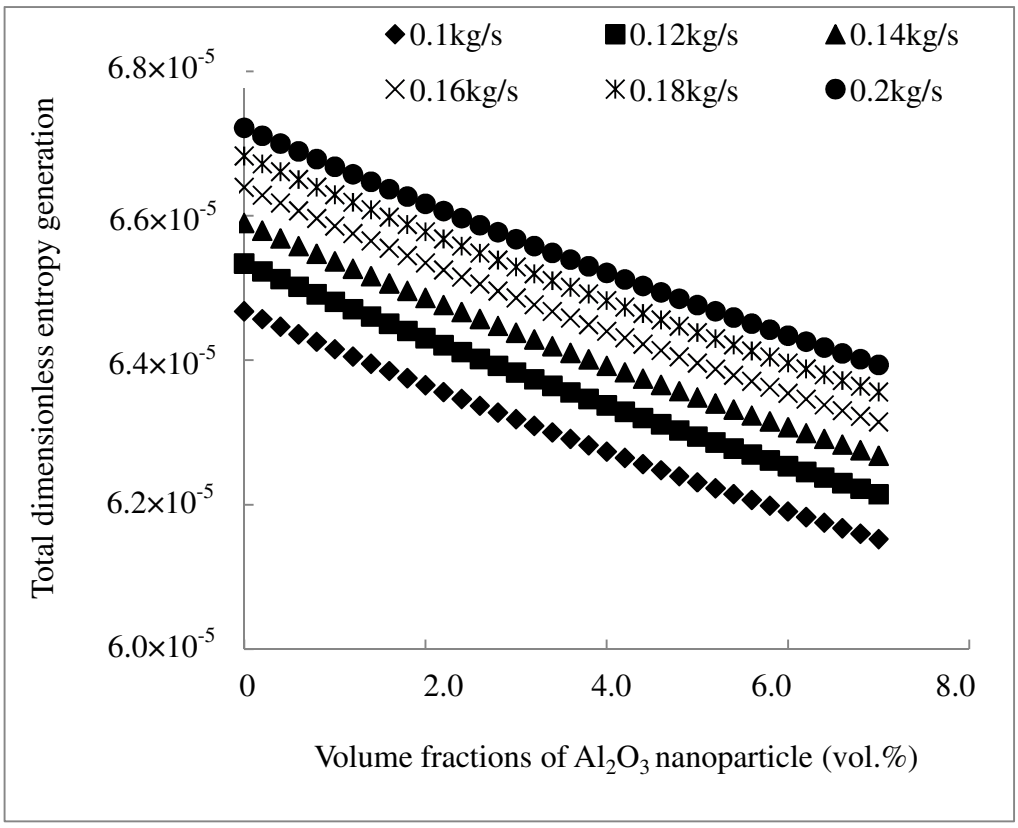

Figure 4.37 Total dimensionless entropy generation of nanofluids using turbulent flow

Mass flow rates from 0.1kg/s to 0.2kg/s are chosen to produce turbulent flow. Although the convective heat transfer increases with mass flow rate, the effect of higher fluid velocity is more pronounced, thus, resulting in lower Stanton number. The convective heat transfer coefficient is calculated from Equations (3.51) and (3.53) while Stanton number from Equation (3.50). The pressure drop of nanofluids also seems to be increasing with mass flow rate. All these factors lead to higher total entropy generation of nanofluids.

4.7.2.3 Total dimensionless entropy generation using different geometry configurations

Geometry configurations considered in this study are tube length and diameter. Figure 4.38 shows that, the total entropy generation decreases with respect to tube length.

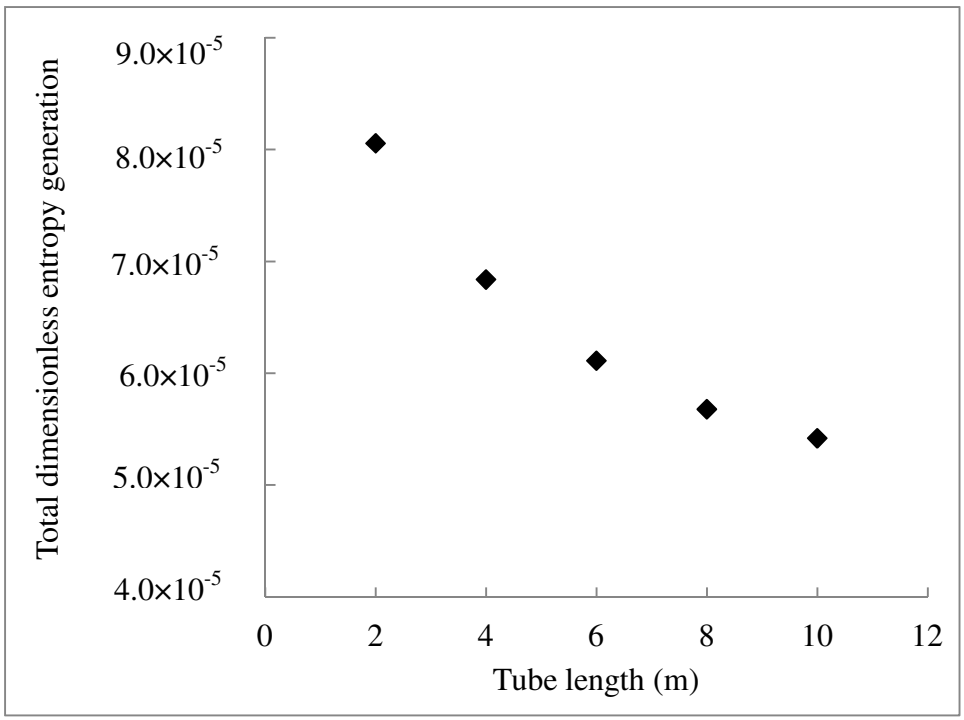

Figure 4.38 Total dimensionless entropy generation of nanofluids with respect to tube length

Parameters used for this study are mass flow rate, $\dot{m}$ (0.01kg/s), tube diameter, d (0.0229m), Al_2O_3 volume fraction (7%), dimensionless temperature difference, τ (0.01) and 300K fluid temperature, T. The considered tube length is from two (2) to ten (10) meters. Laminar flow is created using 0.01kg/s of mass flow rate. One of the possible reasons contributing to this result is the increase of dimensionless length, λ. The dimensionless length, λ is affected by the tube length as given by Equation (3.56). Substitution of higher value of dimensionless length decreases the total dimensionless entropy generation of nanofluids as determined by Equation (3.42). The same operating conditions are used to test the effect of different tube diameters. The only difference is that the tube length is fixed at 5 meter while the tube diameter ranges from 0.01 to 0.03m. The result of this analysis is shown in Figure 4.39.

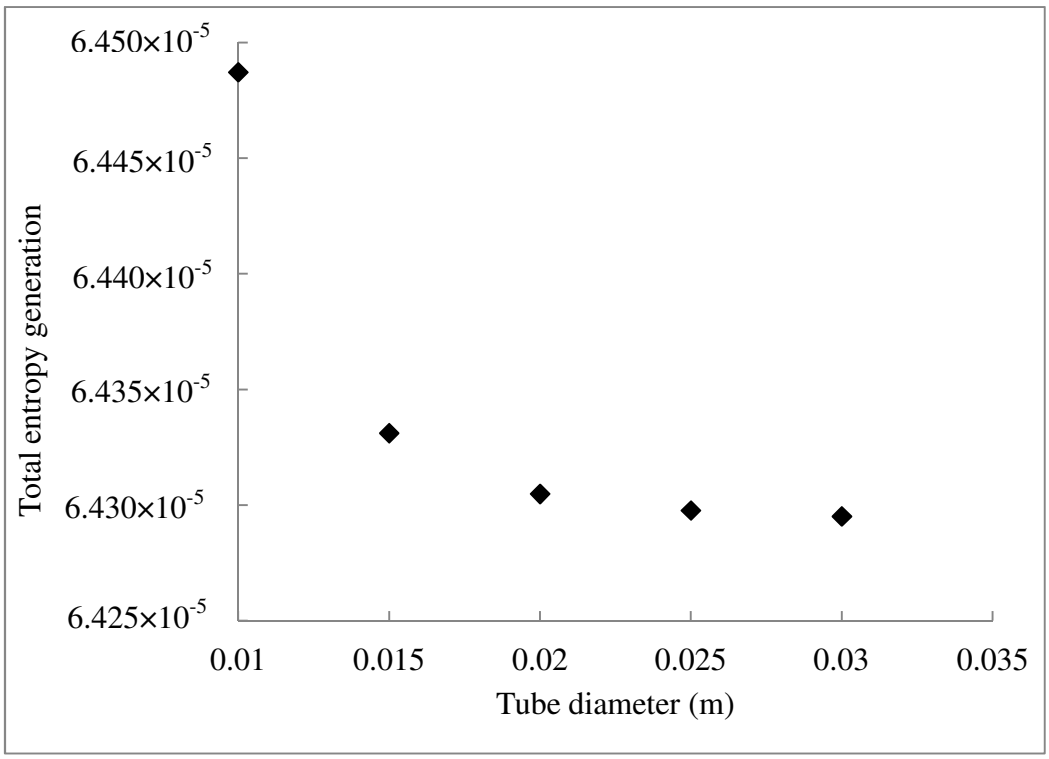

Figure 4.39 Total dimensionless entropy generation of nanofluids with respect to tube diameter

Study implies that there is slight decrease (0.3%) in total dimensionless entropy generation when diameter increases from 0.01 to 0.03 meter. Analysis shows that the fluid pressure drop is inversely proportional to tube diameter. Bigger tube diameter might increase the fluid friction, however, the fluid velocity also decreases at the same time. Combination of lower fluid velocity and higher tube diameter will reduce the pressure drop as given by Equation (3.47). Calculations using Equation (3.42) show that contribution of heat transfers to the entropy generation remain unchanged even though different tube diameters are used. This might be due to increase of Stanton number being compensated by the decrease of dimensionless length.

4.7.2.4 Total dimensionless entropy generation of water based aluminium oxide and titanium dioxide nanofluids

Figure 4.40 compares the total dimensionless entropy generation of Al_2O_3 and TiO_2 nanofluids. The thermo-physical properties of Al_2O_3 and TiO_2 are obtained from the literatures and mathematical correlations.

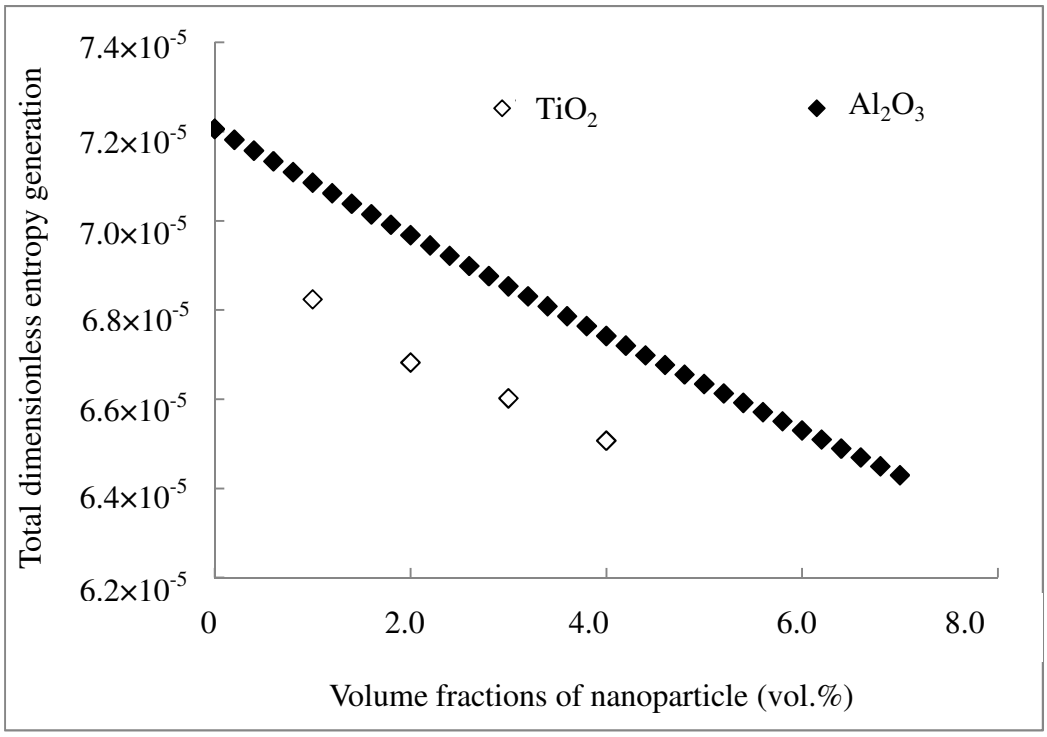

Figure 4.40 Comparison of total dimensionless entropy generation between Al_2O_3 and TiO_2 nanofluids

It is found that entropy generation by TiO_2 nanofluids is lower than Al_2O_3 nanofluids. Addition of 4vol.% of Al_2O_3 nanoparticles reduces the total dimensionless entropy generation by 6.4% compared to 9.7% reductions observed with the use of TiO_2. It might be due to higher thermal conductivity of TiO_2 nanofluids. Thermal conductivity of nanofluids is affected by stability of the suspension, size of the particles, type of particle and etc. In this case, the particle size of Al_2O_3 is 30nm while the TiO_2 is 15nm taken from Murshed et al. (2009). Smaller particle size provides higher surface area to volume ratio which will enhance the heat transfer process.

Figure 4.41 depicts the total entropy generations modelled from the thermo-physical experimental data obtained in the present study. Four types of fluids were considered; water based Al_2O_3 (particle size 13nm and <50nm) nanofluids, water based TiO_2 (particle size: 21nm) nanofluids and water base fluid. The selected particle volume fraction is 0.5%. Study implied that the nanofluids (except Al_2O_3 with particle size: <50nm) have lower entropy generation in comparison to that of water base fluid. In sub-section 4.2, it is found that thermal conductivity of the Al_2O_3 with particle size less than 50nm has lower thermal conductivity compared to the base fluid. Thus, it contributes to higher total dimensionless entropy generation in this analysis.

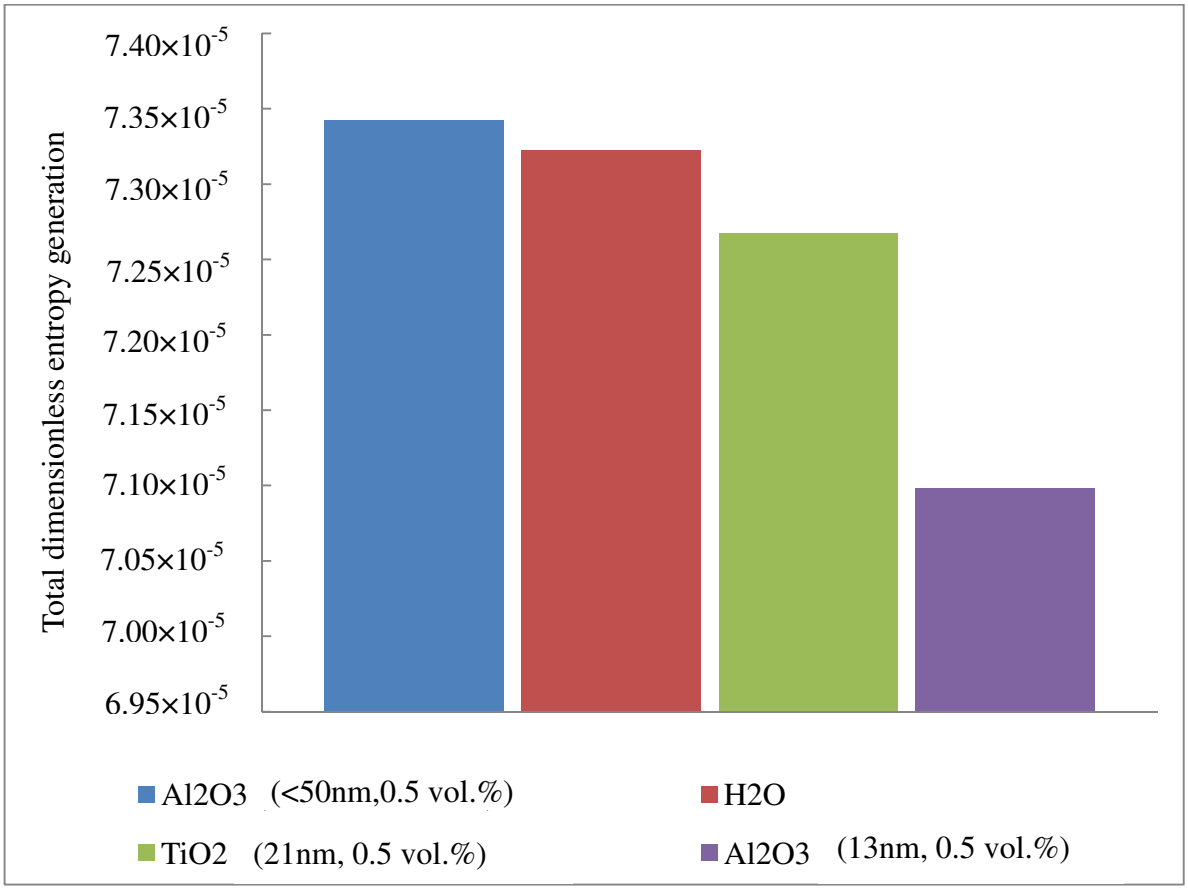

Figure 4.41 Total dimensionless entropy generation of various water-based nanofluids

4.8 Performance investigation of nanofluids as working fluid in a thermosyphon air preheater

This section covers all the major findings on the performance of thermosyphon air preheater operated with nanofluid as a working fluid. Thermosyphon air preheater heat exchanger serves as an alternative option to recover waste heat beside shell and tube heat exchanger.

4.8.1 Comparative studies

Figures 4.42-4.44 depict the relationship between hot air inlet and outlet temperatures at 3 different hot air velocities. The results obtained from present study are compared to the results from Noie (2006).

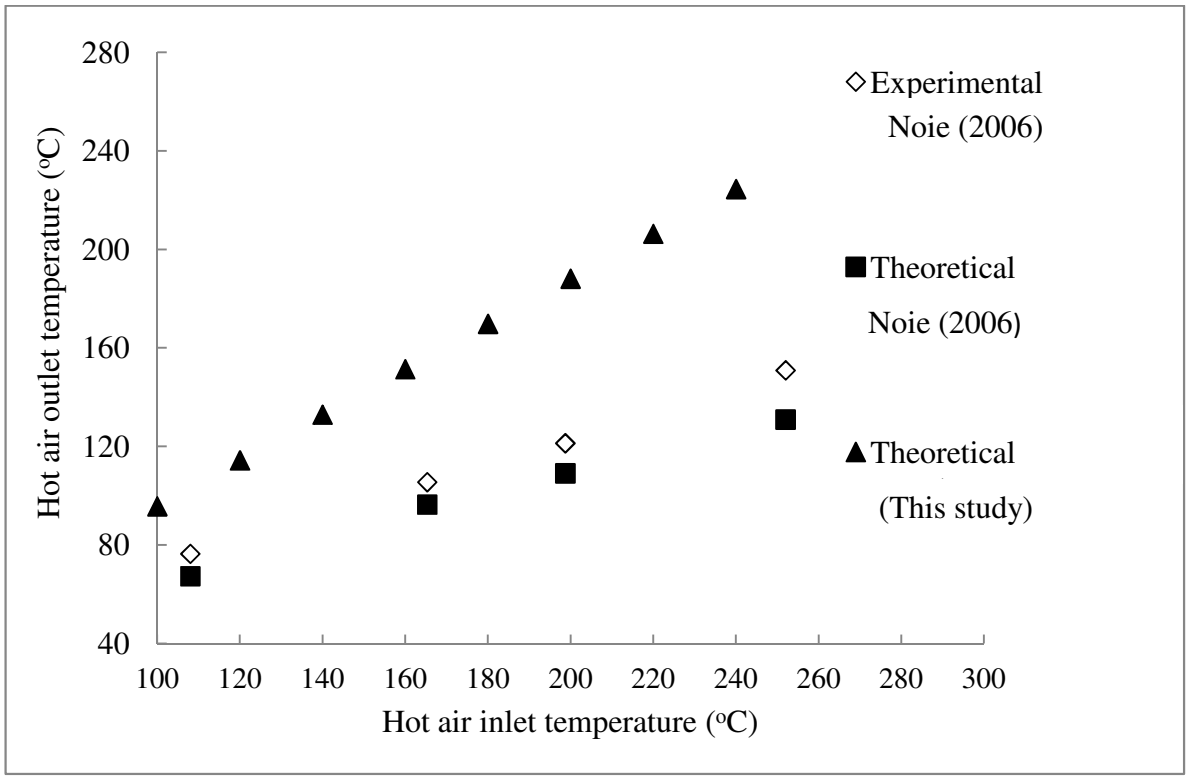

Figure 4.42. Relationship between hot air inlet and outlet temperature at 2.5 m/s hot air velocity

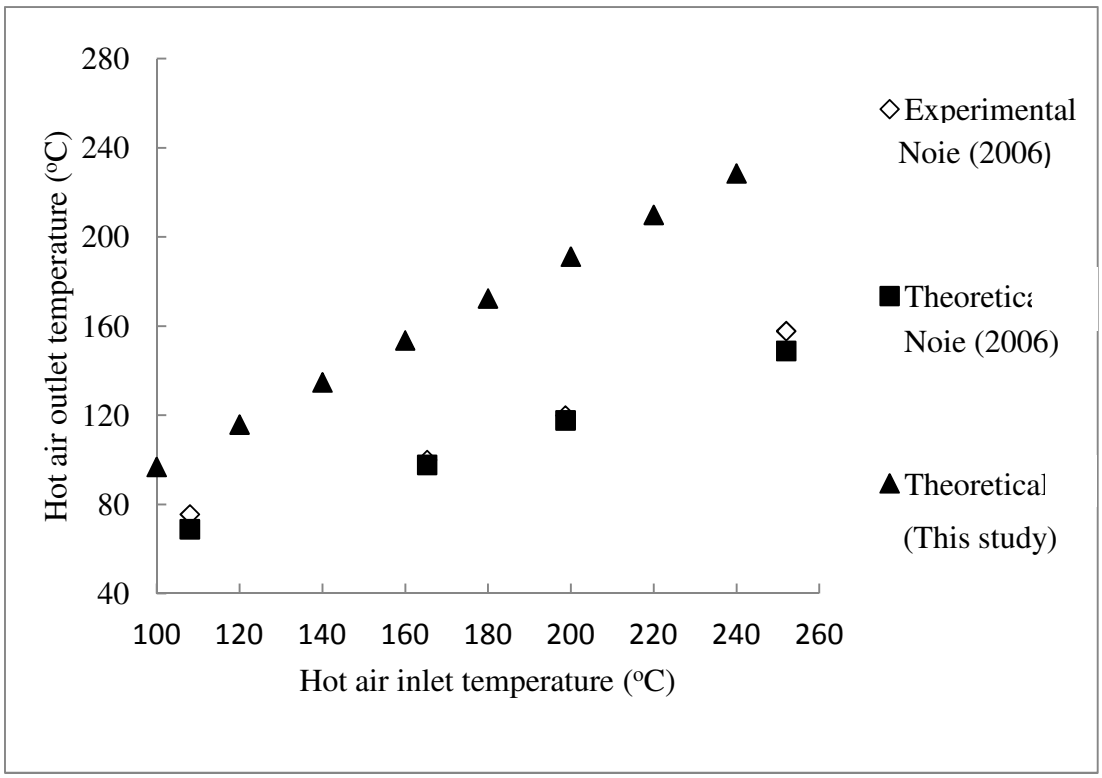

Figure 4.43 Relationship between hot air and outlet temperature at 4.0 m/s hot air velocity

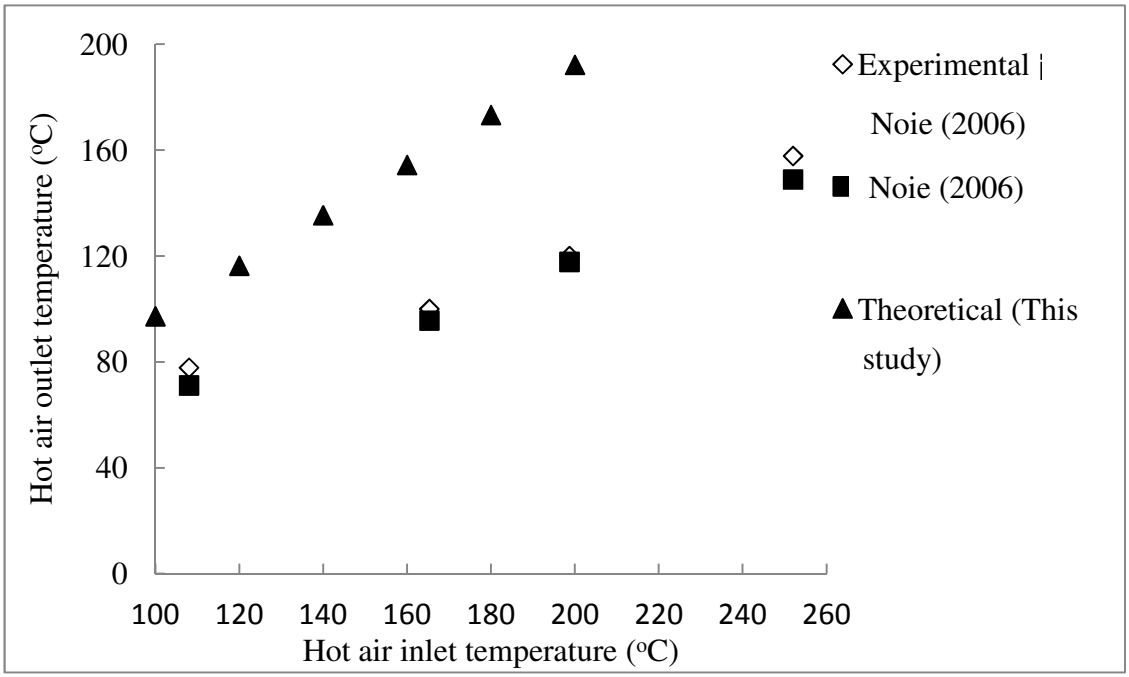

Figure 4.44 Relationship between hot air inlet and outlet temperature at 4.75 m/s hot air velocity

It is found that the results' accuracy is higher at lower hot air inlet temperatures. It is noted that the hot air inlet temperature is proportional to hot air outlet temperature.

Figure 4.45 depicts the relationship between hot air inlet temperature, hot air velocity and absorbed energy at evaporator section.

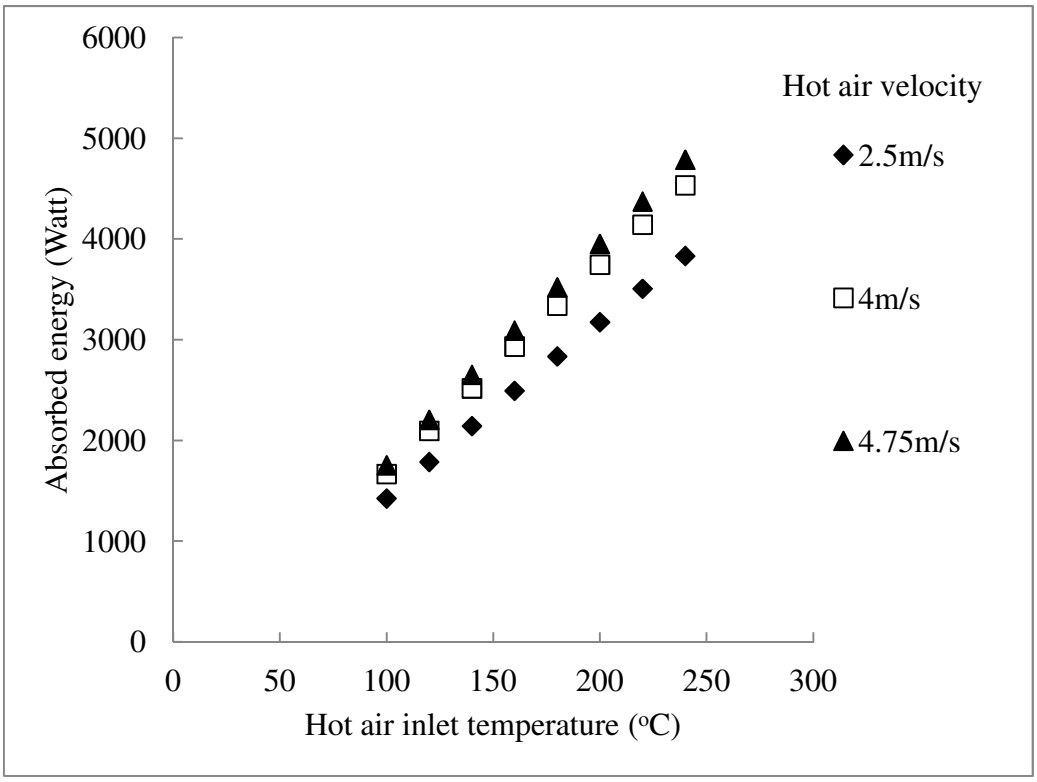

Figure 4.45 Effect of hot air inlet temperature and velocity to energy absorbed at evaporator section

Hot inlet air temperature is proportional to absorbed energy. It is noted that the hot air with higher temperature contains higher amount of heat, hence more heat can be absorbed at the evaporator section. Aside from temperature, the velocity of hot air also plays a crucial role in determining the absorbed energy. Higher augmentation of hot air velocity increases the absorbed energy. Based on Equation (3.82), it is found that the absorbed energy depends on capacity rate, C. Capacity rate is multiplication of hot air mass flow rate and specific heat as shown in Equation (3.73). Increase of the hot air

velocity will increase the hot air mass flow rate. Substitution of this value into Equation (3.82) increases the absorbed energy. In addition, convective heat transfer coefficient of the hot air increases with the increase of hot air velocity as shown in Equation (3.57). Higher convective heat transfer decreases the thermal resistance of the air as shown in Equation (3.62). The large amount of the collective and aggregate movement of hot air molecules contribute to higher heat transfer rates (Incropera et al., 2007).

4.8.2. Influence of nanoparticles volume fraction and hot air velocity on thermal and energy performance of thermosyphon heat exchanger

The following sub-sections describe the thermal and energy performance of thermosyphon heat exchanger operated with nanofluids.

4.8.2.1 Thermal performance of thermosyphon heat exchanger

This section discusses the influence of nanoparticle volume fraction and hot air velocity on the thermal performance of a thermosyphon heat exchanger. The thermal performance analysis includes investigating overall heat transfer coefficient and cold air outlet temperature. From Figure 4.46, it is found that minor differences were created in overall heat transfer coefficient for thermosyphon operated with water and nanofluids.

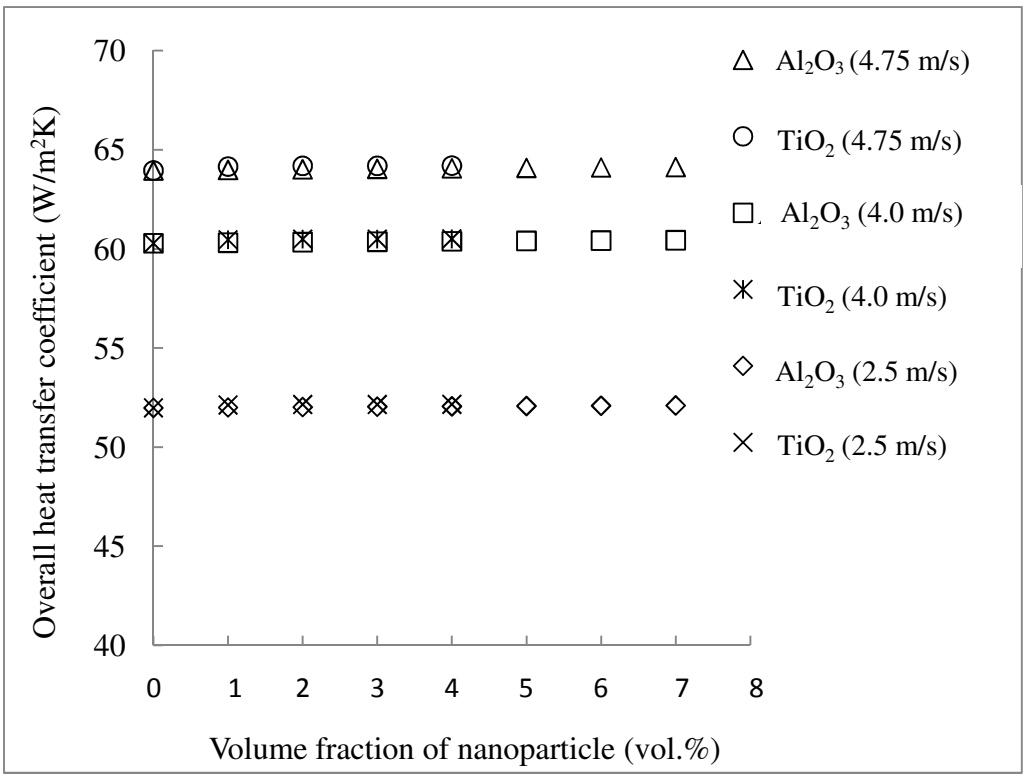

Figure 4.46 Effect of nanoparticles' volume fraction and hot air velocity to overall heat transfer coefficient of heat pipe heat exchanger

Only a slight increase in overall heat transfer coefficient is observed with addition of nanoparticles. From the literatures, the change of heat pipe surface and working fluids thermo-physical properties (thermal conductivity, specific heat and viscosity) are the possible mechanisms contributing to higher efficiency of heat pipe. However, it is noted that the formulations used in the present study only covers the thermo-physical properties of the nanofluids. External surface change is not considered in the analysis. Do and Jang (2010) found that the change of evaporator surface causes substantial effect compared to the change of working fluid thermo-physical properties. The authors revealed that development of thin porous coating layer at the evaporator augments the heat transfer rate by providing additional surface for evaporation. Qu et al. (2010) agreed that Al_2O_3 nanoparticles settlement at the evaporator section of oscillating heat pipe provides major contribution to the thermal performance enhancement of heat pipe.

It is found that, settlements of the nanoparticles occurred at both sides. Thus, Figure 4.46 again proves that the change of working fluid (nanofluids) only provides minor contribution to the heat transfer enhancement of the heat pipe. The surface change in the heat pipe or thermosyphon itself is the main factor for the thermal performance enhancement.

It is noticed that the overall heat transfer coefficient of the thermosyphon operated with TiO_2 nanofluids is slightly higher than Al_2O_3 nanofluids. It is due to higher thermal conductivity of TiO_2 nanofluids compared to that of the Al_2O_3 nanofluids. For the effect of hot air velocity, present study implied that higher velocity enhances the overall heat transfer coefficient. At 7% Al_2O_3 volume fraction, 23% improvement of overall heat transfer coefficient is observed when hot air velocity increases from 2.5m/s to 4.75m/s. The same amount of enhancement is observed for 4% volume fraction of TiO_2. Higher air velocity increases its convective heat transfer which reduces the thermal resistance of air. Eventually, it increases the overall heat transfer coefficient. Similar to section 4.8.1, higher air velocity produces large amount of collective and aggregate movement of hot air molecules. Sample calculation of the water based 1 vol.% Al_2O_3 nanofluid's overall convective heat transfer coefficient is shown in Appendix G. Figure 4.47 depicts the effect of nanoparticle volume fraction and hot air velocity to the cold air outlet temperature.

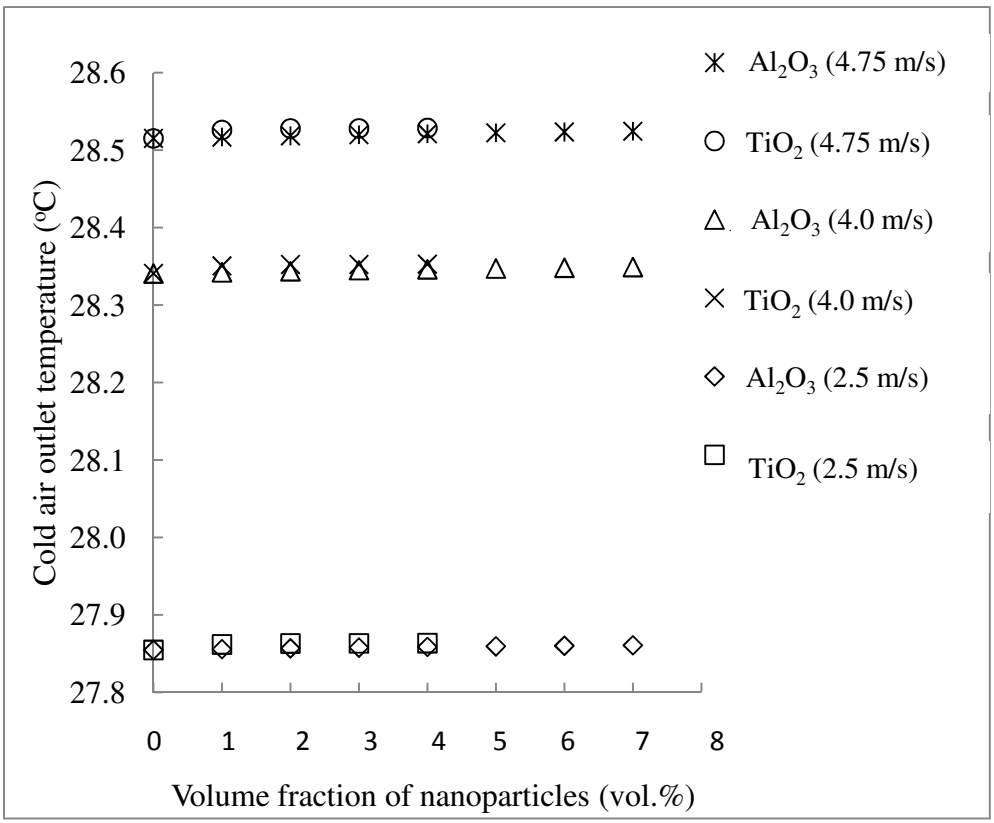

Figure 4.47 Effect of nanoparticles' volume fraction and hot air velocity to cold air outlet temperature of heat pipe heat exchanger

The cold air outlet temperature is associated with the overall heat transfer coefficient. Hence, similar trend is observed in Figure 4.47. Not much increase in the cold air outlet temperature is observed with the augmentation of particle volume fraction. However, both Al_2O_3(7vol.%) and TiO_2(4vol.%) offer 2.4% cold air outlet temperature enhancement when hot air velocity increases from 2.5m/s to 4.75m/s.

4.8.2.2 Energy performance of thermosyphon heat exchanger

This section further analyzes the cold air outlet temperature obtained from section 4.8.2.1. Energy will be supplied to the cold air until its temperature reaches 126.85^{o}C to facilitate fuel combustion process. This value is taken from Saidur et al., (2010). The authors used it in their energy and exergy analysis for industrial boilers. Figures 4.48-4.49 shows the energy required to increase the air temperature to 126.85^{o}C for $Al_2O_3$and TiO_2 nanofluids, respectively.

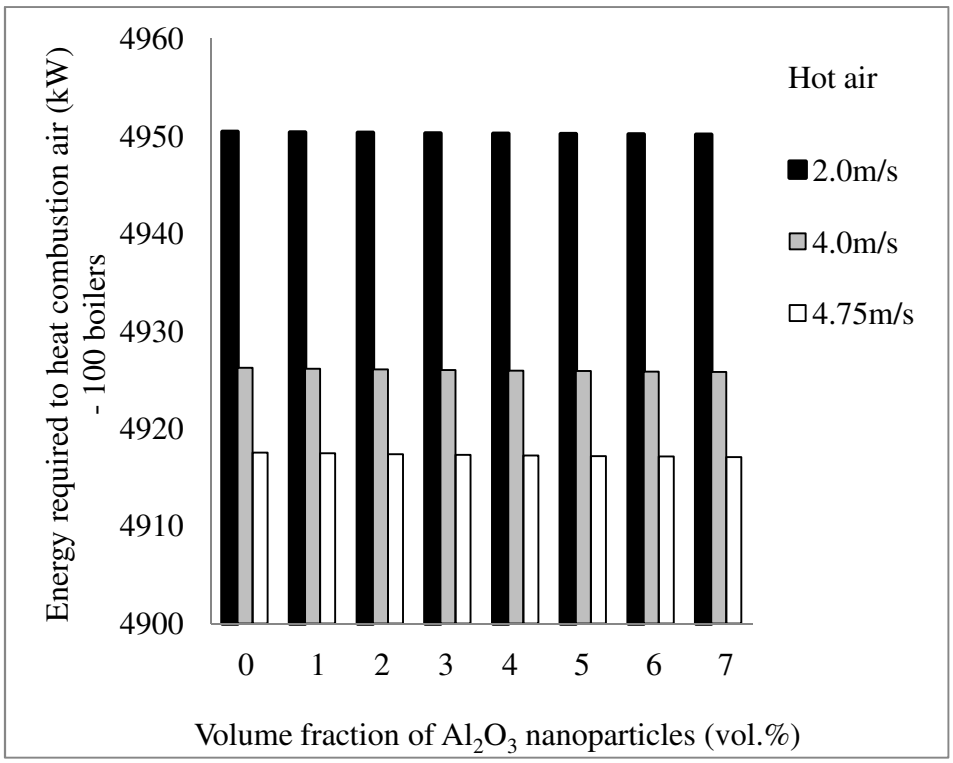

Figure 4.48 Effect of Al_2O_3 nanoparticles' volume fraction and hot air velocity to energy performance of thermosyphon heat exchanger

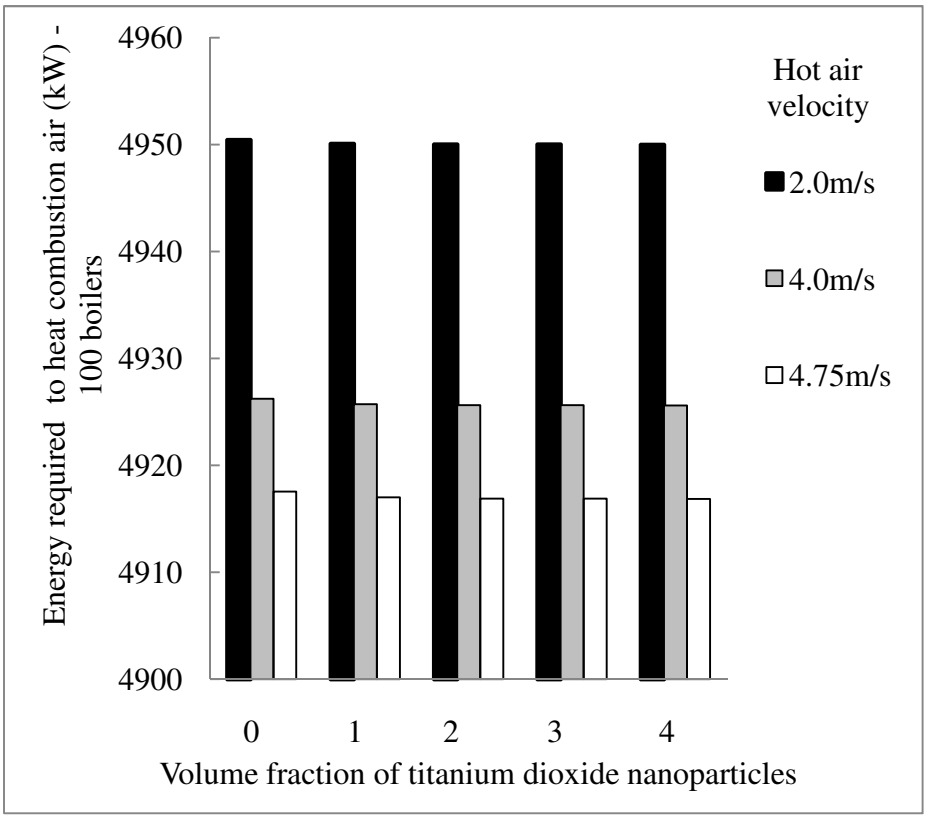

Figure 4.49 Effect of TiO_2 nanoparticles, volume fraction and hot air velocity to energy performance of thermosyphon heat exchanger

This is the total energy required to increase the air to 126.85^{o}C predicted for 100 boilers. It is found that, the required energy decreases with increase of hot air velocity. Similar to section 4.8.2.1, this happened due to decrease of thermal resistance at the evaporator side. Increase in the air velocity produces higher convective heat transfer coefficient which eventually decreases the air thermal resistance. For instance, the required energy reduces 0.67% when hot air velocity increases from 2.0 m/s to 4.75 m/s for 7vol. % of Al_2O_3 nanofluids. Similar reduction percentage is observed for 4vol. % titanium dioxide nanoparticles. However, not much energy difference is found with increasing the nanoparticle volume fraction for two types of nanofluids. The next chapter will describe the conclusions derived from the present study and suggestions for further study.

CHAPTER 5 CONCLUSION AND RECOMMENDATIONS

5.1 Conclusion

All the objectives in the present study are achieved amd the conclusions that can be drawn from this study are:

(a) Thermal conductivity of base fluids increases with addition of nanoparticles. For instance, 8.9% augmentation of thermal conductivity of water based Al_2O_3 (0.5vol. %, particle size:13nm) is observed compared to water/ethylene glycol-based fluid. About 12.9% improvement is observed for the water based Al_2O_3 (0.5vol.%, particle size: 13nm) nanofluid. Water and ethylene glycol/water - based nanofluid containing smaller Al_2O_3 (particle size: 13nm) nanoparticles exhibits higher thermal conductivity compared to Al_2O_3 with less than 50nm particle size.

(b) Density of water or ethylene glycol/water-based nanofluids containing Al_2O_3 or TiO_2 nanoparticles increases with the increase of particle volume fraction. TiO_2 nanofluids exhibit higher density values compared to Al_2O_3 nanofluids (particle size 13 and <50nm). Type of particle has significant effect on nanofluids density rather than particle size. Viscosity of water or water/ethylene glycol nanofluids containing TiO_2 or Al_2O_3 nanoparticles increases with particle loading but decreases with the increase of operating temperature.

(c) With reference to the thermal performance of shell and tube heat exchanger, heat transfer rate is improved with volume fractions for copper nanofluid. About 7.8% heat transfer augmentation was observed for ethylene glycol-based nanofluids containing 1vol.% of copper nanoparticles at 26.3 kg/s and 111.6 kg/s mass flow rate for flue gas and coolant, respectively. For 2vol.% water-based copper nanofluids, 4.53% heat transfer enhancement in laminar flow was recorded. Nanofluid convective heat transfer coefficient and overall heat transfer

coefficient are higher than those of base fluid. About 9.5% and 16.9% enhancements were recorded for ethylene glycol with 1% copper nanoparticles compared to base fluid. Overall heat transfer coefficient of ethylene glycol/water Al_2O_3 (particle size: 13 and <50nm) and TiO_2 are higher than the ethylene glycol/water base fluid. Apart from that, thermal performance of the heat recovery exchanger is increased with flue gas mass flow rate. However, only minor heat transfer enhancement was observed for ethylene glycol based 1 vol.% of copper nanofluids when coolant mass flow rate was increased from 200 to 230 kg/s.

(d) Study also found that application of nanofluids in shell and tube heat exchanger provides opportunity to reduce the size of shell and tube heat exchanger without affecting its thermal performance. Smaller heat exchangers require less materials for fabrication and for processing energy.

(e) Based on the nanofluids flow in a circular tube subjected to a constant wall temperature, total dimensionless entropy generation is reduced with nano particle volume fraction. TiO_2 nanofluids offer lower total dimensionless entropy generation compared to Al_2O_3 nanofluids. For 4 vol. % , about 9.7% and 6.4% reduction of entropy generation are observed for TiO_2 and Al_2O_3 nanofluids, respectively.

(f) Total dimensionless entropy generation increases with the increase of dimensionless temperature difference, τ. Mass flow rate of working fluid influences the total dimensionless entropy generation. 19.6% increase is achieved when mass flow rate increases from 0.01 to 0.02 kg/s for water based 7vol.% Al_2O_3 nanofluids. However only 3.9% increase is found in turbulent flow (from 0.1 to 0.2 kg/s) under the same nanoparticle loading.

(g) About 32.7% reduction of total dimensionless entropy generation can be resulted when tube length is extended from 2 to 10 m for 7vol.% Al_2O_3 nanofluid. However, only 0.3% reduction in entropy generation was achieved when tube diameter increased from 0.01 to 0.02 m.

(h) On the application of thermosyphon air pre-heater, the change of nanofluid thermo-physical properties plays a minor role in improving its thermal performance. Slight increase of overall heat transfer coefficient and cold air outlet temperature is observed with augmentation of nanoparticle volume fraction. TiO_2 nanofluids offer slightly higher overall heat transfer coefficient and cold air outlet temperature compared to Al_2O_3 nanofluids. 23% overall heat transfer enhancement is observed for TiO_2(4vol.%) and Al_2O_3 (7vol.%) nanofluids when hot air velocity increases from 2.5 m/s to 4.75 m/s. 2.4% enhancement of cold air outlet temperature is observed for TiO_2 (4vol.%) and Al_2O_3 (7vol.%) nanofluids when hot air velocity increases from 2.5 m/s to 4.75 m/s. 0.67% reduction is resulted in the energy required to heat the combustion air when velocity increases from 2.5 m/s to 4.75 m/s.

This study found that nanofluid operated shell and tube heat recovery exchanger offers better thermal performance compared to that of base fluid. Analysis was conducted by using Kern and effective-NTU methods. This is the main contribution or novelty of the present work in heat recovery aspect. The application of nanofluids provides an alternative approach for better utilization of energy consumption especially in the industry.

5.2 Recommendations

The recommendations for future or further study are as follows:

(a) From the literature review, it is found that thermal researchers focused only on thermal conductivity and viscosity characteristics of nanofluids. There is lack of research investigating the specific heat of nanofluids. Thus, more study should be conducted in this area.

(b) Stability is an important parameter for obtaining nanofluids with optimum thermal properties and to make nanofluid a pragmatic solution to industry problems. Nanoparticles tend to agglomerate when higher loading is used. More studies should focus on minimizing instability particularly by using surfactants. However, surfactant increases the viscosity characteristic of nanofluids. Research in analyzing the optimum loading of surfactant should be considered.

(c) More experimental studies should be done on using nanofluids in heat recovery exchanger. From the open literatures it is apparent that most of the researchers focused on the fundamental properties of nanofluids. Researchers should switch their attention to the applications of nanofluids especially in heat recovery exchanger.

REFERENCES

Abdelaziz, E. A., Saidur, R., & Mekhilef, S. (2011). A review on energy saving strategies in industrial sector. *Renewable and Sustainable Energy Reviews, 15*(1), 150-168.

ASHRAE Handbook (2001). Physical properties of secondary coolants (Brines), *American Society of Heating, Refrigerating and Air Conditioning Engineers,Inc, Atlanta*. GA.

Batchelor, G. K. (1977). The effect of Brownian motion on the bulk stress in a suspensions of spheres. *J.Fluid Mech, 83*(1).

Beck, M. P., Sun, T.,&Teja, A. S. (2007). The thermal conductivity of alumina nanoparticles dispersed in ethylene glycol. *Fluid Phase Equilibria, 260*(2), 275-278.

Beck, M. P. (2008). Thermal Conductivity of Metal Oxide Nanofluids. Unpublished PhD's thesis, Georgia Institute of Technology.

Bejan, A. (1996). *Entropy generation minimization*. Boca Taron: CRC Press.

Bhattacharya, P. (2005). *Thermal conductivity and colloidal stability of nanofluids.* Arizona State University.

Bianco, V., Chiacchio, F., Manca, O., & Nardini, S. (2009). Numerical investigation of nanofluids forced convection in circular tubes. *Applied Thermal Engineering, 29*(17-18), 3632-3642.

Bianco, V., Nardini, S., & Manca, O. (2011). Enhancement of heat transfer and entropy generation analysis of nanofluids turbulent convection flow in square section tubes. *Nanoscale research letters, 6*(252).

Bobbo,S., Fedele, L., Benetti, A., Colla, L., Fabrizio, M., Pagura, C., et al. (2012). Viscosity of water based SWCNH and TiO_2 nanofluids. *Experimental Thermal and Fluid Science, 36*, 65-71.

Brinkman.H.C. (1952). The viscosity of concentrated suspensions and solution. *J.Chem. Phys, 20*, 571-581.

Charyulu, D. G., Singh, G., & Sharma, J. K. (1999). Performance evaluation of a radiator in a diesel engine-a case study. *Applied Thermal Engineering, 19*(6), 625-639.

Chandrasekar, M., Suresh, S., & Chandra Bose, A. (2010). Experimental investigations and theoretical determination of thermal conductivity and viscosity of Al_2O_3/water nanofluid. *Experimental Thermal and Fluid Science, 34*(2), 210-216.

Chen, H., Ding, Y., He, Y., & Tan, C. (2007). Rheological behaviour of ethylene glycol based titania nanofluids. *Chemical Physics Letters, 444*(4-6), 333-337.

Chen, H., Yang, W., He, Y., Ding, Y., Zhang, L., Tan, C., Alexei,A.L., et al. (2008). Heat transfer and flow behaviour of aqueous suspensions of titanate nanotubes (nanofluids). *Powder Technology, 183*(1), 63-72.

.

Chen, H., Ding, Y., & Lapkin, A. (2009). Rheological behaviour of nanofluids containing tube / rod-like nanoparticles. *Powder Technology, 194*(1-2), 132-141.

Chen, L., & Xie, H. (2010). Properties of carbon nanotube nanofluids stabilized by cationic gemini surfactant. *Thermochimica Acta, 506*(1-2), 62-66.

Chen, Q., Finney, K., Li, H., Zhang, X., Zhou, J., Sharifi, V., et al. (2012). Condensing boiler applications in the process industry. *Applied Energy, 89*, 30-36.

Choi, S. U. S. (2009). Nanofluids: From vision to reality through research. *Journal of Heat Transfer, 131*, 033106-033109.

Chon, C. H., & Kihm, K. D. (2005). Thermal conductivity enhancement of nanofluids by Brownian motion. *Journal of Heat Transfer, 127*, 810.

Colangelo, G., Favale, E., de Risi, A.,& Laforgia, D. (2011). Results of experimental investigations on the heat conductivity of nanofluids based on diathermic oil for high temperature applications. *Applied Energy*, *97*, 828-833.

Corcione, M. (2011). Empirical correlating equations for predicting the effective thermal conductivity and dynamic viscosity of nanofluids. *Energy Conversion and Management, 52*(1), 789-793.

Dagtekin, I., Oztop, H. F., & Sahin, A. Z. (2005). An analysis of entropy generation through a circular duct with different shaped longitudinal fins for laminar flow. *International Journal of Heat and Mass Transfer, 48*(1), 171-181.

De Robertis, E., Cosme, E. H. H., Neves, R. S., Kuznetsov, A. Y., Campos, A. P. C., Landi, S. M., et al. (2012) Application of the modulated temperature differential scanning calorimetry technique for the determination of the specific heat of copper nanofluids. *Applied Thermal Engineering*, *41*,10-17.

Ding, Y., Chen, H., He, Y., Lapkin, A., Yeganeh, M., Siller, L., et al. (2007). Forced convective heat transfer of nanofluids. *Advanced Powder Technology, 18*(6), 813-824.

Duan, F., Kwek, D., & Crivoi, A. (2011). Viscosity affected by nanoparticle aggregation in Al_2O_3-water nanofluids. *Nanoscale Research Letters, 6*, 248.

Duangthongsuk, W., &Wongwises, S. (2007). A critical review of convective heat transfer of nanofluids. *Renewable and Sustainable Energy Reviews, 11*(5), 797-817.

Duangthongsuk, W., & Wongwises, S. (2009). Measurement of temperature-dependent thermal conductivity and viscosity of TiO_2-water nanofluids. *Experimental Thermal and Fluid Science,33*(4), 706-714.

Duangthongsuk, W., & Wongwises, S. (2012). A dispersion model for predicting the

heat transfer performance of TiO_2-water nanofluids under a laminar flow regime. *International Journal of Heat and Mass Transfer, 55*(11-12), 3138-3146.

Do, K. H., Ha, H. J., & Jang, S. P. (2010). Thermal resistance of screen mesh wick heat pipes using the water-based Al_2O_3 nanofluids. *International Journal of Heat and Mass Transfer, 53*(25-26), 5888-5894.

Do, K. H., & Jang, S. P. (2010) Effect of nanofluids on the thermal performance of a flat micro heat pipe with a rectangular grooved wick. *International Journal of Heat and Mass Transfer, 53*(9-10), 2183-2192.

Eastman, J. A., Choi, S., S, L., Yu, W., & Thompson, L. J. (2001). Anomalously increased effective thermal conductivities of ethylene glycol-based nanofluids containing copper nanoparticles. *Applied Physics Letters, 78*(6), 718-720.

Ebrahimnia-Bajestan, E., Niazmand, H., Duangthongsuk, W., & Wongwises, S. (2011). Numerical investigation of effective parameters in convective heat transfer of nanofluids flowing under a laminar flow regime. *International Journal of Heat and Mass Transfer, 54*(19-20), 4376-4388.

Evans, W. J. (2008). Investigation and Identification of Physical Mechanism for Enhanced Thermal Conductivity in Nanofluids Using Molecular Level Modeling. Unpublished PhD's thesis, Rensselaer Polytechnic Institute, New York.

Farajollahi, B., Etemad, S. G., & Hojjat, M. (2010). Heat transfer of nanofluids in a shell and tube heat exchanger. *International Journal of Heat and Mass Transfer, 53*(1-3), 12-17.

Fedele, L., Colla, L., & Bobbo, S. (2012). Viscosity and thermal conductivity measurements of water-based nanofluids containing titanium oxide nanoparticles. *International Journal of Refrigeration, 35(5),* 1359-1366.

Firouzfar, E., Soltanieh, M., Noie, S.H., & Saidi, S.H. (2011). Energy saving in HVAC systems using nanofluid. *Applied Thermal Engineering, 31*, 1543-1545.

Ghadimi, A., Saidur, R., & Metselaar, H. S. C. (2011). A review of nanofluid stability properties and characterization in stationary conditions. *International Journal of Heat and Mass Transfer, 54*(17-18), 4051-4068.

Guo, Z. C., & Fu, Z. X. (2010). Current situation of energy consumption and measures taken for energy saving in the iron and steel industry in China. *Energy, 35*(11), 4356-4360.

Hagens, H., Ganzevles, F. L. A., Van der Geld, C. W. M., & Grooten, M. H. M. (2007). Air heat exchangers with long heat pipes: Experiments and predictions. *Applied Thermal Engineering, 27*(14-15), 2426-2434.

Han, Z. (2008). Nanofluids with Enhanced Thermal Transport Properties. Unpublished PhD's thesis, University of Maryland at College Park, College Park, Maryland.

Hewitt, G. F., Shires, G. L., & Bott, T. R. (1993). *Process heat transfer*. Florida: CRC Press, Inc.

He, Y., Jin, Y., Chen, H., Ding, Y., Cang, D., & Lu, H. (2007). Heat transfer and flow behaviour of aqueous suspensions of TiO_2 nanoparticles (nanofluids) flowing upward through a vertical pipe. *International Journal of Heat and Mass Transfer, 50*(11-12), 2272-2281.

He, Y., Men, Y., Zhao, Y., Lu, H., & Ding, Y. (2009). Numerical investigation into the convective heat transfer of TiO_2 nanofluids flowing through a straight tube under the laminar flow conditions. *Applied Thermal Engineering, 29*(10), 1965-1972.

Hojjat, M., Etemad, S. G., Bagheri, R., & Thibault, J. (2011). Convective heat transfer of non-Newtonian nanofluids through a uniformly heated circular tube. *International Journal of Thermal Sciences, 50*(4), 525-531

Hong, K. S., Hong, T.-K., & Yang, H.-S. (2006). Thermal conductivity of Fe nanofluids depending on the cluster size of nanoparticles. *Appl. Phys. Lett., 88*, 031901

Huminic, G., & Huminic, A. (2013). Numerical analysis of laminar flow heat transfer of nanofluids in a flattened tube. *International Communications in Heat and Mass Transfer, 44, 52-57.*

Hwang, Y. J., Ahn, Y. C., Shin, H. S., Lee, C. G., Kim, G. T., Park, H. S., et al. (2006). Investigation on characteristics of thermal conductivity enhancement of nanofluids. *Current Applied Physics, 6*(6), 1068-1071.

Hwang, Y., Lee, J.-K., Lee, J.-K., Jeong, Y.-M., Cheong, S.-i., Ahn, Y.-C., et al. (2008). Production and dispersion stability of nanoparticles in nanofluids. *Powder Technology, 186*(2), 145-153.

Ijam, A., & Saidur, R. (2012) Nanofluid as a coolant for electronic devices (cooling of electronic devices). *Applied Thermal Engineering*, *32*, 76-82.

Increase Performance Inc. Flue gas calculator. Retrieved 26th March 2011, from http://www.increase-performance.com/calc-flue-gas-prop.html

Incropera, F. P., Dewitt, D. P., Bergman, T. L., & Lavine, A. S. (2007). *Fundamentals of heat and mass transfer* (6th ed.). New York: John Wiley andSons.

Jahar, S. (2011). Performance of nanofluid-cooled shell and tube gas cooler in transcritical CO_2 refrigeration systems. *Applied Thermal Engineering, 31*(14-15), 2541-2548.

Jang, S. P., & Choi, S. U. S. (2004). Role of Brownian motion in the enhanced thermal conductivity of nanofluids. *Applied Physics Letters, 84*(21), 4316-4318.

Jang, S. P., & Choi, S. U. S. (2006). Cooling performance of a microchannel heat sink with nanofluids. *Applied Thermal Engineering, 26*(17-18), 2457-2463.

Jayamaha, L. (2008). *Energy Efficient Building Systems, Green Strategies for Operation*

and Maintenance. Singapore: McgrawHill Education.

Jung, J.-Y., Oh, H.-S., & Kwak, H.-Y. (2009). Forced convective heat transfer of nanofluids in microchannels. *International Journal of Heat and Mass Transfer, 52*(1-2), 466-472.

Jung, J.-Y., & Yoo, J. Y. (2009). Thermal conductivity enhancement of nanofluids in conjunction with electrical double layer (EDL). *International Journal of Heat and Mass Transfer, 52*(1-2), 525-528.

Jung, S., Jo, B., Shin, D., & Banerjee, D. (2010). Experimental Validation of a Simple Analytical Model for Specific Heat Capacity of Aqueous Nanofluids. *SAE Technical Paper 2010-01-1731*.

Kakac, S. & Liu, H.T. (2002). *Heat exchanger selection,rating and thermal design* (2nd ed.). New York: CRC Press.

Keblinski, P., Phillpot, S. R., Choi, S. U. S., & Eastman, J. A. (2002). Mechanisms of heat flow in suspensions of nano-sized particles (nanofluids). *International Journal of Heat and Mass Transfer, 45*(4), 855-863.

Keblinski, P., Eastman, J. A., & Cahill, D. G. (2005). Nanofluids for thermal transport. *Materials Today, 8*(6), 36-44.

Keblinski, P. (2009). Thermal conductivity of nanofluids. In S. Volz (Ed.), *Thermal nanosystems and nanomaterials*: Springer.

Khanafer, K., & Vafai, K. A critical synthesis of thermophysical characteristics of nanofluids. *International Journal of Heat and Mass Transfer, 54*(19-20), 4410-4428.

Kim, D., Kwon, Y., Cho, Y., Li, C., Cheong, S., Hwang, Y., et al. (2009). Convective heat transfer characteristics of nanofluids under laminar and turbulent flow conditions. *Current Applied Physics,* 9(2, Supplement 1), 119-123.

Ko, T. H. (2006). Analysis of optimal Reynolds number for developing laminar forced convection in double sine ducts based on entropy generation minimization principle. *Energy Conversion and Management, 47(6),* 655-670.

Ko, T. H., & Wu, C. P. (2009). A numerical study on entropy generation induced by turbulent forced convection in curved rectangular ducts with various aspect ratios. *International Communications in Heat and Mass Transfer, 36*(1), 25-31.

Kole, M., & Dey, T. K. (2010). Viscosity of alumina nanoparticles dispersed in car engine coolant. *Experimental Thermal and Fluid Science, 34*(6), 677-683.

Kulkarni, D. P., Vajjha, R. S., Das, D. K., & Oliva, D. (2008). Application of aluminum oxide nanofluids in diesel electric generator as jacket water coolant. *Applied Thermal Engineering, 28*(14-15), 1774-1781.

Kulkarni, D. P., Das, D. K., & Vajjha, R. S. (2009). Application of nanofluids in heating buildings and reducing pollution. *Applied Energy 86*(12),2566-2573.

Lee, J.-H., Hwang, K. S., Jang, S. P., Lee, B. H., Kim, J. H., Choi, S. U. S., et al. (2008). Effective viscosities and thermal conductivities of aqueous nanofluids containing low volume concentrations of Al_2O_3 nanoparticles. *International Journal of Heat and Mass Transfer, 51*(11-12), 2651-2656.

Lee, S. W., Park, S. D., Kang, S., Bang, I. C., & Kim, J. H. (2011). Investigation of viscosity and thermal conductivity of SiC nanofluids for heat transfer applications. *International Journal of Heat and Mass Transfer, 54*, 433-438.

Leong.K.C, Yang.C, and Murshed, S. M. S. (2006). A model for the thermal conductivity of nanofluids-the effect of interfacial layer. *J.Nanopart Res, 8*, 245254.

Leong, K. Y., Saidur, R., Kazi, S. N., & Mamun, A. H. (2010). Performance investigation of an automotive car radiator operated with nanofluid-based coolants (nanofluid as a coolant in a radiator). *Applied Thermal Engineering, 30*(17-18), 2685-2692.

Leong, K. Y., Saidur, R., Khairulmaini, M., Michael, Z., & Kamyar, A. (2012). Heat transfer and entropy analysis of three different types of heat exchangers operated with nanofluids. *International Communications in Heat and Mass Transfer, 39*(6), 838-843.

Lin, C.-Y., Wang, J.-C., and Chen, T.-C. (2011). Analysis of suspension and heat transfer characteristics of Al_2O_3 nanofluids prepared through ultrasonic vibration. *Applied Energy*, 88*(12),* 4527-4533.

Liu, D., Tang, G.-F., Zhao, F.-Y., & Wang, H.-Q. (2006). Modeling and experimental investigation of looped separate heat pipe as waste heat recovery facility. *Applied Thermal Engineering, 26*(17-18), 2433-2441.

Liu, M.-S., Lin, M. C.-C., Tsai, C. Y., & Wang, C.-C. (2006). Enhancement of thermal conductivity with Cu for nanofluids using chemical reduction method. *International Journal of Heat and Mass Transfer, 49*(17-18), 3028-3033.

Liu, M.S., Lin, C.C., & Wang, C.C. (2011). Enhancement of thermal conductivityies with Cu, CuO, and carbon nanotube nanofluids and application of MWNT/water nanofluid on a water chiller system. *Nanoscale Research Letters*, *6*(297),1-23

Li, X. F., Zhu, D. S., Wang, X. J., Wang, N., Gao, J. W., & Li, H. (2008). Thermal conductivity enhancement dependent pH and chemical surfactant for Cu-H_2O nanofluids. *Thermochimica Acta, 469*(1-2), 98-103.

Lotfi, R., Rashidi, A. M., & Amrollahi, A. (2012). Experimental study on the heat transfer enhancement of MWNT-water nanofluid in a shell and tube heat exchanger. *International Communications in Heat and Mass Transfer, 39*(1), 108-111.

Lu, W.-Q., & Fan, Q.-M. (2008). Study for the particle's scale effect on some thermophysical properties of nanofluids by a simplified molecular dynamics method. *Engineering Analysis with Boundary Elements, 32*(4), 282-289.

Lundgren, T. S. (1972). Slow flow through stationary random beds and suspensions of spheres. *J. Fluid Mech, 51*(2), 273-299.

Mahbubul, I. M., Saidur, R., & Amalina, M. A. (2012). Latest developments on the viscosity of nanofluids. *International Journal of Heat and Mass Transfer, 55(4),* 874-885.

Mingzheng, Z., Guodong, X., Jian, L., Lei, C., & Lijun, Z. (2012). Analysis of factors influencing thermal conductivity and viscosity in different kinds of surfactant solutions. *Experimental Thermal and Fluid Science, 36*, 22-29.

Mintsa, H. A., Roy, G., Nguyen, C. T., & Doucet, D. (2009). New temperature dependent thermal conductivity data for water-based nanofluids. *International Journal of Thermal Sciences, 48*(2), 363-371.

Moghaddami, M., Mohammadzade, A., & Esfehani, S. A. V. (2011). Second law analysis of nanofluid flow. *Energy Conversion and Management, 52*(2*),* 1397-1405.

Murshed, S. M. S., Leong, K. C., & Yang, C. (2005). Enhanced thermal conductivity of TiO_2--water based nanofluids. *International Journal of Thermal Sciences, 44*(4), 367-373.

Murshed, S. M. S., Leong, K. C., & Yang, C. (2008a). Thermophysical and electrokinetic properties of nanofluids - A critical review. *Applied Thermal Engineering, 28*(17-18), 2109-2125.

Murshed, S. M. S., Leong, K. C., & Yang, C. (2008b). Investigations of thermal conductivity and viscosity of nanofluids. *International Journal of Thermal Sciences, 47*(5), 560-568.

Murshed, S. M. S., Leong, K. C., & Yang, C. (2009). A combined model for the effective thermal conductivity of nanofluids. *Applied Thermal Engineering, 29*(11-12), 2477-2483.

Mousa, M. G. (2011). Effect of nanofluid concentration on the performance of circular heat pipe. *Ain Shams Engineering Journal, 2*(1), 63-69.

Namburu, P. K., Kulkarni, D. P., Misra, D., & Das, D. K. (2007). Viscosity of copper oxide nanoparticles dispersed in ethylene glycol and water mixture. *Experimental Thermal and Fluid Science, 32*(2), 397-402

Nasiri, A., Shariaty-Niasar, M., Rashidi, A. M., & Khodafarin, R. (2012). Effect of CNT structures on thermal conductivity and stability of nanofluid. *International Journal of Heat and Mass Transfer, 55*, 1529-1535.

Nguyen, C. T., Desgranges, F., Roy, G., Galanis, N., Mare, T., Boucher, S., et al. (2007). Temperature and particle-size dependent viscosity data for water-based nanofluids -Hysteresis phenomenon. *International Journal of Heat and Fluid Flow, 28*(6), 1492-1506.

Nguyen, C. T., Desgranges, F., Galanis, N., Roy, G., Maré, T., Boucher, S., et al. (2008). Viscosity data for Al2O3-water nanofluid--hysteresis: is heat transfer enhancement using nanofluids reliable? *International Journal of Thermal Sciences, 47*(2), 103-111.

Noie, S. H. (2006). Investigation of thermal performance of an air-to-air thermosyphon heat exchanger using ϵ-NTU method. *Applied Thermal Engineering, 26*(5-6), 559-567.

Noie-Baghban, S. H., & Majideian, G. R. (2000). Waste heat recovery using heat pipe heat exchanger (HPHE) for surgery rooms in hospitals. *Applied Thermal Engineering, 20*(14), 1271-1282.

Nuntaphan, A., Tiansuwan, J., & Kiatsiriroat, T. (2002). Enhancement of heat transport in thermosyphon air preheater at high temperature with binary working fluid: A case study of TEG-water. *Applied Thermal Engineering, 22*(3), 251-266.

Otanicar, T. P., Phelan, P. E., Prasher, R. S., Rosengarten, G., & Taylor, R. A. (2010). Nanofluid-based direct absorption solar collector. *Journal of renewable and Sustainable Energy, 2*, 033102-033113.

Pandiyarajan, V., Chinna Pandian, M., Malan, E., Velraj, R., & Seeniraj, R. V. (2011). Experimental investigation on heat recovery from diesel engine exhaust using finned shell and tube heat exchanger and thermal storage system. *Applied Energy, 88*(1), 77-87.

Park, K.-J., & Jung, D. (2007). Boiling heat transfer enhancement with carbon nanotubes for refrigerants used in building air-conditioning. *Energy and Buildings, 39*(9), 1061-1064.

Paul, G., Sarkar, S., Pal, T., Das, P. K., & Manna, I. (2012). Concentration and size dependence of nano-silver dispersed water based nanofluids. *Journal of Colloid and Interface Science, 371*(1), 20-27.

Peyghambarzadeh, S. M., Hashemabadi, S. H., Hoseini, S. M., & Seifi Jamnani, M. (2011a). Experimental study of heat transfer enhancement using water/ethylene glycol based nanofluids as a new coolant for car radiators. *International Communications in Heat and Mass Transfer, 38*(9), 1283-1290.

Peyghambarzadeh, S. M., Hashemabadi, S. H., Jamnani, M. S., & Hoseini, S. M. (2011b). Improving the cooling performance of automobile radiator with Al_2O_3/water nanofluid. *Applied Thermal Engineering, 31*(10), 1833-1838.

Phuoc, T. X., & Massoudi, M. (2009). Experimental observations of the effects of shear rates and particle concentration on the viscosity of Fe_2O_3 deionized water nanofluids. *International Journal of Thermal Sciences, 48*(7), 1294-1301.

Prasher, R., Bhattacharya, P., & E.Phelan, P. (2006). Brownian-motion-based convective-conductive model for the effective thermal conductivity of nanofluids. *Journal of Heat Transfer, 128*, 588-595.

Putra, N., Septiadi, W. N., Rahman, H., & Irwansyah, R. (2012). Thermal performance of screen mesh wick heat pipes with nanofluids. *Experimental Thermal and Fluid Science*, *40*, 10-17.

Qu, J., Wu, H.-y., & Cheng, P. (2010). Thermal performance of an oscillating heat pipe with Al_2O_3-water nanofluids. *International Communications in Heat and Mass Transfer, 37*(2), 111-115.

Qu, J., & Wu, H. (2011). Thermal performance comparison of oscillating heat pipes with SiO_2/water and Al_2O_3/water nanofluids. *International Journal of Thermal Sciences, 50*(10), 1954-1962.

Ramesh, K. S., & Dusan, P. S. (2003). *Fundamentals of heat exchanger design*. New Jersey: John Wiley and Sons.

Roberts, N. A., & Walker, D. G. (2010). Convective Performance of Nanofluids in Commercial Electronics Cooling Systems. *Applied Thermal Engineering, 30*(16), 2499-2504.

Saidur, R., Ahamed, J. U., & Masjuki, H. H. (2010). Energy, exergy and economic analysis of industrial boilers. *Energy Policy, 38*(5), 2188-2197.

Sahin, A. Z. (2000). Entropy generation in turbulent liquid flow through a smooth duct subjected to constant wall temperature. *International Journal of Heat and Mass Transfer, 42*(8), 1469-1478.

Sahin.A.Z. (1998). A second law comparison for optimum shape of duct subjected to constant wall temperature and laminar flow. *Heat and mass transfer, 22*, 425-430.

Saneipoor, P., Naterer, G. F., & Dincer, I. (2011). Heat recovery from a cement plant with a Marnoch Heat Engine. *Applied Thermal Engineering, 31*(10), 1734-1743.

Sarit, K. D., Choi, S. U. S., Yu, W., & Pradeep, T. (2008). *Nanofluids science and technology*. New Jersey: Wiley Interscience.

Sarit, K.D. (2009). Process heat transfer. Oxford: Alpha Science.

Shafahi, M., Bianco, V., Vafai, K., & Manca, O. (2010). An investigation of the thermal performance of cylindrical heat pipes using nanofluids. *International Journal of Heat and Mass Transfer, 53*(1-3), 376-383.

Shalchi-Tabrizi, A., & Seyf, H. R. (2012). Analysis of entropy generation and convective heat transfer of Al_2O_3 nanofluid flow in a tangential micro heat sink. *International Journal of Heat and Mass Transfer, 55*(15-16), 4366-4375.

Shi, X., Che, D., Agnew, B., & Gao, J. (2011). An investigation of the performance of compact heat exchanger for latent heat recovery from exhaust flue gases. *International Journal of Heat and Mass Transfer, 54*(1-3), 606-615.

Shima, P. D., Philip, J., & Raj, B. (2010). Influence of aggregation on thermal conductivity in stable and unstable nanofluids. *Appl. Phys. Lett, 97*, 153113.

Sigma Aldrich. (2013).Nanomaterials. Retrieved 4th August 2013, from http://www.sigmaaldrich.com/malaysia.html

Singh, P. K., Anoop, K. B., Sundararajan, T., & Das, S. K. (2010). Entropy generation due to flow and heat transfer in nanofluids. *International Journal of Heat and Mass Transfer, 53*, 4757-4767.

Srimuang, W., & Amatachaya, P. (2012). A review of the applications of heat pipe heat exchangers for heat recovery. *Renewable and Sustainable Energy Reviews, 16*(6), 4303-4315.

Strandberg, R., & Das, D. K. (2010). Influence of temperature and properties variation on nanofluids in building heating. *Energy Conversion and Management, 51*(7), 1381-1390.

Stijepovic, M. Z., & Linke, P. (2011). Optimal waste heat recovery and reuse in industrial zones. *Energy, 36*(7), 4019-4031.

Suresh, S., Venkitaraj, K. P., Selvakumar, P., & Chandrasekar, M. (2012). A comparison of thermal characteristics of Al_2O_3/water and CuO/water nanofluids in transition flow through a straight circular duct fitted with helical screw tape inserts. *Experimental Thermal and Fluid Science, 39*, 37-44.

Taborek, J. (1991). Industrial Heat Exchanger Design Practices. In S. Kakac (Ed.), *Boilers, evaporators condensers*. New York: John Wiley and Sons.Inc.

Teke, I., Agra, Ö., AtayIlmaz, S. Ö., & Demir, H. (2010). Determining the best type of heat exchangers for heat recovery. *Applied Thermal Engineering, 30*(6-7), 577-583.

Teng, T.-P., Hung, Y.-H., Teng, T.-C., Mo, H.-E., & Hsu, H.-G. (2010). The effect of alumina/water nanofluid particle size on thermal conductivity. *Applied Thermal Engineering, 30*(14-15), 2213-2218.

Timofeeva, E. V., Smith, D. S., Yu, W., France, D. M., Singh, D. V., & Routbort, J. L. (2010). Particle size and interfacial effects on thermo-physical and heat transfer characteristics of water-based α-SiC nanofluids. *Nanotechnology, 21*(215703 (10pp)), 21.

Tsai, T.-H., & Chein, R. (2007). Performance analysis of nanofluid-cooled microchannel heat sinks. *International Journal of Heat and Fluid Flow, 28*(5), 1013-1026.

United States, Energy Information Administration. (2011). Annual Energy Outlook 2011 Early Release Overview. Retrieved 26th March 2011,from http://www.eia.gov/forecasts/aeo/pdf/0383er(2011).pdf

US Research Nanomaterials, Inc. (2013). Nanopowders. Retrieved 4th August 2013, from http://us-nano.com/nanopowders

Vajjha.R.S., D.K.Das, & Mahagaonkar.B.M. (2009). Density measurement of different nanofluids and their comparison with theory. *Petroleum Science and Technology, 27*, 612-624.

Vajjha, R. S., & Das, D. K. (2009). Experimental determination of thermal conductivity of three nanofluids and development of new correlations. *International Journal of Heat and Mass Transfer, 52*(21-22), 4675-4682.

Vajjha, R. S., Das, D. K., & Kulkarni, D. P. (2010). Development of new correlations for convective heat transfer and friction factor in turbulent regime for nanofluids. *International Journal of Heat and Mass Transfer, 53*(21-22), 4607-4618.

Velagapudi, V., Konijeti, K.,&Aduru, K. (2008). Empirical correlations to predict thermophysical and heat transfer characteristics of nanofluids. *Thermal Science, 12*, 27-37.

Wang, X.-j., Zhu, D.-s., & Yang, S. (2009). Investigation of pH and SDBS on enhancement of thermal conductivity in nanofluids. *Chemical Physics Letters, 470*(1-3), 107-111.

Wang, X.-Q., & Mujumdar, A. S. (2007). Heat transfer characteristics of nanofluids: a review. *International Journal of Thermal Sciences, 46(1),* 1-19.

Webb.R.L. (1994). *Principles of enhanced heat transfer*. New York: Wiley.

Wen, D., & Ding, Y. (2004). Experimental investigation into convective heat transfer of nanofluids at the entrance region under laminar flow conditions. *International Journal of Heat and Mass Transfer, 47*(24), 5181-5188.

Wu, S., Zhu, D., Li, X., Li, H., & Lei, J. (2009). Thermal energy storage behavior of Al_2O_3-H_2O nanofluids. *Thermochimica Acta, 483*(1-2), 73-77.

Xu, G., Huang, S., Yang, Y., Wu, Y., Zhang, K., & Xu, C. (2013). Techno-economic analysis and optimization of the heat recovery of utility boiler flue gas. *Applied Energy* (in press).

Yang, F., Yuan, X., & Lin, G. (2003). Waste heat recovery using heat pipe heat exchanger for heating automobile using exhaust gas. *Applied Thermal Engineering, 23*(3), 367-372.

Yang, L., Du, K., Ding, Y. H., Cheng, B., & Li, Y. J. (2012). Viscosity-prediction models of ammonia water nanofluids based on various dispersion types. *Powder Technology, 215-216*, 210-218.

Yanjia, W., & Chandler, W. (2010). The Chinese nonferrous metals industry--energy use and CO_2 emissions. *Energy Policy, 38*(11), 6475-6484.

Yilmaz, A. (2009). Minimum entropy generation for laminar flow at constant wall temperature in a circular duct for optmum design. *Heat mass transfer, 45*, 1415-1421.

Yoo, D.-H., Hong, K. S., & Yang, H.-S. (2007). Study of thermal conductivity of nanofluids for the application of heat transfer fluids. *Thermochimica Acta, 455*(1-2), 66-69.

Yousefi, T., Veisy, F., Shojaeizadeh, E., & Zinadini, S. (2012). An experimental investigation on the effect of MWCNT-H_2O nanofluid on the efficiency of flat-plate solar collectors. *Experimental Thermal and Fluid Science, 39*, 207-212.

Yu, W., & Choi, S. U. S. (2003). The role of interfacial layers in the enhanced thermal conductivity of nanofluids: A renovated Maxwell model. *Journal of Nanoparticle Research, 5*, 167-171.

Yu, W., & Choi, S. U. S. (2004). The role of interfacial layers in the enhanced thermal conductivity of nanofluids: A renovated Hamilton–Crosser model. *Journal of Nanoparticle Research, 6*, 355-361.

Yu, W., France, D. M., Choi, S. U. S., & Routbort, J. L. (2007). *Review and assessment of nanofluid technology for transportation and other applications* (No. ANL/ESD/07-9). Argonne: Energy System Division,Argonne National Laboratoryo. Document Number)

Yu, W., Xie, H., Chen, L., & Li, Y. (2009). Investigation of thermal conductivity and viscosity of ethylene glycol based ZnO nanofluid. *Thermochimica Acta, 491*(1-2)*,* 92-96.

Yu, W., Xie, H., Chen, L., & Li, Y. (2010). Investigation on the thermal transport properties of ethylene glycol-based nanofluids containing copper nanoparticles. *Powder Technology, 197*(3), 218-221.

Yu, W., Xie, H., Li, Y., Chen, L., & Wang, Q. (2011). Experimental investigation on the thermal transport properties of ethylene glycol based nanofluids containing low volume concentration diamond nanoparticles. *Colloids and Surfaces A: Physicochemical and Engineering Aspects, 380*(1-3), 1-5.

Zeinali, H. S., Nasr, E. M., & Etemad, S. G. (2007). Experimental investigation of convective heat transfer of Al_2O_3/water nanofluid in circular tube. *International Journal of Heat and Fluid Flow, 28(2),* 203-210.

Zarifi, E., Jahanfarnia, G., & Veysi, F. (2013). Thermal-hydraulic modelling of nanofluids as the coolant in VVER- 1000 reactor core by the porous media approach. *Annals of Nuclear Energy*, *51*,203-212.

Zhang, X., Gu, H., & Fujii, M. (2007). Effective thermal conductivity and thermal diffusivity of nanofluids containing spherical and cylindrical nanoparticles. *Experimental Thermal and Fluid Science, 31*(6), 593-599.

Zhou, S.-Q., & Ni, R. (2008). Measurement of the specific heat capacity of water-based Al_2O_3 nanofluid. *Appl. Phys. Lett, 92*, 093123.

Zhou, L.-P., Bu-XuanWang, Peng, X.-F., Du, X.-Z., & Yang, Y.-P. (2010). Research Article On the Specific Heat Capacity of CuO Nanofluid. *Advances in Mechanical Engineering*, 1-4.

Zhu, D., Li, X., Wang, N., Wang, X., Gao, J., & Li, H. (2009). Dispersion behavior and thermal conductivity characteristics of Al_2O_3-H_2O nanofluids. *Current Applied Physics, 9*(1), 131-139.

APPENDIX A
CURRICULUM VITAE

Leong Kin Yuen obtained his M.Eng in mechanical engineering from University of Malaya, Malaysia and a B.Eng in mechanical engineering from University Tun Hussein Onn, Presently, he is a lecturer at Universiti Pertahanan Nasional Malaysia (UPNM) teaching Heat Transfer, Air Conditioning and Refrigeration, Engineering Drawing and Control Engineering. To date, he has published seven (7) ISI- cited papers where most of the papers are nanofluids related papers. He is also a principle investigator for one of the nanofluids project funded by the Ministry of Higher Education, Malaysia under the FRGS grant to UPNM. He also reviews articles submitted to the International Journal of Heat and Mass Transfer, Heat Transfer- Asian Research and Nano-Micro Letter.

APPENDIX B

LIST OF PUBLICATIONS

1) **K.Y.Leong** ,R. Saidur, T.M.I Mahlia,Y.H.Yau, Performance Investigation of Nanofluids as Coolant in Thermosyphon Air Preheater,-International Communication Heat and Mass Transfer – 39 (2012) 523–529 *(ISI/SCOPUS-Cited Publication- 1.892IF)-Q1*

2) **K.Y.Leong** ,R. Saidur, T.M.I Mahlia,Y.H.Yau, Modeling of shell and tube heat recovery exchanger operated with nanofluid based coolants, International Journal of Heat and Mass Transfer, 55 (4), (2012) 808-816 (*ISI/SCOPUS-Cited Publication-2.407IF) –Q1*

3) **K.Y.Leong**, R.Saidur, T.M.Mahlia, Y.H.Yau, Entropy generation analysis of nanofluid flow in a circular tube subjected to constant wall temperature, International Communication Heat and Mass Transfer, 39(8) (2012) 1169-1175 *(ISI/SCOPUS- Cited Publication-1.8921IF)- Q1*

4) **K.Y.Leong** ,R. Saidur, T.M.I. Mahlia,Y.H.Yau,Predicting size reduction of shell and tube heat recovery exchanger operated with nanofluids based coolants and its associated energy saving, Energy Education Science and Technology Part A, 30(1) (2012)1-14 *(SCOPUS- Cited Publication)*

APPENDIX C

INVITATION AS A REVIEWER

Reviewer Invitation for HMT-D-12-00736R1
1 message

A.R. Balakrishnan <arbala@iitm.ac.in> Tue, Sep 18, 2012 at 9:57 AM
To: leongkinyuen@gmail.com

Ms. Ref. No.: HMT-D-12-00736R1
Title: Heat transfer performance of screen mesh wick heat pipes using silver-water nanofluid
International Journal of Heat and Mass Transfer

Dear Leong,

Given your expertise in this area, I would appreciate receiving your comments on the above paper. I have included the abstract of the manuscript below to provide you with an overview.

If you accept this invitation, your comments would be appreciated by Oct 16, 2012. If you are unable to act as a reviewer at this time, I would greatly appreciate your suggestions for alternate reviewers.

To accept this invitation, please click here:

http://ees.elsevier.com/hmt/l.asp?i=13046&l=L6TA0NHM

To decline this invitation, please click here:

http://ees.elsevier.com/hmt/l.asp?i=13045&l=C2P1S1V6

Alternatively, to register your response using the Elsevier Editorial System please do the following:

1. Go to this URL: http://ees.elsevier.com/hmt/

2. Enter these login details:
Your username is:
Your password is:

3. Click [Reviewer Login]
This takes you to the Reviewer Main Menu.

4. Click [New Reviewer Invitations]

5. Click either [Agree to Review] or [Decline to Review]

I look forward to hearing from you in the near future.

To help you review this manuscript you are granted free access to Scopus for 30 days after accepting this invitation. Scopus is the largest abstract and citation database of research literature and quality web sources. With Scopus, it is easy to find references, similar articles or papers by the same authors.

Yours sincerely,

T. Basak
Associate Editor
International Journal of Heat and Mass Transfer

Reviewer Invitation for HMT-D-12-01542

1 message

A.R. Balakrishnan <arbala@iitm.ac.in> Thu, Sep 13, 2012 at 8:10 PM
To: leongkinyuen@gmail.com

Ms. Ref. No.: HMT-D-12-01542
Title: Convective heat transfer characteristics of CNT nanofluids in a tubular heat exchanger of various lengths for energy efficient cooling/heating system
International Journal of Heat and Mass Transfer

Dear Leong,

Given your expertise in this area, I would appreciate receiving your comments on the above paper. I have included the abstract of the manuscript below to provide you with an overview.

If you accept this invitation, your comments would be appreciated by Oct 11, 2012. If you are unable to act as a reviewer at this time, I would greatly appreciate your suggestions for alternate reviewers.

To accept this invitation, please click here:

http://ees.elsevier.com/hmt/l.asp?i=12790&l=9VTL4BP8

To decline this invitation, please click here:

http://ees.elsevier.com/hmt/l.asp?i=12789&l=CQ8ECD3T

Alternatively, to register your response using the Elsevier Editorial System please do the following:

1. Go to this URL: http://ees.elsevier.com/hmt/

2. Enter these login details:
   Your username is:
   Your password is:

3. Click [Reviewer Login]
This takes you to the Reviewer Main Menu.

4. Click [New Reviewer Invitations]

5. Click either [Agree to Review] or [Decline to Review]

I look forward to hearing from you in the near future.

To help you review this manuscript you are granted free access to Scopus for 30 days after accepting this invitation. Scopus is the largest abstract and citation database of research literature and quality web sources. With Scopus, it is easy to find references, similar articles or papers by the same authors.

Yours sincerely,

T. Basak
Associate Editor
International Journal of Heat and Mass Transfer

A.R. Balakrishnan <arbala@iitm.ac.in> Fri, Dec 14, 2012 at 12:48 PM
To: leongkinyuen@gmail.com

Ms. Ref. No.: HMT-D-12-02108
Title: Mixed convection flow over a solid sphere embedded in a porous medium filled by a nanofluid containing gyrotactic microorganisms
International Journal of Heat and Mass Transfer

Dear Leong,

Given your expertise in this area, I would appreciate receiving your comments on the above paper. I have included the abstract of the manuscript below to provide you with an overview.

If you accept this invitation, your comments would be appreciated by Jan 11, 2013. If you are unable to act as a reviewer at this time, I would greatly appreciate your suggestions for alternate reviewers.

To accept this invitation, please click here:

http://ees.elsevier.com/hmt/l.asp?i=16616&l=2WMG6ZBS

To decline this invitation, please click here:

http://ees.elsevier.com/hmt/l.asp?i=16615&l=KMPMUJ04

Alternatively, to register your response using the Elsevier Editorial System please do the following:

1. Go to this URL: http://ees.elsevier.com/hmt/

2. Enter these login details:
Your username is:
Your password is:

3. Click [Reviewer Login]
This takes you to the Reviewer Main Menu.

4. Click [New Reviewer Invitations]

5. Click either [Agree to Review] or [Decline to Review]

[NML] Article Review Acknowledgement Inbox x

Nano-Micro Letters <editor@nmletters.org> 10/9/12

to me

Dear Dr. Mr Kin Yuen Leong,

Thank you for completing the review of the submission, "Controlling the Properties of Solvent-Free Fe3O4 Nanofluids by Corona Structure," for Nano-Micro Letters. We appreciate your contribution to the quality of our work.

The quality of Nano-Micro Letters depends on both the authors and reviewers who are willing to make contributions. We thank you for your willingness to help.

Yours sincerely

Dr. Liying Zhang
Managing Editor
Nano-Micro Letters
http://www.nmletters.org
Email: editor@nmletters.org

A.R. Balakrishnan <arbala@iitm.ac.in> Mar 17 (10 days ago)

to me, lky_leo501

Ms. Ref. No.: HMT-D-12-01968R1
Title: Effect of Copper Nanofluid in Aqueous Solution of Long Chain Alcohols in the Performance of Heat Pipes
International Journal of Heat and Mass Transfer

Dear Leong,

Given your expertise in this area, I would appreciate receiving your comments on the above paper. I have included the abstract of the manuscript below to provide you with an overview.

If you accept this invitation, your comments would be appreciated by Apr 13, 2013. If you are unable to act as a reviewer at this time, I would greatly appreciate your suggestions for alternate reviewers.

To accept this invitation, please click here:

http://ees.elsevier.com/hmt/l.asp?i=20522&l=0M7IH5HL

To decline this invitation, please click here:

http://ees.elsevier.com/hmt/l.asp?i=20521&l=CMYJXQZZ

Alternatively, to register your response using the Elsevier Editorial System please do the following:

1. Go to this URL: http://ees.elsevier.com/hmt/

2. Enter these login details:
   Your username is: leongkinyuen@gmail.com
   If you need to retrieve password details, please go to: http://ees.elsevier.com/HMT/automail_query.asp.

APPENDIX D

INVITATION TO THE 2ND ANNUAL CONGRESS OF NANO S&T 2012 CHINA

Gmail by Google

Kin Yuen Leong <leongkinyuen@gmail.com>

253-Brochure and Invitation Letter
1 message

Selina <Je3n5@bit-wcd.com>
Reply-To: selina@bitconferences.com
To: leongkinyuen@gmail.com

Thu, Jul 5, 2012 at 10:19 AM

Dear Dr. K.Y. Leong,

The organizing committee is pleased to announce that the 2nd Annual World Congress of Nano-S&T (Nano S&T-2012), which will be held from October 26 to 28, 2012 in Qingdao, China. The congress will consist of 12 streamlines covering topics including: Nanosciences and Technologies, Nanomaterials, Analytical tools for Nanotech, Nano-electronics, Nano IT, Nanocoating, etc. This conference will bring together over 1000 experts and specialists from all over the world.

Based upon your contribution to the field of Nanotechnology, if you agree, we cordially invite you to participate in the meeting to talk about Performance investigation of nanofluids as working fluid in a thermosyphon air preheater..... at **Section 7-2: Nanotech in Heat Transfer and Nano Fluid Engineering** of this grand congress.

Certainly, you can look through the program and select a session at your priority. We will be honored if you can deliver a speech during this event. Your involvement in this congress will be invaluable for the development of the program.

Some speakers' profile and presentation's titles have been released at the conference website so that you can know what specific subjects will be covered by the other speakers. You may log on: http://www.bitconferences.com/nano2012/program.asp.

I am pleased to send you a conference brochure about Nano-S&T2012 in the attachment.

APPENDIX E

INVITATION TO SUBMIT PAPER TO FRONTIER IN HEAT PIPE (FHP)

Frontiers in Heat Pipes (FHP)
4 messages

Zhang, Yuwen <zhangyu@missouri.edu> Sat, Sep 1, 2012 at 5:59 AM
To: "Zhang, Yuwen" <zhangyu@missouri.edu>
Cc: amir faghri <amir.faghri@uconn.edu>

Dear Colleague:

I am pleased to inform you that you have been selected as an active research member of the heat pipe community and to submit an invited paper for special issues of Frontiers in Heat Pipes (FHP), an International Journal. The special issues of FHP are dedicated to recent advances in heat pipes and are set to be published in February 2012. If you accept this invitation, you should inform me of your proposed title by September 15, 2012. The full paper is due on December 20, 2012.

The following are some of the specific advantages Frontiers in Heat Pipes (FHP) have over existing heat and mass transfer journals:

1. Frontiers in Heat Pipes is mainly devoted to the field of heat pipe science and technology. Eight issues of the Journal of Frontiers in Heat Pipes (FHP) have been published since its inception in 2010.
2. Journal issues and volumes are made permanently available electronically on a central technical website (Thermal-Fluids Central) that is used globally free-of-charge by the thermal-fluids community.
3. Premiere open-access and peer-reviewed journal.
4. No cost to authors or readers.
5. No color or page limitation.
6. Unlimited use and distribution resulting in an increased citations and impact.

I am looking forward to hear from you concerning your proposed title by September 15.

Best Regards,

Yuwen Zhang, Ph.D.

James C. Dowell Professor

ASME Fellow and AIAA Associate Fellow

Department of Mechanical and Aerospace Engineering

University of Missouri

E 3411 Thomas & Nell Lafferre Hall

Columbia, MO 65211, USA

Tel: (573) 884-6936

Fax: (573) 884-5090

URL: http://web.missouri.edu/~zhangyu

APPENDIX F

SPPEECH INVITATION FROM NANOSCIENCE AND TECHNOLOGY 2013, CHINA

Invitation Letter

Dear Dr. K.Y. Leong

The organizing committee is pleased to extend to you a formal invitation to give a presentation at **Track 6: Nanotechnology in Energy & Environment** for the upcoming 3rd Annual World Congress of Nanoscience & Technology (Nano S&T-2013), to be held from September 27 to 29, 2013 in Xi'an, China. We feel that your unique and inspirational speech would be the perfect way to kick off the conference.

The comingcongress will be held concurrently with the Euro-Asia Economic Forum, thus national leaders will also attend Nano-S&T.TheEuro-Asia Economic Forumis hosted by:

- Ministry of Commerce of the People's Republic of China
- Ministry of Education of the People's Republic of China
- Ministry of Culture of the People's Republic of China
- Development Research Center of the State Council
- National Energy Administration of the People's Republic of China
- State Administration of Cultural Heritage
- State Administration of Cultural Heritage
- China Development Bank
- The Export-Import Bank of China
- Secretariat of Shanghai Cooperation Organization
- United Nations Development Programme
- Eurasian Economic Community
- The People's Government of Shaanxi Province

The Best Paper Award ($1000) collection is under construction now. For the details, you may click http://www.bitconferences.com/nano2013/CSBJ.asp .

The previous two annual Nanoscience & Technology conferences were great successes and allowed influential industry partners, scientific experts, leaders and policymakers from many different countries to meet, exchange ideasand begin to work together.

The 3rd Annual World Congress of Nanoscience & Technologywill consist of 10tracks covering topics including:new nanoscience and nanotechnology, advanced nanomaterials,nano-electronics, optoelectronics and microsystems, nano-fabrication, characterization &nanometrology, nanomedicine and nanobiotechnology, nanotechnology in energy &the environment, and novel applications of nanotechnology. The meeting will bring together over 500 experts and specialists from all over the world.Please visit our conference website http://www.bitconferences.com/nano2013/program.asp for more information.

We would be honored and gratefulfor your participation in the3rd Annual World Congress of Nanoscience & Technology.

Sincerely yours,

Ms. Ada Wang
Organizing Committee of Nano S&T-2013
East Area, F11, Building 1,
Dalian Ascendas IT Park,
1 Hui Xian Yuan,
Dalian Hi-tech Industrial Zone,
LN 116025, China
Tel: 0086-411-84799609-844
Email: ada@bitconferences.com

APPENDIX G

SAMPLE CALCULATIONS

Some of the sample calculations used in this study are as follows

1) <u>Thermal conductivity enhancement of ethyelene/glycol based 0.5 vol% Al2O3 (13nm) nanofluids</u>

$$k(\text{ethylene glycol/water}) + 0.5\ \text{vol.}\ \%\ Al2O3 - 13nm) = 0.4116$$

$$k(\text{ethylene g; ycol/water}) = 0.378$$

$$\%\ \text{enhancement} = \frac{k_{\text{nanofluids}} - k_{\text{ethylene glycol/water}}}{k_{\text{ethylene glycol/water}}} \times 100\%$$

$$= \frac{0.4116 - 0.378}{0.378} \times 100\% \qquad = 8.9\%$$

2) <u>Shell and tube heat recovery exchanger</u>

Shell side calculation (Convective heat transfer coefficient)

$$\text{Cross flow area, } A_{cf} = (D_s - N_{TC}d_o)B$$

$$N_{TC} = \frac{D_s}{P_T} = \frac{2.09}{0.044450} = 47.019123$$

$$A_{cf} = \big(2.09 - 47.019123(0.0254)\big)1.776 = 1.590788$$

$$\text{Equivalent diameter, } D_e = \frac{4\left(P_t^2 - \frac{\pi d_o^2}{4}\right)}{\pi d_o}$$

$$D_e = \frac{4\left(0.044450^2 - \frac{\pi(0.0254)^2}{4}\right)}{\pi(0.0254)} = 0.073629\ \text{m}$$

$$\text{Flue gas viscosity, } \mu_{fg} = 0.000019\ \frac{Ns}{m^2}$$

$$\text{Flue gas Prandtl number, } Pr_{fg} = 0.759492$$

$$\text{Flue gas Reynolds number } Re_{fg} = \left(\frac{\dot{m}_{fg}}{A_{cf}}\right)\frac{D_e}{\mu_{fg}} = \left(\frac{26.3}{1.590788}\right)\left(\frac{0.073629}{0.000019}\right)$$

$$= 64067.863724$$

$$\text{Flue gas convective heat transfer coefficient , } h_{fg} = \frac{0.36k}{D_e} Re_{fg}^{0.55} Pr_{fg}^{\frac{1}{3}}$$

$$h_{fg} = \frac{0.36(0.000029)}{0.073629} 64067.863724^{0.55} 0.759492^{\frac{1}{3}} = 0.056418$$
$$= 56.418 \frac{W}{m^2K}$$

Tube side calculation (Convective heat transfer coefficient)

1vol. % Cu+H_2O

Thermal conductivity of nanofluids, $k_{nf} = 0.000305 \frac{kW}{mK}$

Density of nanofluid $\rho_{nf} = 1150.421900 \frac{kg}{m^3}$

Specific heat of nanoflui, $c_{p.nf} = 2.516754 \frac{kJ}{kgK}$

Prandtl number of, $Pr_{nf} = 22.222115$

Number of tubes per pass, $N_{t,p}$

$N_{t,p} = N_T = 1024$ since single tube pass is considered

Tube side flow area per pass, $A_{o,t} = \frac{\pi}{4} d_i^2 N_{t,p}$

$$A_{o,t} = \frac{\pi}{4} d_i^2 N_{t,p} = \frac{\pi}{4} (0.0229)^2 (1024) = 0.421810 m^2$$

Nanofluids Reynold number, $Re_{nf} = \frac{\dot{m}_{nf} d_i}{A_{o,t} \mu_{nf}}$

$$Re_{nf} = \frac{(111.6 \times 0.0229)}{(0.421810 \times 0.002697)} = 2246.543355 \text{ (laminar flow)}$$

Nusselt number, $Nu = 3.66$

Nanofluids convective heat transfer coefficient, $h_{nf} = \frac{Nu_{nf} k_{nf}}{d_i}$

$$h_{nf} = \frac{(3.66)(0.000305)}{0.0229} = 48.82 \frac{kW}{m^2K}$$

Overall heat transfer coefficient

Overall heat transfer coefficient, U_o

$$\frac{1}{U_o} = \frac{1}{h_{fg}} + \frac{d_o \ln\left(\frac{d_o}{d_i}\right)}{2k_w} + \frac{1}{h_{nf}}\frac{d_o}{d_i}$$

$$\frac{1}{U_o} = \frac{1}{56.418} + \frac{0.0229\ \ln\left(\frac{0.0254}{0.0229}\right)}{2(395.96)} + \frac{1}{48.82}\frac{0.0254}{0.0229}$$

$$U_o = 24.723411\frac{W}{m^2K}$$

3) <u>Size reduction and energy saving of shell and tube heat exchanger</u>

Estimation of nanofluids convective heat transfer coefficient, $h_{nf} = 49.5\frac{W}{m^2K}$

Estimation of flue gas convective heat transfer coefficient, $h_{fg} = 30\frac{W}{m^2K}$

Overall heat transfer coefficient, $U_o = \frac{1}{\frac{1}{49.5} + \frac{1}{30}} = 18.67924528\frac{W}{m^2K}$

Heat capacity, $Q = 26.3 \times 1149.2766 \times (150 - 35) = 3475987.077W$

$$LMTD = \frac{\left(T_{fg,in} - T_{nf,out}\right) - \left(T_{fg,out} - T_{nf,in}\right)}{In\left(\frac{T_{fg,in} - T_{nf,out}}{T_{fg,out} - T_{nf,in}}\right)}$$

$$= \frac{(150 - 55.46453799) - (35 - 30)}{In\left(\frac{150 - 55.46453799}{35 - 30}\right)} = \frac{90.9831837}{2.95473}$$

$$= 30.45903442$$

Required heat transfer area, $A = \frac{Q}{LMTD \times U}$

$$A = \frac{Q}{LMTD \times U} = \frac{3475987.077}{(30.45903442)(18.67924528)} = 6109.458181$$

Shell diameter, $D_s = 0.637\sqrt{\frac{CL}{CTP}}\left[\frac{(A)(PR)^2\left(d_{t,o}\right)}{L}\right]^{1/2}$

$$D_s = 0.637\sqrt{\frac{1}{0.93}}\left[\frac{(6109.458181)(1.75)^2(0.0254)}{5}\right]^{1/2} = 6.439753015m$$

$$\text{Number of tubes, } N_t = 0.785\left(\frac{CTP}{CL}\right)\frac{(D_s)^2}{(PR)^2(d_{to})^2}$$

$$\text{Number of tubes, } N_t = 0.785\left(\frac{0.93}{1}\right)\frac{(6.439753015)^2}{(1.75)^2(0.0254)^2} = 15323.13038$$

Number of tubes per pass,

$N_{t,p} = N_T = 15323.13038$ since single tube pass is considered

$$\text{Tube side flow area per pass, } A_{o,t} = \frac{\pi}{4}d_i^2 N_{t,p}$$

$$\text{Tube side flow area per pass, } A_{o,t} = \frac{\pi}{4}0.0229^2(15323.13038) = 6.311147683$$

For 1 vol.% Copper +Ethylene glycol

$$\text{Nanofluids Reynold number, } Re_{nf} = \frac{\dot{m}_{nf}d_i}{A_{o,t}\mu_{nf}}$$

$$Re_{nf} = \frac{\dot{m}_{nf}d_i}{A_{o,t}\mu_{nf}} = \frac{60 \times 0.0229}{6.767221121 \times 0.014561307} = 14.94932983 \text{ laminar flow}$$

$\text{Nusselt number, } Nu = 3.66$

$$\text{Nanofluids convective heat transfer coefficient, } h_{nf} = \frac{Nu_{nf}k_{nf}}{d_i}$$

$$h_{nf} = \frac{3.66 \times 0.000295643}{0.0229} = 47.23\frac{W}{mK} \quad \sim 49.5\frac{W}{mK} \text{ (Prediction)}$$

Assume tube is made from copper with 8933kg/m^3 (density)

$$\text{Cross section area of tube} = \frac{\pi}{4}0.0254^2 - \frac{\pi}{4}0.0229^2 = 0.00009483682823 \text{ m}^2$$

$$\text{Volume of the tube} = 0.00009483682823 \times 5 = 4.7419144115 \times 10^{-4}\text{m}^3$$

$$\text{Mass of tubes (overall)} = 8933 \times 4.7419144115 \times 10^{-4} \times 15323.13038$$

$$= 649915.46375 \text{ kg}$$

Energy required for material processingfor 1000 boilers (tube side)

$= 1.17517 \times 649915.46375 \times 1000$ =76286705.54 kWh

Assume tube is made from steel with 7854kg/m^3 (density)

Cross section area of shell $= \frac{\pi}{4}6.453753015^2 - \frac{\pi}{4}6.439753015^2$

$= 0.141789886\ \mathrm{m}^2$

Volume of shell $= 0.141789886 \times 5 = 0.70894943$

Mass of shell $= 0.70894943 \times 7854 = 5568088.816$ kg

Energy required for material processingfor 1000 boilers (shell side)

$5568088.816 \times 0.45224 \times 1000 = 2518112.486$ kWh

Total energy consumption $= 2518112.486 + 76286705.54 = 78804818.03$ kWh

Energy saving $=$ Energy consumption$_{\mathrm{bf}}$ $-$ Energy consumption $_{\mathrm{bf}}$

$= 84737707.93 - 78804818.03 = 5932.889906$MWh

4) Entropy generation analysis

Thermo-physical properties of water based (1 vol.%) Al_2O_3 nanofluids

$$\frac{k_{eff}}{k_f} = 1.0 + 1.0112\emptyset_p + 2.4375\emptyset_p\left(\frac{47}{d_p(nm)}\right) - 0.0248\,\emptyset_p\left(\frac{k_p}{0.613}\right)$$

$$\frac{k_{eff}}{0.613} = 1.0 + 1.0112(0.01) + 2.4375(0.01)\left(\frac{47}{30}\right) - 0.0248\,(0.01)\left(\frac{36}{0.613}\right)$$

Thermal conductivity of nanofluids, $k_{eff} = k_{nf} = 0.633679594\,\frac{W}{mK}$

$$\frac{\mu_{nf}}{0.000855} = \frac{1}{(1-\emptyset)^{2.5}} = \frac{1}{(1-0.01)^{2.5}}$$

Vicosity of nanofluid, $\mu_{nf} = 0.000876755\,\frac{Ns}{m^2}$

Density of nanofluid, $\rho_{nf} = (1-\emptyset)\rho_f + \emptyset\rho_p$

$= (1-0.01)997.0089731 + (0.01)\,(3970)$

$= 1026.738883\,\frac{kg}{m^3}$

Specific heat of nanofluid, $c_{p,nf} = \frac{(1-\emptyset)\rho_f c_{p,f} + \emptyset\rho_p c_{p,p}}{\rho_{nf}}$

$$= \frac{(1-0.01)(997.0089731)(4179)+(0.01)(3970)(765)}{1026.738883}$$

$$= 4046.993896 \frac{J}{kgK}$$

Dimensionless wall temperature difference, $\tau = \frac{T_w - 300}{T_w} = 0.02$

Wall temperature, $T_w = 306.122449$

Cross section area (circular tube) $= \frac{\pi}{4} d^2 = \frac{\pi}{4} 0.0229^2 = 4.118706509 \times 10^{-4}$

Velocity of nanofluids, $u_{nf} = \frac{\dot{m}}{\rho_{nf} A_c} = \frac{0.01}{(1026.738883)(4.118706509 \times 10^{-4})}$

$$= 0.023644103 \frac{m}{s^2}$$

Eckert number, $Ec = \frac{u_{nf}^2}{C_{p,nf} T_w} = \frac{0.023644103^2}{4046.993896 \times 306.122449} = 4.51251 \times 10^{-10}$

Nanofluids Reynolds number, $Re_{nf} = \frac{4\dot{m}_{nf}}{\pi d_h \mu_{nf}}$

$= \frac{(4)(0.01)}{\pi(0.0229)(0.000876755)} = 634.0743717$ (laminar flow)

Convective heat transfer coefficient, $h_{nf} = \frac{Nuk_{nf}}{d_h}$

$h_{nf} = \frac{(3.66)(0.633679594)}{0.0229} = 101.2780486 \frac{W}{m^2 K}$

Stanton number, $St = \frac{h_{nf}}{\rho_{nf} u_{nf_{nf}} c_{p,nf}}$

$$= \frac{101.2780486}{(1026.738883)(0.023644103)(4046.993896)}$$

$$= 0.001029991$$

Dimensionless length of a circular tube, $\lambda = \frac{L}{D} = \frac{5}{0.0229} = 218.3406114$

Friction factor, $f = \frac{64}{Re} = \frac{64}{634.0743717} = 0.100934532$

Total dimensionless entropy generation, Ψ

$$\Psi = \frac{1}{1-e^{-4St\lambda}}\left\{\ln\left[\frac{1-\tau e^{-4St\lambda}}{1-\tau}\right]-\tau\left(1-e^{-4st\lambda}\right)+\frac{1}{8}f\frac{Ec}{St}\ln\left[\frac{e^{4st\lambda}-\tau}{1-\tau}\right]\right\}$$

$$= 7.08586\times10^{-5}$$

5) Thermosyphon air preheater

Properties of air

$$\rho_{air} = 0.938006\,\frac{kg}{m^3}$$

$$\mu_{air} = 2.18274\times10^{-5}\,\frac{Ns}{m^2}$$

$$Pr = 0.6954$$

$$c_{p,air} = 1011.3\,\frac{J}{kgK}$$

Thermal resistance of air side (evaporator)

Air Reynolds number, $Re_{D,max} = \frac{\rho_{air}u_{max}d_o}{\mu_{air}}$

$$Re_{D,max} = \frac{0.9380006(1.367295402)(0.015)}{2.18274\times10^{-5}} = 881.3678843$$

Colburn factor $j = 0.14Re^{-0.328}\left(\frac{S_t}{S_l}\right)^{-0.502}\left(\frac{f_s}{d_o}\right)^{0.031}$

$$= 0.14(881.3678843)^{-0.328}\left(\frac{0.03}{0.03}\right)^{-0.502}\left(\frac{0.01}{0.015}\right)^{0.031}$$

$$= 0.014950566$$

Convective heat transfer coefficient of air $h_{air,eva} = \frac{j\,\rho_{air}u_{max}C_{p,air}}{Pr_{air}^{2/3}}$

$$h_{air,eva} = \frac{j\,\rho_{air}u_{max}C_{p,air}}{Pr_{air}^{2/3}}$$

$$= \frac{(0.014950566)(0.938006)(1.367295402)(1011.3)}{0.6954^{\frac{2}{3}}}$$

$= 24.70486532$

Fin efficency, $\eta_f = \frac{\tanh ml}{ml}$

$$m = \sqrt{\frac{2h_{air,eva}}{k_{fin}\, f_{thickness}}} = \sqrt{\frac{2(24.70486532)}{(239.19)(0.0004)}} = 22.72504428$$

$$\eta_f = \frac{\tanh ml}{ml} = \frac{\tanh(22.72504428 \times 0.015)}{(22.72504428 \times 0.015)} = 0.962987276$$

Total surface temperature effectiveness, η_o

$$\eta_o = 1.0 - (1.0 - 0.962987276) \times \frac{11.221686}{13.67169192} = 0.969620061$$

Air thermal resistance , $R_{air,eva} = \frac{1}{(24.70486532)(0.969620061\ )} = 0.041746101$

Thermal resistance of air side (condenser)

Same calculation as evaporator side

Air thermal resistance , $R_{air,condenser} = 0.034452879$

Thermal resistance of working fluid at evaporator

Water based (1 vol.%) Al_2O_3 nanofluids

Convective heat transfer coefficient, $h_{nf/eva}$

$$\frac{h_{nf,eva}}{k_{nf}}\left(\frac{\mu_{nf}^2}{\rho_{nf,l}(\rho_{nf,l} - \rho_{nf,g})g}\right)^{1/3} = \left(\frac{4}{3}\right)^{\frac{1}{3}} \frac{1}{Re_{nf}^{1/3}}$$

$$\frac{h_{nf,eva}}{0.704815957}\left(\frac{0.000287073^2}{987.97546(987.97546 - 40.286476)9.81}\right)^{1/3} = \left(\frac{4}{3}\right)^{\frac{1}{3}} \frac{1}{30_{nf}^{1/3}}$$

$$h_{nf.eva} = 12.01471751 \frac{kW}{m^2K}$$

Thermal resistance of nanofluids at evaporator, $R_{nf,eva} = \frac{1}{\left(\frac{\alpha_{nf}}{\alpha_{air}}\right) h_{nf,eva}}$

$$R_{nf,eva} = \frac{1}{\left(\frac{34.0992248}{196.2631628}\right) 12014.71751} = 0.00047905$$

Thermal resistance of working fluid at condenser

Water based (1 vol.%) Al_2O_3 nanofluids

Convective heat transfer coefficient, $h_{nf,cond}$

$$\frac{h_{nf,cond}}{k_{nf}}\left(\frac{\mu_{nf}^2}{\rho_{nf,l}(\rho_{nf,l}-\rho_{nf,g})g}\right)^{1/3} = \frac{4}{3}\left(\frac{4}{3Re_{nf}}\right)^{\frac{1}{3}}$$

$$h_{nf,cond} = 6.775680502\frac{kW}{m^2K}$$

Thermal resistance of nanofluids at condenser, $R_{nf,condenser}$

$$R_{nf,condenser} = \frac{1}{\left(\frac{\alpha_{nf}}{\alpha_{air}}\right) h_{nf,cond}} = 0.000849457$$

Overall heat transfer coefficient at evaporator, $= \frac{1}{0.041746101 + 0.00047905}$

$= 23.68256796$

Overall heat transfer coefficient at condenser $= \frac{1}{0.034452879 + 0.000849457}$

28.32673729

Total overall heat transfer coefficient at both sides $= 52.00930525\frac{W}{m^2K}$